REDUCING DEGRADATION OF INTRACELLULAR COFACTORS TO IMPROVE BIOCONVERSION TO OXIDIZED CHEMICALS AND PRODUCTION OF RECOMBINANT PROTEINS BY *ESCHERICHIA COLI*

by

QI HAN

(Under the Direction of Mark A. Eiteman)

ABSTRACT

Microorganisms are widely used to synthesize chemicals. One set of microbial conversions involves the transfer of electron from a starting material to a microbial electron carrier (such as NAD^+): A + NAD^+ → B + NADH. L-xylulose formation is a good example of this microbial conversion, which is a rare sugar generated from xylitol by an NAD^+-dependent xylitol 4-dehydrogenase (XDH) from *Pantoea ananatis.* Since the general conversion of A to B (or the specific example of xylitol to L-xylulose) involves the utilization of NAD^+ and the formation of NADH, the continued presence of NAD^+ is necessary to drive the process.

Two fundamental challenges exist, however. First, to drive the reaction forward at a fast rate toward the product, a relatively high ratio of NAD^+/NADH is required. Second, microbes continually degrade both NAD^+ and NADH as part of biochemical recycling that occurs in living systems, which will lead essentially to a loss of NAD(H) availability.

Using the conversion of xylitol to L-xylulose as a model system, we co-expressed water-forming NADH oxidase (NOX) from *Streptococcus pneumoniae* with XDH to regenerate NAD^+, and also modified the biochemical pathways involved in NAD(H) degradation. Controlled batch process demonstrated that the final equilibrium L-xylulose/xylitol ratio was correlated to an

elevated ratio of NAD^+/NADH. The *E. coli* strain (MEC697) with deletions of the *nadR nudC mazG* genes in the degradation pathway of NAD(H) increased the total amount of NAD(H) and delayed the degradation of this cofactor, further improving the conversion of xylitol to L-xylulose. As a potential platform for enhancing formation of the oxidized biochemical product, MEC697 also successfully improved the conversion of galactitol to L-tagatose, with almost a 60% increase in the final product.

In addition, MEC697 reduced the acetate formation when grown on glucose and improved β-galactosidase production. Using steady-state cultures, we demonstrated the enhanced total NAD(H) in MEC697 delayed the threshold growth rate for acetate formation to beyond 0.27 h^{-1}. At the 1 liter scale, a batch process with 10 g/L glucose, MEC697 as the host strain for recombinant protein production reduced acetate by about 50% and doubled the formation of β-galactosidase.

INDEX WORDS: *Escherichia coli,* Rare sugars, Recombinant protein, NAD^+/NADH, Xylitol 4-dehydrogenase, NADH oxidase, β-galactosidase, Glucose, Glycerol, Xylitol, L-xylulose, Acetate, Batch process, Chemostat

REDUCING DEGRADATION OF INTRACELLULAR COFACTORS TO IMPROVE BIOCONVERSION TO OXIDIZED CHEMICALS AND PRODUCTION OF RECOMBINANT PROTEINS BY *ESCHERICHIA COLI*

by

QI HAN

B.A., Southwest University, China, 2009

M.S., Southwest University, China, 2012

A Dissertation Submitted to the Graduate Faculty of the University of Georgia in Partial Fulfillment of the Requirements for the Degree

DOCTOR OF PHILOSOPHY

ATHENS, GEORGIA

2018

REDUCING DEGRADATION OF INTRACELLULAR COFACTORS TO IMPROVE BIOCONVERSION TO OXIDIZED CHEMICALS AND PRODUCTION OF RECOMBINANT PROTEINS BY *ESCHERICHIA COLI*

by

QI HAN

Major Professor:	Mark A. Eiteman
Committee:	Jim R. Kastner
	Ramaraja P. Ramasamy
	William N. Lanzilotta

Electronic Version Approved:

Suzanne Barbour
Dean of the Graduate School
The University of Georgia
December 2018

DEDICATION

TO MY FAMILY

TABLE OF CONTENTS

CHAPTER 1

INTRODUCTION

Nicotinamide adenine dinucleotide (NAD^+) or its reduced form (NADH) is a cofactor for 433 enzymes in over 740 biochemical reactions (Chen and Liu, 2014). The interest in industry for enzymatic transformations which use NAD(H) dependent biotransformation is growing rapidly (Chenault and Whitesides, 1987; Palmore et al., 1998; Schmid et al., 2001; Van Der Donk and Zhao, 2003). However, the need for purified enzymes and the high cost of NAD(H) are disadvantages for the efficient and economic conversions using the enzymatic transformations. To improve and simplify NAD(H) dependent conversions, whole-cell catalysts with overexpression of the target NAD^+-dependent enzymes is a promising alternative. In such a process, cells synthesize NAD(H), and during the oxidation of carbon sources regenerate the resulting NADH into NAD^+ by the reduction of oxygen under aerobic conditions.

A significant improvement for NAD^+-dependent biotransformation can be achieved using whole-cells when a regeneration pathway is engineered. Glucose catabolism involves the formation of NADH. Under fully aerobic growth conditions, the respiratory chain will utilize NADH and continuously regenerate NAD^+. An oxidative or reductive biotransformation process relies on the appropriate balance of NAD^+ and NADH, which serve as a significant driving force for product formation. Studies have investigated multiple approaches to improve cofactor balance using emerging technologies, such as promoter engineering, structural synthetic biotechnology, systems metabolic engineering, and cofactor regeneration (Dueber et al., 2009;

Na et al., 2010; Lee et al., 2012; Su et al., 2017). For example, a whole-cell biocatalyst with overexpression of NAD^+-dependent (2R,3R)-2,3-butanediol dehydrogenase was used to produce acetoin. After introducing a NADH oxidase to regenerate NAD^+, the recombinant strain displayed a higher biocatalytic efficiency in the production of acetoin (Xiao et al., 2010). Although, increasing the balance between NAD^+ and NADH is important in such biotransformations, an often-overlooked challenge for using whole-cells for NAD^+-dependent bioconversions is the loss of NAD(H) availability by cellular degradation. The central premise of this work is that removing the cofactor degradation pathways using metabolic engineering strategies will enhance or prolong a NAD^+-mediated bioconversion.

In this research, we demonstrate that reducing the catabolic NAD(H) pathways results in more NAD(H) available to accomplish the NAD^+-dependent oxidations. One of the goals of this research is to develop metabolically engineering strains and microbial fermentation processes capable of producing the oxidized chemicals in high yield and final titer. The oxidation of xylitol into L-xylulose by an NAD^+-dependent xylitol 4-dehydrogenase was examined as one model system. In this dissertation, Chapter 3 focuses on creating a high NAD^+/NADH ratio to increase the driving force for oxidative biotransformations. In addition, a water-forming NADH oxidase and the use of glucose or glycerol as the carbon source were also investigated for improving L-xylulose production. Chapter 4 focuses on increasing the L-xylulose yield by preventing total NAD(H) degradation in *E. coli*. The phosphate in growth medium and several gene knockouts related to the catabolic NAD(H) pathways were examined to enhance the pool size of total NAD(H) and consequently delay the cofactor degradation. Interestingly, a new strain constructed in Chapter 4 also exhibited ability to eliminate acetate when grown on glucose. Thus, Chapter 5 mainly focuses on analyzing the physiological characteristics of the new knockout strain in

chemostat fermenters and validating its application in recombinant proteins generation. Among the improvement observed are less acetate accumulation and an increase in the titer of β-galactosidase in controlled batch fermentation. These studies demonstrates that reducing NAD(H) is crucial for diving NAD^+-dependent biotransformations and can be a methodology for enhancing formation of the oxidized biochemical product. These results also provide new insights into strategies for reducing acetate to improve recombinant protein production in *E. coli*.

References

Chen, X., S. Li, and L. Liu. 2014. Engineering redox balance through cofactor systems. *Trends Biotechnol*. 32(6): 337-343.

Chenault, H. K. and G. M. Whitesides. 1987. Regeneration of nicotinamide cofactors for use in organic synthesis. *Appl. Biochem. Biotechnol*. 14(2): 147-197.

Dueber, J. E., G. C. Wu, G. R. Malmirchegini, T. S. Moon, C. J. Petzold, A. V. Ullal, K. L. Prather, and J. D. Keasling. 2009. Synthetic protein scaffolds provide modular control over metabolic flux. *Nat. Biotechnol*. 27(8): 753.

Lee, J. W., D. Na, J. M. Park, J. Lee, S. Choi, and S. Y. Lee. 2012. Systems metabolic engineering of microorganisms for natural and non-natural chemicals. *Nat. Chem. Biol*. 8(6): 536.

Na, D., T. Y. Kim, and S. Y. Lee. 2010. Construction and optimization of synthetic pathways in metabolic engineering. *Curr. Opin. Microbiol*. 13(3): 363-370.

Palmore, G. T. R., H. Bertschy, S. H. Bergens, and G. M. Whitesides. 1998. A methanol/dioxygen biofuel cell that uses NAD^+-dependent dehydrogenases as catalysts: application of an electro-enzymatic method to regenerate nicotinamide adenine dinucleotide at low overpotentials. *J Electroanal. Chem*. *443*(1): 155-161.

Schmid, A., J. S. Dordick, B. Hauer, A. Kiener, M. Wubbolts, and B. Witholt. 2001. Industrial biocatalysis today and tomorrow. *Nature*, 409(6817): 258.

Su, L., Y. Shen, W. Zhang, T. Gao, Z. Shang, and M. Wang. 2017. Cofactor engineering to regulate NAD^+/NADH ratio with its application to phytosterols biotransformation. *Microb. Cell Fact.* 16(1): 182.

Van Der Donk, W. A. and H. Zhao. 2003. Recent developments in pyridine nucleotide regeneration. *Curr*. *Opin Biotechnol*. 14(4): 421-426.

Xiao, Z., C. Lv, C. Gao, J. Qin, C. Ma, Z. Liu, P. Liu, L. Li, and P. Xu. 2010. A novel whole-cell biocatalyst with NAD^+ regeneration for production of chiral chemicals. *PloS One*. 5(1): e8860.

CHAPTER 2

LITERATURE REVIEW

Rare sugars and applications

According to the rules for classification from International Society of Rare Sugars (ISRS), common sugars are comprised four hexoses (D-glucose, D-galactose, D-mannose, D-fructose) and three pentoses (D-xylose, D-ribose, and L-arabinose). Twenty-nine other hexoses, pentoses and modified sugars (i.e., by deoxygenation, methylation, etc.) are classified as "rare sugars" (Graber et al., 1988; Liu and Thorson, 1994; Salas, 1999). Succinctly, rare sugars are monosaccharides that rarely exist in nature (Granström et al., 2004) .

Rare sugars have applications in pharmaceutical and food industry that include 1) antiviral drugs, 2) anti-cancer or tumor treatments, and 3) drug building blocks (Beerens et al., 2012). For example, L-ribose is the sugar moiety in lamivudien used for anti-hepatitis B virus therapy (Mathé and Gosselin, 2006). L-xylose, L-gulose and L-galactose are used to produce L-nucleosides (Jeong et al., 1993; Ma et al., 1997; Woodyer et al., 2008). In cancer and tumor treatments, D-allose is an effective therapeutic agent when used in conjunction with radiation (Bicher, 1997), and L-glucose can be used with other cancer treatments to improve the therapy (Lim et al., 2011). In addition, D-arabinose and D-lyxose can be starting material for the synthesis of antitumor agents (Moran et al., 1993; Goodwin et al., 1998; Savage et al., 2006).

Some rare sugars or sugar alcohols taste sweet but can not be metabolized at a significant rate by humans. Thus, some relatively inexpensive sugar alcohols including sorbitol, xylitol, and

mannitol are used extensively as low calorie sweeteners in the US, while D-tagatose and D-psicose have been proposed as sugar substitutes (Kroger et al., 2006).

Chemical synthesis for rare sugars production

Chemical synthesis is one option available for rare sugar production. For example, xylitol is synthesized chemically on an industrial scale of 40,000-50,000 tonnes annually (Heikkilä et al., 2005). In this process, pure D-xylose is hydrogenated to xylitol on a Raney nickel catalyst at about 125°C and a hydrogen pressure of 3 bar (Albert et al., 1980). Similarly, methods to synthesize L-gulose and L-idose using 2-(trimethylsilyl) thiazole have been reported (Dondoni et al., 1997), and D- and L-gulose and talose can be prepared from the diastereomeric allylic alcohol (Harris et al., 2000). However, chemical synthesis of rare sugars is often a tedious process that requires high reaction temperatures and expensive catalysts.

Enzymes for rare sugars production

In contrast to chemical synthesis, bioconversions that generate rare sugars use ambient temperatures. A general strategy for the enzymatic interconversion of all monosaccharides in the cell-free system has been proposed using combinations of keto-aldol isomerases, epimerases, and oxidoreductases (Granström et al., 2004).

Keto-aldol isomerases or aldose isomerases (EC 5.3.1.X) catalyze an intramolecular redox reaction, and exchange the carbonyl group between the C1 and C2 positions (Izumori, 2006). As fairly promiscuous biocatalysts, isomerases are specific to rare sugars that contain the same functional groups on C1 and C2 positions. For example, D-psicose, L-fructose, D-ribose and L-tagatose each have a carbonyl and aldehyde group at the C1 and C2 positions, respectively. L-rhamnose isomerase from *Bacillus pallidus* Y25 catalyzes the conversion of these four monosaccharides, respectively to D-allose, L-mannose, D-ribulose, and L-talose

(Poonperm et al., 2007). Isomerases are enzymes that are reversible and always result in an equilibrium between two or more sugars. Therefore, yield can be reduced and downstream processing is often complicated (Beerens et al., 2012). Glucose-6-phosphate isomerase from *Pyrococcus furiosus,* for example, simultaneously generates L-tagatose and L-galactose from L-talose, or D-ribose and D-arabinose from D-ribulose (Yoon et al., 2009).

Epimerases (EC 5.1.3.X) are responsible for catalyzing the reorientation of a hydroxyl group to convert monosaccharides into epimers (Samuel et al., 2002). As a potential bridge between some rare sugars, epimerases can shorten a synthetic route by modifying carbonyl groups at the C3, C4 or C5 positions. For instance, D-tagatose 3-epimerase from *Pseudomonas sp*. ST-24 alters the C3 position of D-tagatose, L-sorbose, L-psicose and D-fructose to form, respectively, D-sorbose, L-tagatose, L-fructose and D-psicose (Itoh et al., 1995; Itoh et al., 1996; Takeshita et al., 2000a). Unfortunately, most epimerases require sugars to have a phosphate or nucleotide group in order to drive the reaction. This requirement often prevents the widespread commercial use of many epimerases (Beerens et al., 2012). Similarly, *Escherichia coli* UDP-galactose 4-epimerase (EC 5.1.3.2) can bridge between D-glucose and D-galactose but uses UDP-glucose or UDP-galactose as the substrates (Kim et al., 2011).

Oxidoreductases (EC 1.1.X.X) catalyze the interconversion of monosaccharides with their corresponding sugar alcohols (Salas, 1999). Oxidoreductases can serve as a bridge between D- and L-sugars by a two-step reduction and oxidation process with a sugar alcohol intermediate. For example, synthesis of L-gulose from D-glucose can be accomplished by first using aldehyde reductase (EC 1.1.1.21) to form the intermediate D-sorbitol and then using mannitol 1-dehydrogenase (EC 1.1.1.255) to oxidize the sugar alcohol (Woodyer et al., 2010). The principal disadvantage of the industrial application of oxidoreductases, in a purely enzymatic process for

rare sugar production, is the need for expensive cofactors $NAD^+/NADP^+$ as cosubstrates (Beerens et al., 2012). However, there is typically no need to supply the cofactors in a microbial process since microbes themselves synthesize the cofactors.

Microbial processes for rare sugars production

Although an immobilized enzyme process can show high conversion to a desired rare sugar, such a process often requires costly cofactors (Berenguer and Fernandez, 2010) as well as the regeneration of the cofactor in the correct oxidation state. In contrast, using an intact organism is advantageous because the cofactors are generated by the microbe and remain within the cell. Whole cell methods for rare sugar production can be classified as either a resting cell process or a growing cell process.

A resting cell process uses biocatalyticly active but non-growing cells. Such cells are washed suspensions of microbes which are used as a source of enzymes for studies of biotransformations (Wilson, 1938). The resting cell method generally has the advantages of high specificity for the desired conversion, simple purification of products because a minimal medium is used and the potential for high volumetric productivity and cell repeated use. A growing cell process is an alternative microbial method for the synthesis of rare sugars. In this case, cells are provided ample nutrients for their growth, including carbon, nitrogen and potentially oxygen. For both the resting cell and growing cell processes, a rare sugar precursor is taken up by the cells and further converted into the desired sugar by active enzymes within the cell.

Both enzymatic and microbial processes must have a “driving force” for the conversion of one sugar into another sugar to occur effectively. There are three general categories for driving forces.

a) NADH or NADPH formation during sugar oxidation.

Pentose or hexose alcohols can be oxidized by NAD(P)$^+$-dependent dehydrogenases to their sugar forms. During the reaction process, the electrons are transferred to NAD$^+$/NADP$^+$ to form the reduced cofactor NADH/NADPH. In order for a sugar conversion to proceed, the oxidized form of the cofactor (NAD$^+$/NADP$^+$) must be regenerated, for example, by a secondary oxidizing agent such as oxygen in the presence of an appropriate biocatalyst. So, continuously providing oxygen can serve as a driving force to ensure a continuous supply of NAD$^+$/NADP$^+$ for the dehydrogenase.

Many NAD$^+$-dependent sugar alcohol dehydrogenases exist that can be used to generate rare sugars. For example, the NAD$^+$-dependent mannitol-1-dehydrogenase (MDH, EC 1.1.1.255) from *Apium graveolens* can oxidize the C1 hydroxyl of ribitol to produce L-ribose (Woodyer et al., 2008). An active culture of engineered *E. coli* resulted in 55% conversion of 100 g/L ribitol in 72 h. Similarly, NAD$^+$-dependent MDH can convert D-sorbitol to L-gulose and galactitol to L-galactose in high yields (Woodyer et al., 2010). L-xylulose formation from xylitol is another example of a sugar oxidation that is relevant to this work. Using cells that have been grown to a stationary phase, *E. coli* expressing the NAD$^+$-dependent xylitol dehydrogenase (XDH, EC 1.1.1.10) from *B. pallidus* or *Pantoea ananatis* converts xylitol to L-xylulose (Aarnikunnas et al., 2006; Takata et al., 2010).

b) NADH or NADPH consumption during sugar reduction.

Many important conversions are reduction reactions and therefore require NADH or NADPH as the electron source. In these cases, regeneration of the reduced cofactor requires some energy input.

One example of a microbial reduction is the conversion of D-xylose to xylitol. Research has focused on the conversion of D-xylose to xylitol by *Saccharomyces cerevisiae* and *Candida spp* with $NADP^+$-dependent xylose reductase (XR, EC 1.1.1.307) under anaerobic conditions (Bruinenberg et al., 1983; Bruinenberg, 1986). Because NADPH is consumed during the reaction, the main challenge with the yeast process is NADPH deficiency (Kötter and Ciriacy, 1993). By manipulating the metabolism, increased NADPH can lead to more xylitol accumulation (Granström et al., 2007).

NAD(P)H regeneration can also be accomplished in an enzymatic process. For NADH, the desired enzymatic conversion is often coupled with formate oxidation into CO_2 via formate dehydrogenase (FDH). For example, allitol formation from D-psicose has been coupled to the oxidation of formate by FDH. FDH continuously supplies NADH as a driving force, and the irreversible generation of CO_2 ensures that the direction of the process remains toward allitol formation (Takeshita et al., 2000b). Of course, the process requires formate, which is consumed during its oxidation.

c) No net change in oxidation state during the reaction

A third category involves conversions that have no net change in cofactors. Several approaches exist under this category. When oxidoreductases are used to interconvert ketoses and aldoses through a sugar alcohol intermediate, two steps for the conversion are required. Examples include the conversion of D-galactose to D-tagatose through the intermediate D-galactitol and L-xylulose to L-xylose through the intermediate D/L-xylitol. In contrast, isomerases require just one step to interconvert two sugars without the participation of cofactors. For example, L-arabinose isomerase (L-AI, EC 5.3.1.4) from various microbes including *Acidothermus cellulolytics* and *Bacillus stearothermophilus* isomerizes D-galactose to D-

tagatose (Prabhu et al., 2008; Cheng et al., 2010a; Cheng et al., 2010b). This specific reaction occurs between C1 and C2. This category of conversions involve equilibria and therefore only the high concentration of the substrate serves as the driving force.

Metabolic pathways related to NAD(H) biosynthesis and degradation

During the growth of *E. coli*, NAD^+ and its phosphorylated analog ($NADP^+$) contribute 12% of all biochemical reactions involved in almost all major metabolic pathways (Reed et al., 2003), which drive a quick interconversion between $NAD(P)^+$ and NAD(P)H. The change of NAD(H) pool is also rapid, with a half-life of nearly 90 min (Cheng and Roth, 1995). Cells will tightly regulate a homeostasis of NAD(H) pool by maintaining a dynamic balance in a network of NAD^+ biosynthesis, decomposition and recycling pathways.

The cell can synthesize NAD(H) through *de novo* pathway or pyridine nucleotide cycles. The *de novo* pathway in *E. coli* is composed of two routes: upstream route from L-aspartate (L-Asp) to nicotinic acid mononucleotide (NaMN) and downstream route from NaMN to NAD^+ (Fig. 1-1). L-aspartate is derived from oxaloacetate, which is an intermediate in TCA cycle. Three consecutive steps convert L-Asp into NaMN: L-aspartate oxidase (NadB, EC 1.4.3.2) encoded by *nadB* catalyzes the oxidation of L-aspartate to iminoaspartate (IA) (Hossain et al., 2014); quinolinate synthase (NadA, EC 2.5.1.72) encoded by *nadA* condenses IA with DHAP to form quinolinic acid (Qa) (Saunders et al., 2008); quinolinate phosphoribosyltransferase (NadC, EC 2.4.2.19) encoded by *nadC* catalyzes the phosphoribosylation of Qa with supply of PRPP to generate NaMN (Bhatia and Calvo, 1996). The downstream route initially from NaMN involves two reactions: NaMN adenylyltransferase (EC 2.7.7.18) encoded by *nadD* converts NaMN to NaAD; ATP-dependent NAD^+ synthetase (EC 6.3.5.1) encoded by *nadE* further catalyzes the amidation of NaAD to generate NAD^+ (Spencer and Preiss, 1967; Lau et al., 2009).

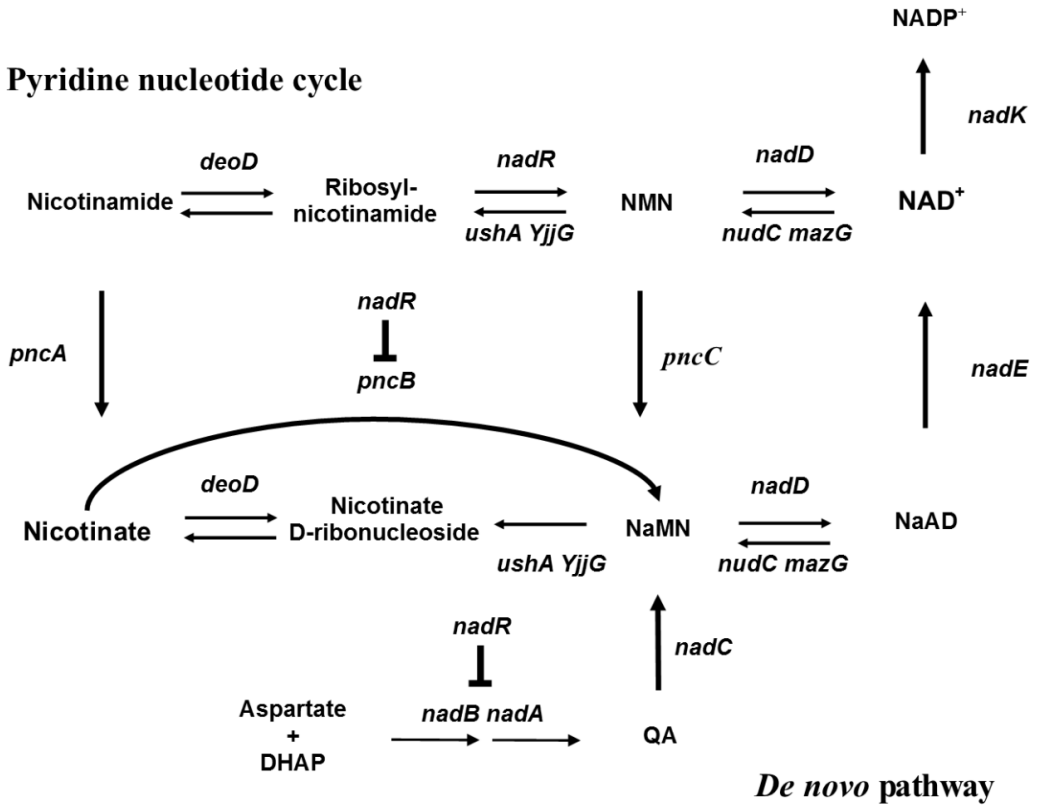

Figure 1-1. NAD^+ metabolism in *Escherichia coli*. Key genes and the corresponding enzymes are: *pncA*, nicotinamidase; *pncB*, nicotinic acid phosphoribosyltransferase; *pncC*, nicotinamide-nucleotide amidase; *deoD*, purine-nucleoside phosphorylase; *ushA*, UDP-sugar hydrolase; *nadA*, quinolinate synthetase; *nadB*, L-aspartate oxidase; *nadC*, quinolinate phosphoribosyltransferase; *nadD*, nicotinate-nucleotide adenylytransferase; *nadE*, NAD^+ synthetase; *nadR*, HTH-type transcriptional regulator; *nudC*, NADH diphosphatase; *mazG*, nucleoside triphosphate pyrophosphohydrolase. Chemical intermediates include: NaMN, nicotinic acid mononucleotide and NMN, nicotinamide mononucleotide. Other genes code for enzymes shown to convert NaMN into N-ribosyl-nicotinamide or NMN into nicotinate D-ribonucleoside.

The pyridine nucleotide cycle (PNC) allows the cell to utilize the pyridine ring and other byproducts of NAD^+ consumption within the cell (Penfound and Foster, 1996). In *E. coli*, nicotinic acid phosphoribosyltransferase (EC 6.3.4.21) encoded by *pncB* together with nicotinamide deamidase (EC 3.5.1.19) encoded by *pncA* can respectively utilize nicotinamide (Nm) and nicotinic acid (Na) to supply NaMN precursor for NAD^+ synthesis (Fig. 1-1) (Foster and Baskowsky-Foster, 1980). The PNC plays a substantial role in response to the environment and takes precedence over the *de novo* pathway whenever these precursors are available in the medium.

NAD(H) synthesis is also influenced by cellular regulation. In order to respond to the change of overall NAD^+ pool or the distribution of NAD(P)/NAD(P)H components between aerobic and anaerobic growth conditions, regulatory mechanisms exist to control the NAD^+ biosynthetic machinery. The tri-functional NadR protein containing the N-terminal helix-turn-helix DNA-binding domain showed specific binding activity on the DNA fragments of upstream regions of *nadA, nadB* and *pncB* genes (Penfound and Foster, 1999; Raffaelli et al., 1999; Grose et al., 2005), and regulates the transcription of genes in the major routes of NAD^+ biosynthesis (Fig. 1-1).

The homeostasis of NAD(H) pool is associated with degradative reactions that catalyze NAD^+ or NADH as the substrate, and the resulting intermediates may undergo further hydrolysis, recycling, or excretion. In *E. coli*, a NADH pyrophosphatase encoded by *nudC* belongs to "Nudix" hydrolases family of genes and was reported to catalyze the hydrolysis of NADH with high activity (Frick and Bessman, 1995). Another Nudix hydrolase coded by *nudE* also showed enzymatic activity toward NAD(H) (O'Handley et al., 1998). Mutant *E. coli* with deletions of *nudC*, *nudE* or both genes resulted in over 50% reduction of pyrophosphatase

activity (Heuser et al., 2007). Several other candidates, such as *ushA* coding a UDP-sugar hydrolase and *mazG* coding a nucleoside triphosphate pyrophosphohydrolase, also hydrolyze NAD^+ and NADH (Zhang and Inouye, 2002; Wang et al., 2014). Moreover, as a route of NAD^+ utilization, NAD^+ kinase encoded by *nadK* can convert NAD^+ to $NADP^+$ for modulating and maintaining the balance between the pools of NAD^+ and $NADP^+$ (Johansson et al., 2005).

Approaches to accumulate intracellular NAD(H)

The influence of genes in the NAD^+ biosynthesis pathway has been studied previously to enhance NAD(H) pools. For example, nicotinic acid phosphoribosyltransferase coded by *pncB* and NAD^+ synthetase coded by *nadE* are thought to be rate limiting steps in NAD(H) synthesis (Imsande and Pardee, 1962; Heuser et al., 2007). Indeed, overexpressing *pncB* in *E. coli* resulted in a 2-fold increase in NAD(H) (San et al., 2002), and in a recombinant *Salmonella typhimurium* overexpressing the *pncB* gene, a 5-fold increase of NAD(H) was attained in the presence of 0.1 mM nicotinic acid (Wubbolts et al., 1990). Similarly, overexpression of *pncB* in a succinate-generating strain of *E. coli* doubled the NAD(H) concentration and improved the formation of this target biochemical (Ma et al., 2013). Another means to increase NAD(H) formation was accomplished by overexpressing the NAD^+ transporter Ntt4 and supplementing the biotransformation medium with NAD^+ leading to a 40% increase in NAD(H) and a 60% increase in dihydroxyacetone (Zhou et al., 2013).

Metabolic pathways related to acetate formation

Glycolysis as the main route of carbon source metabolism utilizes 72% of the carbon supply. However, considerable amounts of acetate accumulate during aerobic *E. coli* fermentation at high growth rates (Åkesson et al., 1999). Acetyl-CoA to acetate and pyruvate to acetate are the two major aerobically active pathways in *E. coli* for the acetate formation. In the

pathway converting acetyl-CoA to acetate, phosphotransacetylase (EC 2.3.1.8) encoded by *pta* gene reversibly converts acetyl-CoA and inorganic phosphate to acetyl phosphate and CoA, while acetate kinase (EC 2.7.2.1) encoded by *ackA* further converts acetyl phosphate and ADP to generate acetate and ATP (Rose et al., 1954). The acetyl-CoA to acetate pathway is considered essential for balanced carbon flux and ATP production during exponential growth under both aerobic and anaerobic conditions (Chang et al., 1999; Avison et al., 2001). Acetate generation can also occur directly from pyruvate using pyruvate oxidase (EC 1.2.2.2) encoded by *poxB* gene to convert pyruvate, ubiquinone and H_2O to acetate, ubiquinol and CO_2 (Steinsiek and Bettenbrock, 2014). Pyruvate oxidase is more active during the late exponential and stationary phases, whereas phosphotransacetylase and acetate kinase are mainly activated during exponential cell growth (Chang and Cronan, 1983; Chang et al., 1994; Dittrich et al., 2005).

Acetate formation during the cell growth is undesirable not only because it leads to inefficient utilization of carbon source but the compound inhibits recombinant protein production and cell growth (Koh et al., 1992; Nakano et al., 1997; March et al., 2002). Acetate is detrimental to the synthesis of RNA, DNA, protein and lipid, especially impacts those proteins involved in *E. coli* transcription-translation machinery, the general stress response and regulation (Blankenhorn et al., 1999; Arnold et al., 2001). Generally, the formation of acetate in *E. coli* is caused by an imbalance between the glycolytic and the TCA cycle fluxes, activating the acetate pathways (Majewski and Domach, 1990; Delgado and Liao, 1997; Farmer and Liao, 1997). Indeed, the rate of acetate formation is directly related to the cell growth rate or the rate at which cells consume glucose. *E. coli* start to accumulate acetate when the cells grow above a threshold growth rate, and this threshold also corresponds to the time that cells reach their maximum oxygen consumption rate (Eiteman and Altman, 2006). Several strains grown in defined medium

have demonstrated that this threshold growth rate is in the range of 0.14-0.17 h^{-1} for fed-batch processes (Korz et al., 1995) and 0.35-0.48 h^{-1} for accelerostats or chemostats (Paalme et al., 1997; Vemuri et al., 2006a).

Approaches to eliminate acetate during microbial production of recombinant proteins

Acetate formation is always a major challenge for industrial application of *E. coli* in recombinant protein generation. Consequently, many engineering approaches have focused on the elimination of acetate to maximize the protein production. These approaches can be classified in two strategies: process modification or genetic modification.

For the process modification strategy, a simple and straightforward approach is a fed-batch process to maintain a low cell growth rate, which also means sacrificing the fast growth rate of *E. coli* (Jensen and Carlsen, 1990; Vidal et al., 2005). Since acetate is an extracellular by-product, directly removing acetate from the cell culture by dialysis-fermentors as it is generated also reduces the inhibitory effects of acetate on cell growth (Nakano et al., 1997; Fuchs et al., 2002), though this approach does not prevent carbon being diverted unnecessarily to acetate rather than to biomass. The pH-stat or controlling DO also serve as tools to reduce acetate formation (Johnston et al., 2003; Shen et al., 2004). In addition to those operational processes, medium composition impacts acetate formation. For example, replacing glucose with fructose decreases acetate and increases protein yield by 65% (Aristidou et al., 1999). Similarly, a medium supplemented with yeast extract, methionine or glycine achieves the same goals (Han et al., 1993). However, altering the medium composition increases the costs and might complicate downstream processes.

Genetic modification to alter central metabolism in *E. coli* can reduce acetate. The simplest approach is to disrupt the acetate synthesis pathways. As noted above, the key pathways

involved in acetate formation are pyruvate oxidase which converts pyruvate to acetate and phosphotranscetylase/acetate kinase which together convert acetyl CoA into acetate. Blocking those two pathways is effective in reducing the acetate (Bauer et al., 1990; Hahm et al., 1994; Abdel-Hamid et al., 2001), but an increase of pyruvate relative to PEP in the knockout strains leads to a much lower growth rate (Chang et al., 1999). Because a high glucose consumption rate is strongly linked to acetate formation, another approach is to disable glucose uptake. The deletion of *ptsG* and *ptsHI* genes in phosphoenolpyruvate:sugar phosphotransferase system (PEP-PTS) decreased acetate formation but also significantly reduced specific growth rate (Ponce, 1999; Picon et al., 2005). Diversion of pyruvate, or its precursor PEP, directly to the TCA cycle can also eliminate the formation of acetate. Overexpression of the native PEP carboxylase in *E. coli* amplifies this anaplerotic reaction to reduce acetate formation by 60% (Farmer and Liao, 1997). Unfortunately, the enzymatic utilization of PEP results in a lower PEP pool for the PTS-mediated uptake of glucose and such a process also reduces cell growth (Gokarn et al., 2000). Overexpressing pyruvate carboxylase from *Rhizobium etli* in *E. coli* increased carbon flux in the TCA cycle and led to a 60% reduction of acetate formation (Gokarn et al., 2001; March et al., 2002). Manipulating the NAD^+/NADH ratio also reduces acetate generation. A greater redox ratio of NADH/NAD^+ was correlated with acetate overflow (Vemuri et al., 2006a). Removing the "excess" NADH by overexpressing a NADH oxidase in an *arcA* strain eliminated acetate production and resulted in a 120% increase of recombinant protein production (Vemuri et al., 2006b).

References

Aarnikunnas, J. S., A. Pihlajaniemi, A. Palva, M. Leisola and A. Nyyssola. 2006. Cloning and expression of a xylitol 4-dehydrogenase gene from *Pantoea ananatis*. *Appl. Environ. Microbiol.* 72(1): 368-377.

Abdel-Hamid, A. M., M. M. Attwood, and J. R. Guest. 2001. Pyruvate oxidase contributes to the aerobic growth efficiency of *Escherichia coli*. *Microbiology*. 147(6): 1483-1498.

Åkesson, M., E. N. Karlsson, P. Hagander, J. P. Axelsson, and A. Tocaj. 1999. On-line detection of acetate formation in *Escherichia coli* cultures using dissolved oxygen responses to feed transients. *Biotechnol. Bioeng*. 64(5): 590-598.

Albert, R., A. Strätz and G. Vollheim. 1980. Die katalytische Herstellung von Zuckeralkoholen und deren Verwendung. *Chem. Ing. Tech.*. 52(7): 582-587.

Aristidou, A.A., K. Y. San, and G. N. Bennett. 1999. Improvement of biomass yield and recombinant gene expression in *Escherichia coli* by using fructose as the primary carbon source. *Biotechnol. Progr*. 15(1): 140-145.

Arnold, C. N., J. McElhanon, A. Lee, R. Leonhart, and D. A. Siegele. 2001. Global analysis of *Escherichia coli* gene expression during the acetate-induced acid tolerance response. *J. Bacteriol*. *183*(7): 2178-2186.

Avison, M.B., R. E. Horton, T. R. Walsh, and P. M. Bennett. 2001. *Escherichia coli* CreBC is a global regulator of gene expression that responds to growth in minimal media. *J. Biol. Chem*. 276: 26955-26961.

Bauer, K.A., A. R. I. E. Ben-Bassat, M. Dawson, V. T. De La Puente, and J. O. Neway. 1990. Improved expression of human interleukin-2 in high-cell-density fermentor cultures of

Escherichia coli K-12 by a phosphotransacetylase mutant. *Appl. Environ. Microbiol.* 56(5): 1296-1302.

Beerens, K., T. Desmet and W. Soetaert. 2012. Enzymes for the biocatalytic production of rare sugars. *J. Ind. Microbiol. Biotechnol.* 39(6): 823-834.

Berenguer-Murcia, A. and R. Fernandez-Lafuente. 2010. New trends in the recycling of NAD (P) H for the design of sustainable asymmetric reductions catalyzed by dehydrogenases. *Curr. Org. Chem.* 14(10): 1000-1021.

Bhatia, R. and K. C. Calvo. 1996. The sequencing, expression, purification, and steady-state kinetic analysis of quinolinate phosphoribosyl transferase from *Escherichia coli*. *Arch. Biochem. Biophys*. 325(2): 270-278

Bicher, A., K. Ault, A. Kimmelman, D. Gershenson, E. Reed, and B. Liang. 1997. Loss of heterozygosity in human ovarian cancer on chromosome 19q. *Gynecol. Oncol*. 66(1): 36-40.

Blankenhorn, D., J. Phillips, and J. L. Slonczewski. 1999. Acid-and base-induced proteins during aerobic and anaerobic growth of *Escherichia coli* revealed by two-dimensional gel electrophoresis. *J. Bacteriol*. 181(7): 2209-2216.

Bruinenberg, P. M. 1986. The NADP (H) redox couple in yeast metabolism. *A. Van. Leeuw.* 52(5): 411-429.

Bruinenberg, P. M., J. P. Van Dijken, and W. A. Scheffers. 1983. An enzymic analysis of NADPH production and consumption in *Candida utilis*. *J. Gen. Microbiol.* 129(4): 965-971.

Chang, D.E., S. Shin, J. S. Rhee, and J. G. Pan. 1999. Acetate metabolism in a *pta* mutant of *Escherichia coli* w3110: Importance of maintaining acetyl coenzyme a flux for growth and survival. *J. Bacteriol*. 181(21): 6656-6663.

Chang, Y. Y. and J. E. Cronan. 1983. Genetic and biochemical analyses of *Escherichia coli* strains having a mutation in the structural gene (*poxB*) for pyruvate oxidase. *J. Bacteriol*. 154(2): 756-762.

Chang, Y. Y., A. Y. Wang, and J. E. Cronan Jr. 1994. Expression of *Escherichia coli* pyruvate oxidase (*PoxB*) depends on the sigma factor encoded by the rpoS (*katF*) gene. *Mol. Microbiol*. 11(6): 1019-1028.

Cheng, L. F., W. M. Mu, and B. Jiang. 2010a. Thermostable L-arabinose isomerase from *Bacillus stearothermophilus* IAM 11001 for D-tagatose production: gene cloning, purification and characterisation. *J. Sci. Food Agr*. 90(8): 1327-1333.

Cheng, L. F., W. M. Mu, T. Zhang, and B. Jiang. 2010b. An L-arabinose isomerase from *Acidothermus cellulolytics* ATCC 43068: cloning, expression, purification, and characterization. *Appl. Microbiol. Biotechnol*. 86(4): 1089-1097.

Cheng, W. and Roth, J., 1995. Isolation of NAD cycle mutants defective in nicotinamide mononucleotide deamidase in *Salmonella typhimurium*. *J. Bacteriol*. 177(23): 6711-6717.

Delgado, J. and J. C. Liao. 1997. Inverse flux analysis for reduction of acetate excretion in *Escherichia coli*. *Biotechnol. Progr*. 13(4): 361-367.

Dittrich, C. R., R. V. Vadali, G. N. Bennett, and K. Y. San. 2005. Redistribution of metabolic fluxes in the central aerobic metabolic pathway of *E. coli* mutant strains with deletion of the *ackA-pta* and *poxB* pathways for the synthesis of isoamyl acetate. *Biotechnol. Progr*. 21(2): 627-631.

Dondoni, A., A. Marra, and A. Massi. 1997. Carbohydrate homologation by the use of 2-(Trimethylsilyl) thiazole. Preparative scale synthesis of rare sugars: l-Gulose, l-Idose, and the disaccharide subunit of bleomycin A2. *J. Org. Chem.* 62(18): 6261-6267.

Eiteman, M. A. and E. Altman. 2006. Overcoming acetate in *Escherichia coli* recombinant protein fermentations. *Trends Biotechnol*. 24(11): 530-536.

Farmer, W. R. and J. C. Liao 1997. Reduction of aerobic acetate production by *Escherichia coli*. *Appl. Environ. Microbiol*. 63(8): 3205-3210.

Foster, J. W. and A. M. Baskowsky-Foster. 1980. Pyridine nucleotide cycle of *Salmonella typhimurium*: in vivo recycling of nicotinamide adenine dinucleotide. *J. Bacteriol*. 142(3): 1032-1035.

Frick, D. N. and M. J. Bessman. 1995. Cloning, purification, and properties of a novel NADH pyrophosphatase evidence for a nucleotide pyrophosphatase catalytic domain in MutT-like enzymes. *J. Biol. Chem.* 270(4): 1529-1534.

Fuchs, C., D. Köster, S. Wiebusch, K. Mahr, G. Eisbrenner, and H. Märkl. 2002. Scale-up of dialysis fermentation for high cell density cultivation of *Escherichia coli*. *J. Biotechnol*. 93(3): 243-251.

Gokarn, R., J. Evans, J. Walker, S. Martin, M. Eiteman, and E. Altman. 2001. The physiological effects and metabolic alterations caused by the expression of *Rhizobium etli* pyruvate carboxylase in *Escherichia coli*. *Appl. Microbiol. Biotechnol.* 56(1-2): 188-195.

Gokarn, R. R., M. A. Eiteman, and E. Altman. 2000. Metabolic analysis of *Escherichia coli* in the presence and absence of the carboxylating enzymes phosphoenolpyruvate carboxylase and pyruvate carboxylase. *Appl. Environ. Microbiol.* 66(5): 1844-1850.

Goodwin, T. E., K. R. Cousins, H. M. Crane, P. O. Eason, T. E. Freyaldenhoven, C. C. Harmon, B. K. King, C. D. LaRocca, R. L. Lile, and S. G. Orlicek. 1998. Synthesis of two new maytansinoid model compounds from carbohydrate precursors. *J. Carbohyd. Chem.* 17(3): 323-339.

Graber, M., A. Morin, F. Duchiron, and P. F. Monsan. 1988. Microbial polysaccharides containing 6-deoxysugars. *Enzyme Microb. Tech.* 10(4): 198-206.

Granström, T. B., G. Takata, M. Tokuda, and K. Izumori. 2004. Izumoring: a novel and complete strategy for bioproduction of rare sugars. *J Biosci Bioeng.* 97(2): 89-94.

Granström, T. B., K. Izumori, and M. Leisola. 2007. A rare sugar xylitol. Part I: the biochemistry and biosynthesis of xylitol. *Appl. Microbiol. Biotechnol.* 74(2): 277-281.

Grose, J.H., U. Bergthorsson, and J. R. Roth. 2005. Regulation of NAD synthesis by the trifunctional NadR protein of *Salmonella enterica*. *J. Bacteriol*. 187(8): 2774-2782.

Hahm, D.H., J. Pan, and J. S. Rhee. 1994. Characterization and evaluation of a *pta* (phosphotransacetylase) negative mutant of *Escherichia coli* HB101 as production host of foreign lipase. *Appl. Microbiol. Biotechnol*. 42(1): 100-107.

Han, K., J. Hong, and H. C. Lim. 1993. Relieving effects of glycine and methionine from acetic acid inhibition in *Escherichia coli* fermentation. *Biotechnol. Bioeng*. 41(3): 316-324.

Harris, J. M., M. D. Keranen, H. Nguyen, V. G. Young, and G. A. O'Doherty. 2000. Syntheses of four D- and L-hexoses via diastereoselective and enantioselective dihydroxylation reactions. *Carbohydr Res.* 328(1): 17-36.

Heikkilä, H., H. Ojamo, A. Miasnikov, V. Ravanko, and M. Tylli. 2005. Process for the production of xylitol. U.S. Patent 6,911,565.

Heuser, F., K. Schroer, S. Lütz, S. Bringer-Meyer, and H. Sahm. 2007. Enhancement of the NAD (P)(H) pool in *Escherichia coli* for biotransformation. *Eng. Life Sci*. 7(4): 343-353.

Hossain, G.S., J. Li, H. D. Shin, G. Du, L. Liu, and J. Chen. 2014. L-Amino acid oxidases from microbial sources: types, properties, functions, and applications. *Appl. Microbiol. Biotechnol*. 98(4): 1507-1515.

Imsande, J., and A. B. Pardee. 1962. Regulation of pyridine nucleotide biosynthesis in *Escherichia coli*. *J. Biol. Chem*. 237(4): 1305-1308.

Itoh, H. and K. Izumori. 1996. Enzymatic production of L-tagatose and L-fructose from L-sorbose and L-psicose, respectively. *J. Ferment. Bioeng.* 81(4): 351-353.

Itoh, H., T. Sato, T. Takeuchi, A. R. Khan and K. Izumori. 1995. Preparation of D-sorbose from D-tagatose by immobilized D-tagatose 3-epimerase. *J. Ferment. Bioeng.* 79(2): 184-185.

Izumori, K. 2006. Izumoring: a strategy for bioproduction of all hexoses. *J. Biotechnol.* 124(4): 717-722.

Jensen, E.B. and R. Carlsen. 1990. Production of recombinant human growth hormone in *Escherichia coli*: expression of different precursors and physiological effects of glucose, acetate, and salts. *Biotechnol. Bioeng*. 36(1): 1-11.

Jeong, L. S., R. F. Schinazi, J. W. Beach, H. O. Kim, S. Nampalli, K. Shanmuganathan, A. J. Alves, A. McMillan, C. K. Chu, and R. Mathis. 1993. Asymmetric synthesis and biological evaluation of. beta.-L-(2R, 5S)-and. alpha.-L-(2R, 5R)-1, 3-oxathiolane-pyrimidine and-purine nucleosides as potential anti-HIV agents. *J. Med. Chem.* 36(2): 181-195.

Johansson, T., C. Oswald, A. Pedersen, S. Tornroth, M. Okvist, B. G. Karlsson, J. Rydstrom, and U. Krengel. 2005. X-ray structure of domain I of the proton-pumping membrane protein transhydrogenase from *Escherichia coli*. *J. Mol. Biol*. 352: 299-312.

Johnston, W.A., M. Stewart, P. Lee, and M. J. Cooney. 2003. Tracking the acetate threshold using DO-transient control during medium and high cell density cultivation of recombinant *Escherichia coli* in complex media. *Biotechnol. Bioeng*. 84(3): 314-323.

Kim, H. J., S. Y. Kang, J. J. Park and P. Kim. 2011. Novel activity of UDP-galactose-4-epimerase for free monosaccharide and activity improvement by active site-saturation mutagenesis. *Appl Biochem Biotechnol.* 163(3): 444-451.

Koh, B. T., U. Nakashimada, M. Pfeiffer, and M. G. Yap. 1992. Comparison of acetate inhibition on growth of host and recombinant *E. coli* K12 strains. *Biotechnol. Lett*. 14(12): 1115-1118.

Korz, D.J., U. Rinas, K. Hellmuth, E. A. Sanders, and W. D. Deckwer. 1995. Simple fed-batch technique for high cell density cultivation of *Escherichia coli*. *J. Biotechnol*. *39*(1): 59-65.

Kötter, P. and M. Ciriacy. 1993. Xylose fermentation by *Saccharomyces cerevisiae*. *Appl. Microbiol. Biotechnol*. 38(6): 776-783.

Kroger, M., K. Meister and R. Kava. 2006. Low-calorie sweeteners and other sugar substitutes: A review of the safety issues. *Compr. Rev. Food Sci. F*. 5(2): 35-47.

Lau, C., Niere, M. and M. Ziegler. 2009. The NMN/NaMN adenylyltransferase (NMNAT) protein family. *Front Biosci*. 14: 410-431.

Lim, Y. R. and D. K. Oh. 2011. Microbial metabolism and biotechnological production of D-allose. *Appl. Microbiol. Biotechnol.* 91(2): 229-235.

Liu, H. W. and J. S. Thorson. 1994. Pathways and mechanisms in the biogenesis of novel deoxysugars by bacteria. *Annu. Rev. Microbiol.* 48(1): 223-256.

Ma, J., D. Gou, L. Liang, R. Liu, X. Chen, C. Zhang, J. Zhang, K. Chen, and M. Jiang. 2013. Enhancement of succinate production by metabolically engineered *Escherichia coli* with co-expression of nicotinic acid phosphoribosyltransferase and pyruvate carboxylase. *Appl. Microbiol. Biotechnol.* 97(15): 6739-6747.

Ma, T., J. S. Lin, M. G. Newton, Y. C. Cheng and C. K. Chu. 1997. Synthesis and anti-hepatitis B virus activity of 9-(2-deoxy-2-fluoro-beta-L-arabinofuranosyl) purine nucleosides. *J. Med. Chem.* 40(17): 2750-2754.

Majewski, R. A. and M. M. Domach. 1990. Simple constrained-optimization view of acetate overflow in *E. coli*. *Biotechnol. Bioeng*. 35(7): 732-738.

March, J. C., M. A. Eiteman, and E. Altman. 2002. Expression of an anaplerotic enzyme, pyruvate carboxylase, improves recombinant protein production in *Escherichia coli*. *Appl. Microbiol. Biotechnol*. 68(11): 5620-5624.

Mathé, C. and G. Gosselin. 2006. L-Nucleoside enantiomers as antivirals drugs: a mini-review. *Antiviral research.* 71(2): 276-281.

Moran, E. J., J. E. Tellew, Z. Zhao and R. W. Armstrong. 1993. Dehydroamino acid derivatives from D-arabinose and L-serine: Synthesis of models for the azinomycin antitumor antibiotics. *J. Org. Chem.*. 58(27): 7848-7859.

Nakano, K., M. Rischke, S. Sato, and H. Märkl. 1997. Influence of acetic acid on the growth of *Escherichia coli* K12 during high-cell-density cultivation in a dialysis reactor. *Appl. Microbiol. Biotechnol*. 48(5): 597-601.

O'Handley, S. F., D. N. Frick, C. A. Dunn, and M. J. Bessman. 1998. Orf186 represents a new member of the Nudix hydrolases, active on adenosine (5′) triphospho (5′) adenosine, ADP-ribose, and NADH. *J. Biol. Chem*. 273(6): 3192-3197.

Paalme, T., R. Elken, A. Kahru, K. Vanatalu, and R. Vilu. 1997. The growth rate control in *Escherichia coli* at near to maximum growth rates: the A-stat approach. *A. Van Leeuwe. J. Microb*. 71(3): 217-230.

Penfound, T. and J. W. Foster. 1996. Biosynthesis and recycling of NAD. *Escherichia coli and Salmonella: cellular and molecular biology. ASM Press, Washington, DC*: 721-730.

Penfound, T. and J. W. Foster. 1999. NAD-dependent DNA-binding activity of the bifunctional NadR regulator of *Salmonella typhimurium*. *J. Bacteriol*. 181(2): 648-655.

Picon, A., M. J. Teixeira de Mattos, and P. W. Postma. 2005. Reducing the glucose uptake rate in *Escherichia coli* affects growth rate but not protein production. *Biotechnol. Bioeng.* 90(2): 191-200.

Ponce, E. 1999. Effect of growth rate reduction and genetic modifications on acetate accumulation and biomass yields in *Escherichia coli*. *J. Biosci. Bioeng*. 87(6): 775-780.

Poonperm, W., G. Takata, H. Okada, K. Morimoto, T. B. Granstrom, and K. Izumori. 2007. Cloning, sequencing, overexpression and characterization of L-rhamnose isomerase from *Bacillus pallidus* Y25 for rare sugar production. *Appl. Microbiol. Biotechnol.* 76(6): 1297-1307.

Prabhu, P., M. K. Tiwari, M. Jeya, P. Gunasekaran, I. W. Kim, and J. K. Lee. 2008. Cloning and characterization of a novel L-arabinose isomerase from *Bacillus licheniformis*. *Appl. Microbiol. Biotechnol.* 81(2): 283-290.

Raffaelli, N., T. Lorenzi, P. L. Mariani, M. Emanuelli, A. Amici, S. Ruggieri, and G. Magni. 1999. The *Escherichia coli* NadR regulator is endowed with nicotinamide mononucleotide adenylyltransferase activity. *J. Bacteriol*. 181(17): 5509-5511.

Reed, J. L., T. D. Vo, C. H. Schilling, and B. O. Palsson. 2003. An expanded genome-scale model of *Escherichia coli* K-12 (i JR904 GSM/GPR). *Genome Biol.* 4(9): R54.

Rose, I. A., M. Grunberg-Manago, S. R. Korey, and S. Ochoa. 1954. Enzymatic phosphorylation of acetate. *J. Biol. Chem.* 211:737–756.

Salas, J. 1999. Genes and enzymes involved in deoxysugar biosynthesis in bacteria. *Nat. Prod. Rep.* 16(3): 283-299.

Samuel, J. and M. E. Tanner. 2002. Mechanistic aspects of enzymatic carbohydrate epimerization. *Nat. Prod. Rep.* 19(3): 261-277.

San, K.Y., G. N. Bennett, S. J. Berríos-Rivera, R. V. Vadali, Y. T. Yang, E. Horton, F. B. Rudolph, B. Sariyar, and K. Blackwood. 2002. Metabolic engineering through cofactor manipulation and its effects on metabolic flux redistribution in *Escherichia coli*. *Metab. Eng*. 4(2): 182-192.

Saunders, A.H., A. E. Griffiths, K. H. Lee, R. M. Cicchillo, L. Tu, J. A. Stromberg, C. Krebs, and S. J. Booker. 2008. Characterization of quinolinate synthases from *Escherichia coli*, *Mycobacterium tuberculosis*, and *Pyrococcus horikoshii* indicates that [4Fe-4S] clusters are common cofactors throughout this class of enzymes. *Biochemistry*. 47(41): 10999-11012.

Savage, P. B., L. Teyton, and A. Bendelac. 2006. Glycolipids for natural killer T cells. *Chem. Soc. Rev.* 35(9): 771-779.

Shen, Y. L., Y. Zhang, A. Y. Sun, X. X. Xia, D. Z. Wei, and S. L. Yang. 2004. High-level production of soluble tumor necrosis factor-related apoptosis-inducing ligand (Apo2L/TRAIL) in high-density cultivation of recombinant *Escherichia coli* using a combined feeding strategy. *Biotechnol. Lett*. 26(12): 981-984.

Spencer, R. L. and J. Preiss. 1967. Biosynthesis of diphosphopyridine, Nucleotide the purification and the properties of diphosphopyridine nucleotide synthetase from *Escherichia coli* B. *J. Biol. Chem*. 242(3): 385-392.

Steinsiek, S., S. Stagge, and K. Bettenbrock. 2014. Analysis of *Escherichia coli* mutants with a linear respiratory chain. *PloS One*. 9(1): e87307.

Takata, G., W. Poonperm, K. Morimoto and K. Izumori. 2010. Cloning and overexpression of the xylitol dehydrogenase gene from *Bacillus pallidus* and its application to L-xylulose production. *Biosci. Biotechnol. Biochem*. 74(9): 1807-1813.

Takeshita, K., A. Suga, G. Takada, and K. Izumori. 2000a. Mass production of D-psicose from D-fructose by a continuous bioreactor system using immobilized D-tagatose 3-epimerase. *J. Biosci. Bioeng.* 90(4): 453-455.

Takeshita, K., Y. Ishida, G. Takada, and K. Izumori. 2000b. Direct production of allitol from D-fructose by a coupling reaction using D-tagatose 3-epimerase, ribitol dehydrogenase and formate dehydrogenase. *J. Biosci. Bioeng.* 90(5): 545-548.

Vemuri, G. N., E. Altman, D. P. Sangurdekar, A. B. Khodursky, and M. A. Eiteman. 2006a. Overflow metabolism in *Escherichia coli* during steady-state growth: transcriptional regulation and effect of the redox ratio. *Appl. Microbiol. Biotechnol.* 72(5): 3653-3661.

Vemuri, G. N., M. A. Eiteman, and E. Altman. 2006b. Increased recombinant protein production in *Escherichia coli* strains with overexpressed water-forming NADH oxidase and a deleted ArcA regulatory protein. *Biotechnol. Bioeng*. 94(3): 538-542.

Vidal, L., P. Ferrer, G. Alvaro, M. D. Benaiges, and G. Caminal. 2005. Influence of induction and operation mode on recombinant rhamnulose 1-phosphate aldolase production by *Escherichia coli* using the T5 promoter. *J. Biotechnol*. 118(1): 75-87.

Wang, L., Y. J. Zhou, D. Ji, X. Lin, Y. Liu, Y. Zhang, W. Liu, and Z. K. Zhao. 2014. Identification of UshA as a major enzyme for NAD degradation in *Escherichia coli*. *Enzyme .Microb. Technol.* 58: 75-79.

Wilson, P.W. 1938. Respiratory enzyme systmes in symbiotic nitrogen fixation I: The "Resting Cell" Technique as a Method for Study of Bacterial Metabolism. *J. Bacteriol*. 35(6): 601.

Woodyer, R. D., N. J. Wymer, F. M. Racine, S. N. Khan, and B. C. Saha. 2008. Efficient production of L-ribose with a recombinant *Escherichia coli* biocatalyst. *Appl. Microbiol. Biotechnol.* 74(10): 2967-2975.

Woodyer, R. D., T. N. Christ, and K. A. Deweese. 2010. Single-step bioconversion for the preparation of L-gulose and L-galactose. *Carbohydr. Res.* 345(3): 363-368.

Wubbolts, M. G., P. Terpstra, J. B. van Beilen, J. Kingma, H. A. Meesters, and B. Witholt. 1990. Variation of cofactor levels in *Escherichia coli*. Sequence analysis and expression of the *pncB* gene encoding nicotinic acid phosphoribosyltransferase. *J. Biol. Chem*. 265(29): 17665-17672.

Yoon, R. Y., S. J. Yeom, C. S. Park, and D. K. Oh. 2009. Substrate specificity of a glucose-6-phosphate isomerase from *Pyrococcus furiosus* for monosaccharides. *Appl. Microbiol. Biotechnol.* 83(2): 295-303.

Zhang, J. and M. Inouye. 2002. MazG, a nucleoside triphosphate pyrophosphohydrolase, interacts with Era, an essential GTPase in *Escherichia coli*. *J. Bacteriol*. 184(19): 5323-5329

Zhou, Y. J., W. Yang, L. Wang, Z. Zhu, S. Zhang, and Z. K. Zhao. 2013. Engineering NAD^+ availability for *Escherichia coli* whole-cell biocatalysis: a case study for dihydroxyacetone production. *Microb. Cell Fact.* 12(1): 103.

CHAPTER 3

COUPLING XYLITOL DEHYDROGENASE WITH NADH OXIDASE IMPROVE L-XYLULOSE PRODUCTION IN *ESCHERICHIA COLI* CULTURE[1]

[1] Han, Q. and M.A. Eiteman. 2017. *Enzyme and Microbial Technology*. 106, 106-113.

Reprinted here with permission of publisher.

Abstract

Escherichia coli expressing NAD^+-dependent xylitol 4-dehydrogenase (XDH) from *Pantoea ananatis* and growing on glucose or glycerol converts xylitol to the rare sugar L-xylulose. Although blocking potential L-xylulose consumption (L-xylulosekinase, *lyxK*) or co-expression of the glycerol facilitator (GlpF) did not significantly affect L-xylulose formation, co-expressing XDH with water-forming NADH oxidase (NOX) from *Streptococcus pneumoniae* increased L-xylulose formation in shake flasks when glycerol was the carbon source. Controlled batch processes at the 1 liter scale demonstrated that the final equilibrium L-xylulose/xylitol ratio was correlated to the intracellular NAD^+/NADH ratio, with 69% conversion of xylitol to L-xylulose and a yield of 0.88 g L-xylulose/g xylitol attained for MG1655/pZE12-*xdh*/pCS27-*nox* growing on glycerol. Intermittently feeding carbon source was ineffective at increasing the final L-xylulose concentration because introduction of carbon source was accompanied by a reduction in NAD^+/NADH ratio. A batch process using 12 g/L glycerol and 22 g/L xylitol generated over 14 g/L L-xylulose after 80 h, corresponding to 65% conversion and a yield of 0.89 g L-xylulose/g xylitol consumed.

Introduction

Rare sugars are pentoses, hexoes and their derivatives that are found in the low abundance in nature (Granström et al., 2004). Interest in rare sugars has recently increased because of their potential applications in pharmaceutical and food industries including antiviral drugs (Jeong et al., 1993; Ma et al., 1997; Mathé and Gosselin, 2006), anti-cancer or tumor treatments (Moran et al. 1993), drug building blocks (Goodwin et al., 1998), and as low-calorie sweeteners (Kroger et al., 2006). L-xylulose is a rare ketopentose which inhibits yeast α-glucosidase (Muniruzzaman et al., 1996) and is an indicator of hepatitis or liver cirrhosis (Hiroshi et al., 1976). This pentose is also a precursor of other rare sugars such as L-xylose or L-lyxose (Bhuiyan et al., 1998; Jokela et al., 2002). The more readily available, less expensive, and structurally similar sugar alcohol xylitol can serve as an ideal substrate for L-xylulose. Further investigation demonstrated that the NAD^+-dependent xylitol 4-dehydrogenase (XDH) from *Pantoea ananatis*, *Alcaligenes* sp., or *Bacillus pallidus* were able to catalyze xylitol to generate L-xylulose (Doten et al., 1985; Khan et al., 1991; Aarnikunnas et al., 2006; Poonperm et al., 2007):

$$\text{xylitol} + NAD^+ \rightarrow \text{L-xylulose} + NADH + H^+ \quad (1)$$

For the production of oxidized biochemicals using oxidoreductases such as XDH, an approach is using the purified enzymes to mediate the conversion, whereas requires the supply of expensive cofactors (e.g., NAD^+ or $NADP^+$) as cosubstrates has discouraged this strategy (Berenguer and Fernandez, 2010). Instead, a growing cell are able to syntheses those cofactor during the growth and essentially allow the system to recycle cofactors. A growing cell approach involves cultivating the whole cell in a growth medium which contains xylitol and therefore allows for the conversion of xylitol into L-xylulose during growth on another carbon source.

The conversion of xylitol to L-xylulose has been achieved using *Escherichia coli* expressing XDH from these *P. ananatis, Alcaligenes sp.* and *B. pallidus* (Khan et al., 1991; Aarnikunnas et al., 2006; Takata et al., 2010). The greatest conversion (defined as L-xylulose generated per mass xylitol initially supplied) of 82% was achieved using *P. ananatis* XDH with 5 g/L xylitol (Aarnikunnas et al., 2006).

Both enzymatic and microbial processes require a driving force for the conversion. Because the specific conversion of L-xylulose from xylitol involves the formation of NADH, the continued presence of NAD^+ by NADH oxidation is necessary to drive the desired conversion. Multiple means can accomplish the cofactor regeneration including delivery of an oxidizing agent (such as O_2), using more oxidized substrates, promoting pathways which generate less NADH or by direct enzyme oxidization. In growing cells, metabolic processes continually turn over NADH/NAD^+, and strategies which favor elevated oxidation of NADH would seem likely to enhance L-xylulose formation.

In this study, we have expressed the *xdh* gene from *P. ananatis* and the *nox* gene coding water-forming NADH oxidase (NOX) from *Streptococcus pneumoniae* (Vemuri et al., 2006a) to study the effect of NADH regeneration on L-xylulose production in cells growing on glucose or glycerol in shake flasks and controlled batch processes.

Materials and Methods

Strains

Escherichia coli MG1655 was used in this study (Table 1-1). The *lyxK* coding L-xylulokinase was knocked out resulting in strain MEC342 by transducing MG1655 with the corresponding Keio (FRT)Kan deletion (Baba et al., 2006). In knockout strains, forward primers

external to the target gene and reverse primers within the kanamycin resistance cassette were used to check for proper chromosomal integration.

Plasmids Construction

The *xdh* gene from *P. ananatis* (ATCC 43072) expressing NAD^+-dependent xylitol 4-dehydrogenase (Aarnikunnas et al., 2006) was synthesized by GenScript (Piscataway, USA) as a codon optimized gene for *E. coli*. Glycerol facilitator gene (*glpF*) from MG1655 and NADH oxidase gene (*nox*) from *Streptococcus pneumoniae* were PCR-amplified using MG1655 genome and pTrc99A-*nox* (Vemuri et al., 2006a) respectively as the template. Using various primers, PCR products were gel-isolated, restriction enzyme digested, and ligated into pZE12-*luc* (Lutz et al., 1997) or pCS27 (Shen and Liao, 2008) to yield the plasmids listed in Table 1-1. These plasmids, pZE12-*xdh* pZE12-*xdh-glpF*, pCS27-*glpF* and pCS27-*nox*, were transformed into selected strains by electroporation.

Growth Medium

The defined medium for shake flask experiments contained (per L): 13.3 g KH_2PO_4, 4.0 g $(NH_4)_2HPO_4$, 1.2 g $MgSO_4 \cdot 7H_2O$, 13.0 mg $Zn(CH_3COO)_2 \cdot 2H_2O$, 1.5 mg $CuCl_2 \cdot 2H_2O$, 15.0 mg $MnCl_2 \cdot 4H_2O$, 2.5 mg $CoCl_2 \cdot 6H_2O$, 3.0 mg H_3BO_3, 2.5 mg $Na_2MoO_4 \cdot 2H_2O$, 100 mg Fe(III) citrate, 8.4 mg $Na_2EDTA \cdot 2H_2O$, 1.7 g citric acid, and 4.5 mg thiamine·HCl. The defined medium for all modes of operation in a controlled bioreactor contained (per L): 1.8 g KH_2PO_4, 3.175 g $K_2HPO_4 \cdot 3H_2O$, 2.5 g K_2SO_4, 4.38 g NH_4Cl, 25.0 mg $Na_2(EDTA) \cdot 2H_2O$, 0.15 g $MgSO_4 \cdot 7H_2O$, 20 mg citric acid, 0.25 mg $ZnSO_4 \cdot 7H_2O$, 0.125 mg $CuCl_2 \cdot 2H_2O$, 1.25 mg $MnSO_4 \cdot H_2O$, 0.875 mg $CoCl_2 \cdot 6H_2O$, 0.06 mg H_3BO_3, 0.25 mg $Na_2MoO_4 \cdot 2H_2O$, 5.5 mg $FeSO_4 \cdot 7H_2O$, and 20 mg thiamine·HCl. The medium was adjusted to a pH of 7.0 with 30%

(w/v) NaOH. Either medium contained 50 mg ampicillin/L or 100 mg kanamycin/L as appropriate to the strain.

Fermentation

Growth in shake flasks was accomplished by first inoculating from plate culture a strain into 3 mL Lysogeny Broth (LB) and grown overnight at 37°C. Then, 1 mL culture was used to inoculate 50 mL defined medium containing 5 g/L xylitol and 5 g/L carbon source (glucose or glycerol) in 250 mL baffled shake flasks maintained at 37°C with an agitation of 250 rpm. Triplicate shake flask cultures were induced at the time of inoculation with 0.5 mM IPTG, and sampled at 48 h for measurement of xylitol, L-xylulose, and the activities of XDH and NOX.

For duplicate batch or intermittent fed-batch fermentations, shake flask cultures as described above which attained an OD of 3 were used to inoculate a 2.5 L bioreactor (Bioflo 2000, New Brunswick Scientific Co., Edison, NJ) containing 1 L of defined medium with 5 g/L xylitol and 10 g/L glucose or glycerol. Cultures were induced at 2 h with 0.5 mM IPTG. The agitation was maintained at 500 rpm, and air flow rate was controlled at 1.0 L/min to ensure a dissolved oxygen concentration above 40% of saturation. The pH was maintained at 7.0 with 30% (w/v) NH_4OH, and the temperature was 37°C. For intermittent fed-batch cultures, an additional 2 g of the same carbon source in about 2 mL DI water was added to the medium every 5-6 h after cell growth had first plateaued.

Mass yield of L-xylulose is the quantity of L-xylulose formed divided by the amount of xylitol consumed (g/g). Conversion is the mass of L-xylulose formed divided by the mass of xylitol initially supplied (g/g). Xylitol was never completely converted to L-xylulose, and the conversion of xylitol is also equal to the fraction of xylitol consumed multiplied by the yield.

We also calculated an equilibrium ratio "R" which is the final L-xylulose formed divided by the xylitol remaining (g/g).

Quantification of NAD^+ and NADH

NAD^+ or NADH extraction was prepared by lysing cells with acid or base in 50°C water bath. Two 1 mL aliquots from the batch culture were centrifuged (20,000×g for 1 min), and the centrifugates separately resuspended in 250 μL 0.2 M HCl (for NAD^+) or 250 μL 0.2 M NaOH (for NADH). The cofactors were extracted from cells in a 50°C water bath for 10 minutes. After cooling in an ice bath, 250 μL of 0.1 M NaOH (for NAD^+) or 250 μL 0.1 M HCl (for NADH) was added to neutralize the lysates. The cell-free extracts were then centrifuged (20,000×g for 5 min), and the supernatants were used to determine the concentration of NAD^+ or NADH.

The intracellular concentration of NAD^+ and NADH was measured by the enzymatic cycling assay (Bernofsky and Swan, 1973). The reaction mixture contained 1.0 M Bicine buffer (pH 8.0 adjusted with 20% NaOH), 40 mM EDTA (pH 8.0 adjusted with 20% NaOH), 16.6 mM phenanzinium ethylsulfate (PES), 4.2 mM thiazolyl blue tetrazolium bromide (MTT), absolute ethanol, and 500 U/mL alcohol dehydrogenase (EC 1.1.1.1, Sigma-Aldrich C., St. Louis, MO, Cat.A7011). NAD^+ or NADH transfers the reducing equivalents from ethanol ultimately to MTT. By measuring the reduced MTT at 570 nm, the rate of MTT reduction was proportional to the concentration of NAD^+ or NADH.

Enzyme Activity

Enzyme activities were measured from 10 mL of culture which had been centrifuged (5,000×g for 5 min at 4°C) and washed three times before resuspending in 5 mM phosphate buffer (pH 7.0). Cell-free extracts were prepared by lysing cells with 0.1 mm glass beads (BioSpec Products, Inc., Bartlesville, OK, USA), and centrifuging (11,000×g for 10 min at 4°C).

The cell-free extract was used to determine XDH (Aarnikunnas et al. 2006) and NOX (Vemuri et al. 2006b) activities. Briefly for the XDH assay, the reaction mixture contained 50 mM Tris/glycine buffer (pH 7.0 adjusted with 20% NaOH), 500 mM xylitol, 1 mM NAD^+, and 10 mM $MgCl_2$. One unit of XDH activity was defined as the amount of enzyme to generate 1.0 μmol of NADH per min. For the NOX assay, the reaction mixture contained 125 mM phosphate buffer (pH 7.0), 2.9 mM NADH, and 5 mM dipotassium EDTA. One unit of NOX activity was defined as the amount of enzyme to consume 1.0 μmol of NADH per min. Total protein concentrations (Pierce BCA protein assay kit, Pierce Biotech, Inc.) were used to calculate specific activity using albumin as the protein standard.

Results

Comparison of L-xylulose formation in various strains and carbon sources

In order to compare the effect of different carbon sources on the cell growth and L-xylulose formation from xylitol, we firstly grew MG1655/pZE12-*xdh* in triplicate in 50 mL defined medium with 5 g/L glucose or 5 g/L glycerol. The specific growth rate and specific activity of XDH was found greater using glucose as the sole carbon source (0.50 h^{-1}, 5.3 U/mg) when compared to using glycerol (0.34 h^{-1}, 1.1 U/mg) (Table 1-2). However, the final concentration of L-xylulose was observed greater when glycerol was the carbon source (approx. 2.5 g/L versus 1.8 g/L). Although the yield based on xylitol consumed was greater for glucose (0.87 g/g) than for glycerol (0.77 g/g), the conversion of xylitol to L-xylulose (Fig. 2-1) was greater for glycerol (0.44 g/g) than for glucose (0.31 g/g).

Substrate transportation and product metabolism are two major concerns when utilize *E. coli* for the whole-cell generation of L-xylulose. The wild-type *E. coli* can not utilize xylitol as

the carbon source but a membrane channel , glycerol facilitator protein (GlpF), was reported to aid xylitol transport (Heller et al., 1980). To demonstrate whether GlpF affects L-xylulose conversion, we overexpressed XDH and GlpF with two genes expressed in a single plasmid (MG1655/pZE12-*xdh*-*glpF*) or in the separated plasmids (MG1655/pZE12-*xdh*/pCS27-*glpF*) and compared the L-xylulose formation. Either growing on glucose or glycerol, the strain with overexpression of GlpF showed only a modest benefit to L-xylulose conversion or yield (Fig. 2-1). On the other hand, the yield of L-xylulose observed in MG1655/pZE12-*xdh* was less than the maximum theoretical yield (0.99 g/g). L-xylulokinase encoded by *lyxK* gene has been reported to convert L-xylulose to L-xylulose-5P, which can be further utilized by the central metabolism (Di Luccio et al., 2007). To examine whether this enzyme impact the final L-xylulose conversion, we constructed MEC342 with *lyxK* gene knockout and transformed it with pZE12-*xdh* to further compare the bioconversion of L-xylulose from xylitol. As shown in Fig. 2-1, MEC342 did not lead to a significant change in L-xylulose formation compared to the wildtype.

The conversion of xylitol to L-xylulose by XDH involves in NAD^+ formation and NADH generation. We hypothesized the inefficient regeneration of NAD^+ from NADH may limit the L-xylulose formation. In order to overcome the limitation of NADH oxidation and make more NAD^+ available for the desire conversion, we overexpressed *nox* coding a water-forming NADH oxidase (NOX) and transformed MG1655 with pZE12-*xdh* and pCS27-*nox*. During growth on glucose, MG1655 pZE12-*xdh*/pCS27-*nox* had no effect on the conversion of L-xylulose. Surprisingly, a significant increase of L-xylulose formation was occurred for cells grown on glycerol (Fig. 2-1). The yield of L-xylulose from xylitol was also greater within the expression of NOX both on glucose (0.89 g/g) and glycerol (0.84 g/g).

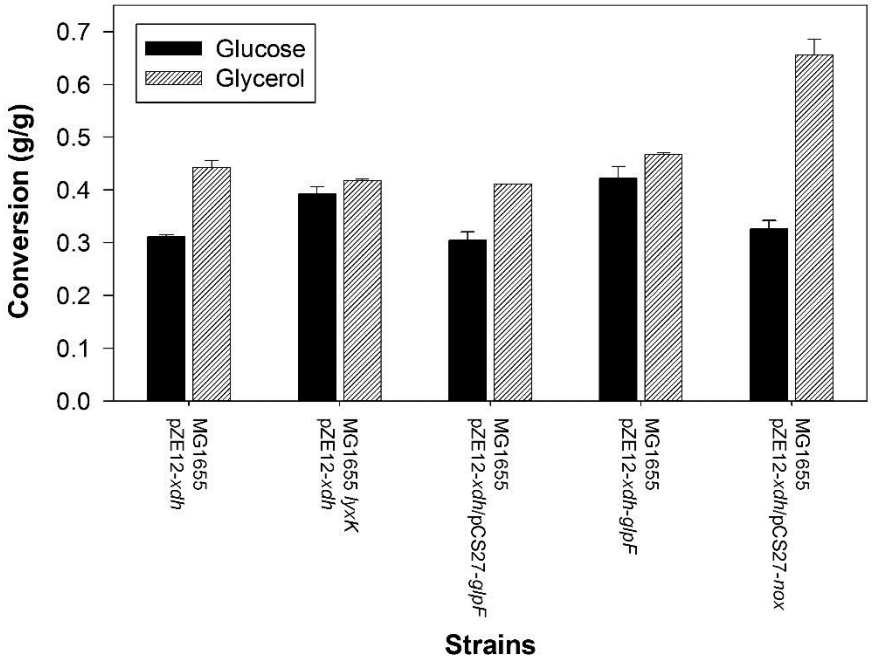

Figure 2-1. Comparison of *E. coli* strains for the conversion of 5 g/L xylitol to L-xylulose after 48 h in shake flask cultures using either 5 g/L glucose or 5 g/L glycerol as carbon/energy source. Conversion is the mass of L-xylulose generated divided by the initial mass of xylitol provided. Error bars indicate standard deviation. See Table 1-1 for more information about the strains.

L-xylulose production in the controlled batch processes

The comparison of various strains during the shake flask experiments found the greatest L-xylulose formation observed in the strain with overexpression of both XDH and NOX during growth on glycerol. However, shake flask experiments used in the relatively fast growing cultures might led to inconstant results due to the limited control over environmental conditions, such as pH and oxygenation. Therefore, we utilized the controlled batch studies at the 1 liter scale to exam the production of L-xylulose. All batches were completed in duplicate with 5 g/L xylitol and 10 g/L glycerol or 10 g/L glucose using MG1655/pZE12-*xdh* and MG1655/pZE12-*xdh*/pCS27-*nox*.

Using glucose as the carbon source, MG1655/pZE12-*xdh* converted 66% of the xylitol to L-xylulose with a yield of 0.89 g L-xylulose/g xylitol (Fig. 2-2). For MG1655/pZE12-*xdh*/pCS27-*nox*, about 53% of the xylitol was converted to L-xylulose with a yield of 0.82 g L-xylulose/g xylitol (Fig. 2-3). Both strain cultures found the concentrations of L-xylulose and xylitol ultimately reached an equilibrium. A significant difference between these two strains is the equilibrium ratio R of L-xylulose formed divided by xylitol remaining: the ratio R in MG1655/pZE12-*xdh* was 2.41 (±0.52) g L-xylulose/g xylitol), while the value of R in MG1655/pZE12-*xdh*/pCS27-*nox* was 1.42 (±0.09) g/g.

Using glycerol as the carbon source, 70% of the xylitol was converted to L-xylulose in MG1655/pZE12-*xdh* with a yield of 0.90 g L-xylulose/g xylitol (Fig. 2-4). MG1655/pZE12-*xdh*/pCS27-*nox* converted 69% of the xylitol to L-xylulose with a yield of 0.88 g L-xylulose/g xylitol (Fig. 2-5). Similar as growing glucose, the glycerol-grown cells also found the final L-xylulose and xylitol concentrations approach an equilibrium but resulted in greater values of R: 3.03 (±0.15) g/g or 3.22 (±0.06) g/g, respectively, for MG1655/pZE12-*xdh* and MG1655/pZE12-

xdh/pCS27-*nox*. The L-xylulose formation during growth on glycerol led to a higher final L-xylulose to xylitol ratio than growth on glucose.

As the equation 1 shown, continuous supply of NAD^+ can provide the driving force for more L-xylulose formation. Therefore, we also measured the intracellular concentrations of NAD^+ and NADH during each of the four sets of batch studies. At the time of carbon source depletion, MG1655/pZE12-*xdh* attained the total NAD(H) concentration in about 8.5 μmol/g DCW (glucose) and 7.5 μmol/g DCW (glycerol) (Fig. 2-2 & 2-4). The concentration of cofactors in MG1655/pZE12-*xdh*/pCS27-*nox* were less than 6.0 μmol/g DCW at the time of either glucose or glycerol exhaustion (Fig. 2-3 & 2-5).

In addition to measure the intracellular NAD(H) concentrations, we also compared the NAD^+/NADH ratio among the four bath processes (Fig. 2-6). When the carbon source was still present in the cell cultures, the NAD^+/NADH ratios were low (1.0-3.0). After the carbon source was depleted, this redox ratios were increased. The growth of MG1655/pZE12-*xdh*/pCS27-*nox* on glycerol obtained the highest NAD^+/NADH ratio in a range of 5.0-6.2. A further comparison of the final NAD^+/NADH with the final equilibrium ratio (L-xylulose/xylitol) found there is a strong correlation between these two ratios that the greater values of NAD^+/NADH led to greater equilibrium ratios (Fig. 2-7). Interestingly, the carbon source utilized by the strain overexpressing NADH oxidase had the different effect on NAD^+/NADH ratio and equilibrium ratio of L-xylulose/xylitol: cells growing on glucose reduced the NAD^+/NADH ratio and the equilibrium ratio, while cells growing on glucose increased both ratios.

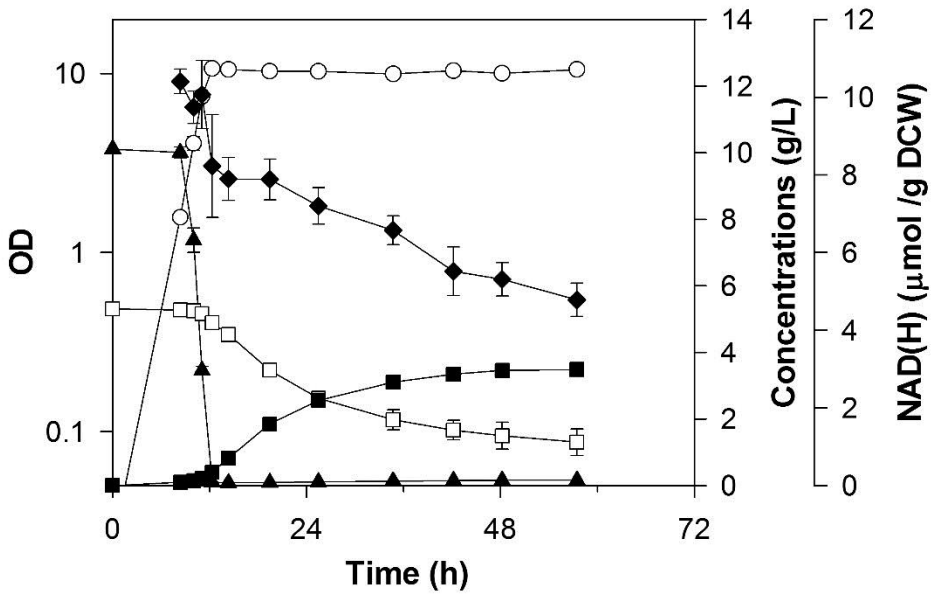

Figure 2-2. L-xylulose formation from 5 g/L xylitol during batch growth of MG1655/pZE12-*xdh* on glucose: OD (○); glucose (▲); xylitol (□); L-xylulose (■); Total NAD(H) (◆).

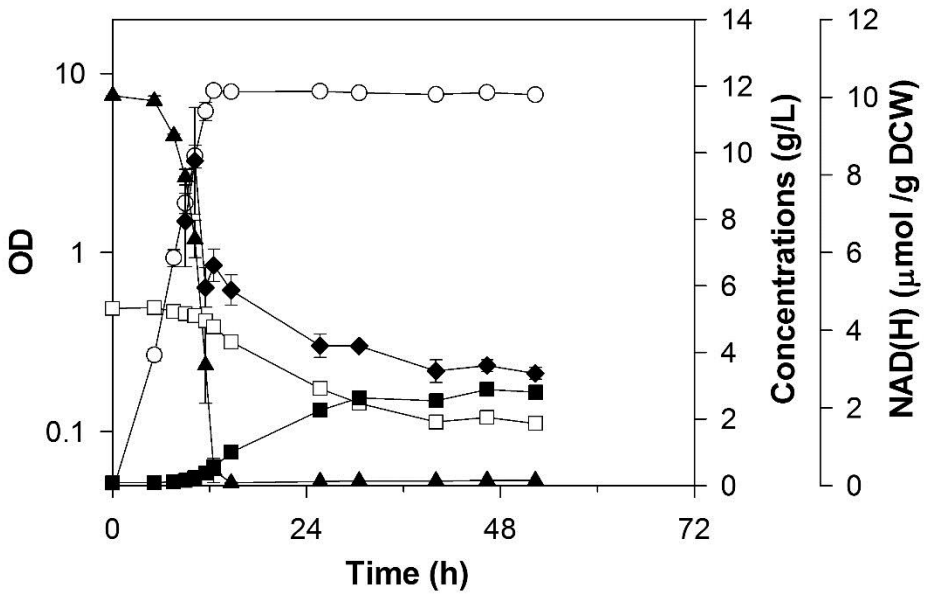

Figure 2-3. L-xylulose formation from 5 g/L xylitol during batch growth of MG1655/pZE12-*xdh*/pCS27-*nox* on glucose: OD (○); glucose (▲); xylitol (□); L-xylulose (■); Total NAD(H) (◆).

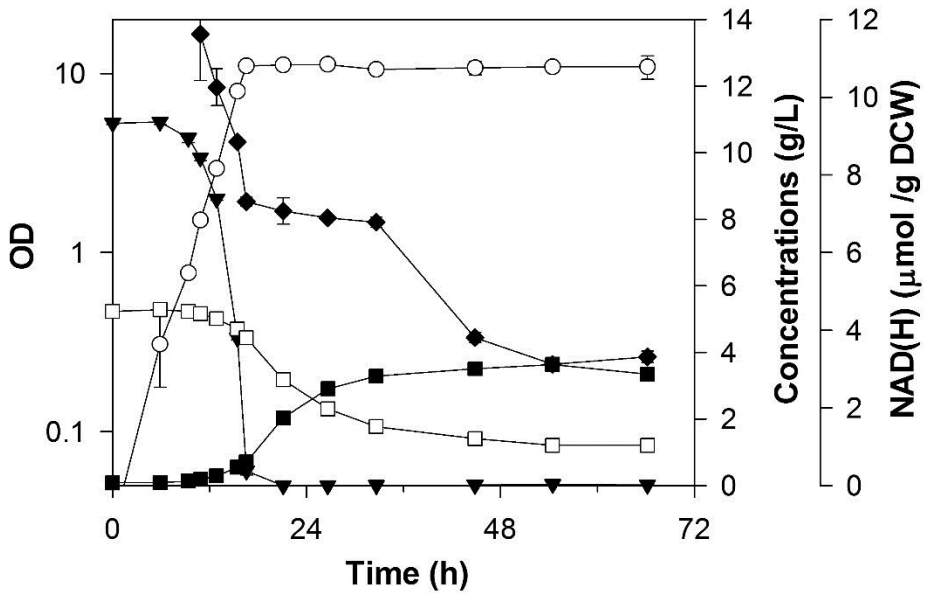

Figure 2-4. L-xylulose formation from 5 g/L xylitol during batch growth of MG1655/pZE12-*xdh* on glycerol: OD (○); glycerol (▼); xylitol (□); L-xylulose (■); Total NAD(H) (◆).

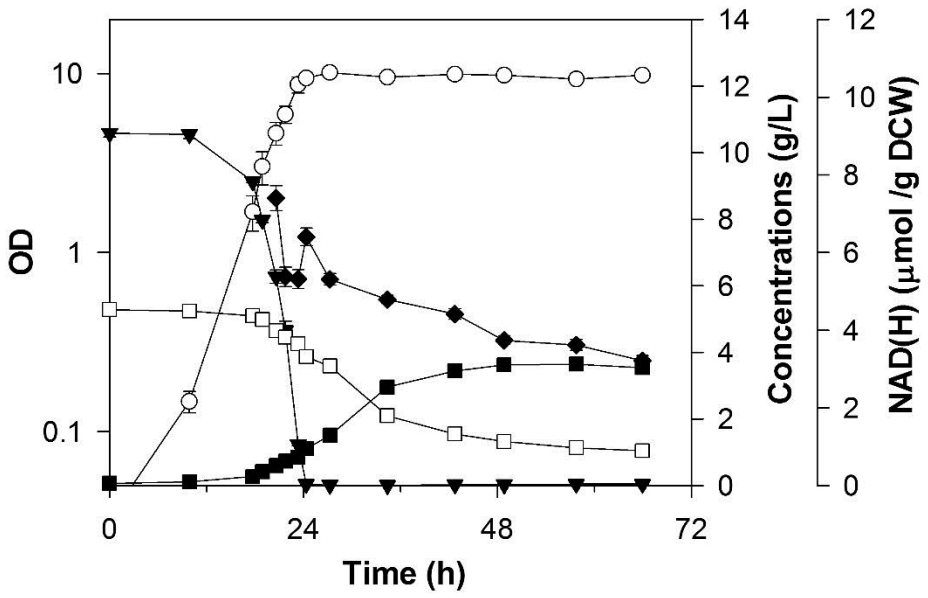

Figure 2-5. L-xylulose formation from 5 g/L xylitol during batch growth of MG1655/pZE12-*xdh*/pCS27-*nox* on glycerol: OD (○); glycerol (▼); xylitol (□); L-xylulose (■); Total NAD(H) (◆).

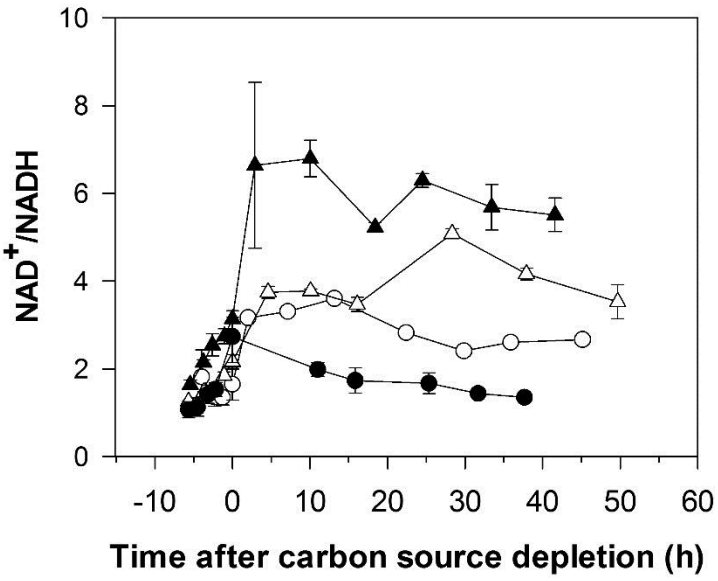

Figure 2-6. The NAD^+/NADH ratio in *E. coli* growing on glucose or glycerol: MG1655/pZE12-*xdh* on glucose (○); MG1655/pZE12-*xdh* on glycerol (△); MG1655/pZE12-*xdh*/pCS27-*nox* on glucose (●); MG1655/pZE12-*xdh*/pCS27-*nox* on glycerol (▲). The time is normalized for each substrate to the approximate time after the carbon/energy source was depleted.

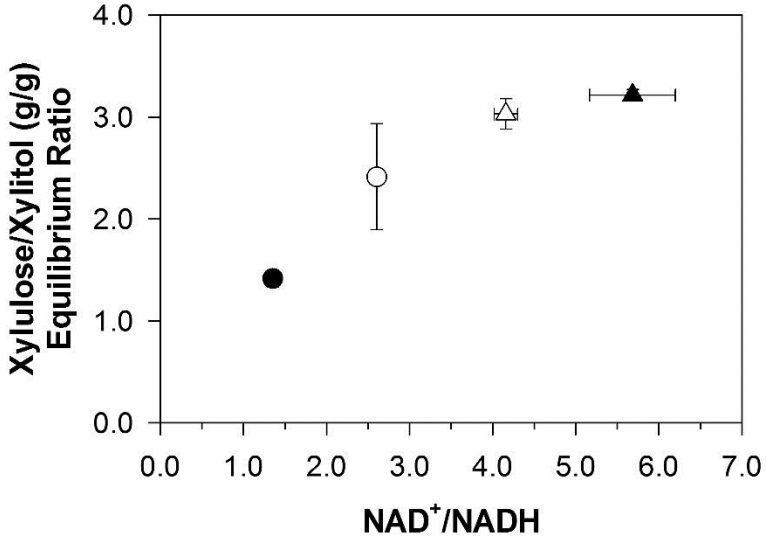

Figure 2-7. Relationship between NAD^+/NADH and the equilibrium ratio R of L-xylulose/xylitol (g/g) in *E. coli* growing on glucose or glycerol: MG1655/pZE12-*xdh* on glucose (○); MG1655/pZE12-*xdh* on glycerol (△); MG1655/pZE12-*xdh*/pCS27-*nox* on glucose (●); MG1655/pZE12-*xdh*/pCS27-*nox* on glycerol (▲).

Intermittent Fed-Batch Processes for L-xylulose production

From the controlled batch process, the formation of L-xylulose dramatically increased when the carbon sources were low, and this quick formation further continued after the carbon sources were exhausted. It's suspected that reintroducing the carbon source after its initial depletion could prolong the L-xylulose formation. We therefore completed the intermittent fed-batch by adding an additional 2 g carbon source (glucose or glycerol) three times into the 1 liter bioreactor at 5-6 h intervals after its initial depletion. MG1655/pZE12-*xdh* and MG1655/pZE12-*xdh*/pCS27-*nox* were tested respectively using glucose or glycerol as the carbon source. All experiments exhibited a reversal of the desired reaction. Particularly, the results with glycerol using MG1655/pZE12-*xdh*/pCS27-*nox* are shown in Fig. 2-8. Each addition of glycerol was accompanied by a decrease in L-xylulose and an increase in xylitol. And the interruption of feeding carbon source during the progress of fermentation led the cell only attained 58% of L-xyluloes conversion and 0.85 g/g of yield, which are less than the values observed in the batch processes.

The NAD^+ and NADH concentrations were also measured during one interval that glycerol was added into the cell cultures. As shown in Fig. 2-9, a pulse of glycerol resulted in a dramatic decrease in NAD^+/NADH ratio, which corresponded to a portion of the L-xylulose converted back into xylitol. The formation of L-xylulose commenced again only when glycerol were totally consumed, a time which also corresponded to an increasing NAD^+/NADH ratio.

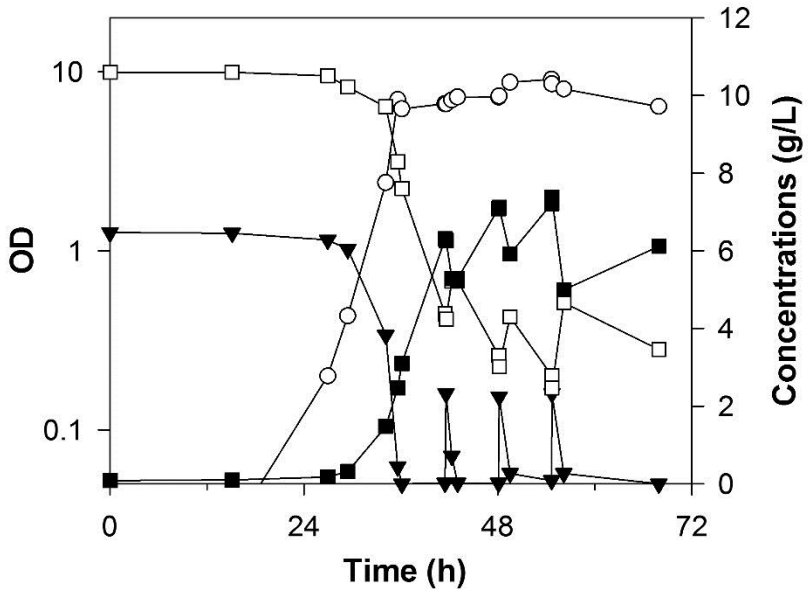

Figure 2-8. L-xylulose formation from 10 g/L xylitol during growth of MG1655/pZE12-*xdh*/pCS27-*nox* on glycerol. Three times at 7 h intervals after the initial glycerol was depleted, an additional 2 g/L of glycerol was added to the fermenter: OD (○); glycerol (▼); xylitol (□); L-xylulose (■).

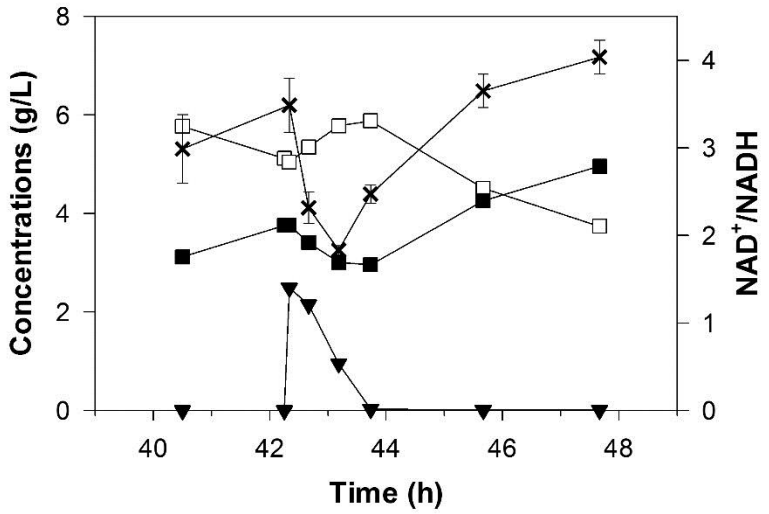

Figure 2-9. Culture dynamics at the time when an additional 2 g/L of glycerol was added during the conversion of xylitol to L-xylulose for MG1655/pZE12-*xdh*/pCS27-*nox*: glycerol (▼); xylitol (□); L-xylulose (■); NAD^+/NADH (✖).

Batch Process using Greater Concentrations

In both shake flask experiments and controlled batch processes, the overexpression of NOX benefits L-xylulose production when the strain is growing on glycerol. Unfortunately, the intermittent feeding strategy source is not able to further improve the final L-xylulose conversion. Because an equilibrium exists between L-xylulose and xylitol, the simple and best approach for increasing the final L-xylulose production is using a higher concentration of xylitol. Thus, a batch process was performed using about 12 g/L glycerol and 22 g/L xylitol with MG1655/pZE12-*xdh*/pCS27-*nox* (Fig. 2-10). After 72 h growth, the conversion of L-xylulose from xylitol reached to 65% with a productivity of 0.19 g/L·h and a yield of 0.89 g L-xylulose/g xylitol. Ultimately, the final equilibrium ratio was about 2.50.

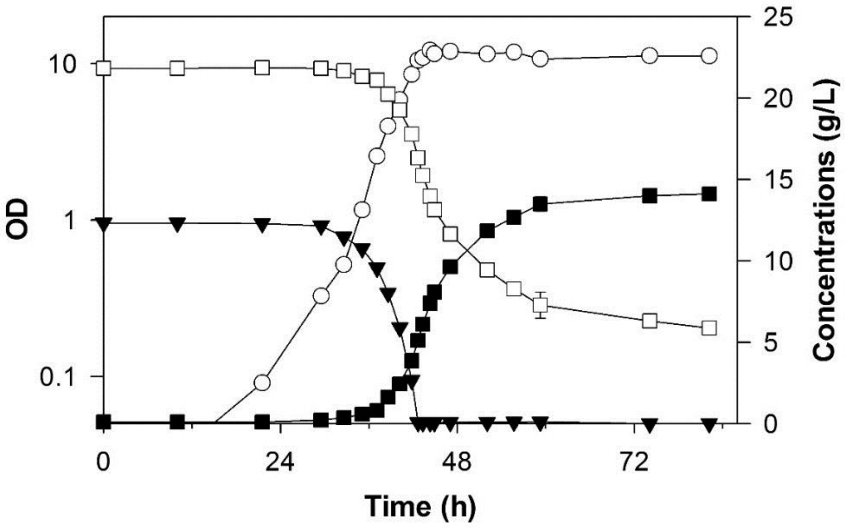

Figure 2-10. L-xylulose formation from 22 g/L xylitol during batch growth of MG1655/pZE12-*xdh*/pCS27-*nox* on glycerol. OD (○); glycerol (▼); xylitol (□); L-xylulose (■).

Discussion

This study demonstrates that the NAD^+/NADH ratio is important for driving the synthesis of biochemicals mediated by NAD(H)-dependent enzymes. In this study, the NAD^+/NADH ratio exhibited a positive correlation with the final ratio R of L-xylulose generated to xylitol remained. Former researchers found that altering the NAD^+/NADH ratio could shift the equilibria between a pair of oxidized and reduced chemicals. For example, the change of NAD^+/NADH ratio of *Bacillus subtilis* from 0.83 to 2.5 resulted in a 2-fold increase in the production of acetoin (Bao et al., 2014). Indeed, our study of intermittent fed-batch (Fig. 2-9) further demonstrate how quickly the equilibrium between biochemical can be shifted simply by providing carbon source because of altering the balance between NAD^+ and NADH.

The selection of carbon source is essential for maintaining the desired NAD^+/NADH ratio during the whole-cell formation of oxidized chemicals. Similar to our studies, there are several reports that manipulate the NAD^+/NADH ratio by comparing glucose and sorbitol to control the metabolite distribution of ethanol and acetate (San et al., 2002). In the current study, the NAD^+/NADH ratio found in growth of *E. coli* on glycerol was greater than the growth on glucose, and this ratio was correlated to an elevated equilibrium ratio R of L-xylulose to xylitol.

Introducing a water-forming NADH oxidase would expected to assist oxidation of intracellular NADH in cases where normally oxidation processes were saturated. NOX overexpression exhibited different performance on the NAD^+/NADH ratio and L-xylulose formation due to the two carbon sources examined. In particular, the NAD^+/NADH ratio was slightly raised during growth on glycerol but reduced during growth on glucose. The cellular response to NOX overexpression likely involved a complex interplay between growth rate, metabolic fluxes, and differential expression level during growth on different carbon sources.

When utilize *E. coli* as the whole-cell catalyst, the limitations of substrate transportation and potential mechanisms for products consumption should be carefully examined. The *lyxK* knockout had no impact on the final L-xylulose formation, which suggested the presence of L-xylulokinase is not the reason to explain why the L-xylulose yield was lower than the theoretical value. The uptake of xylitol in *E. coli* does not depend on any active-transportation but on a glycerol facilitator (GlpF), especially when both glycerol and xylitol were present in the cell cultures (Heller et al., 1980; Fu et al., 2002). Since the membrane expression level of GlpF significantly affects glycerol transportation rate and further impacts xylitol uptake (Sweet et al., 1990), a greater transport rate could cause glycerol-grown cells to maintain a greater intracellular xylitol concentration, which could result in a higher conversion to L-xylulose.

The results from four batch studies found a significant decrease in total NAD(H) after carbon source depleted. When the cell maintained a high level of intracellular NAD(H), NAD^+ biosynthesis is repressed and NAD^+ degradation is activated (Foster and Moat, 1980). Because the synthesis of NAD(H) relies on energy such as ATP, cell would likely trigger the mechanism of NAD^+ degradation, which was suspected to hinder the continuous supply of NAD^+ for an efficient NAD^+-dependent biotransformations. Indeed, the reduction of total NAD(H) was accompanied with a decline of NAD^+/NADH ratio in this study. Since NAD^+ degradation will affect the NAD^+/NADH ratio and equilibrium between xylitol and L-xylulose, further studies are underway to improve the performance of whole-cell biotransformation of L-xylulose by means of maintaining cell with a high intracellular NAD(H) level.

Acknowledgments

The authors thank Sarah Lee for her technical assistance. The authors declare she has no conflicts of interests.

References

Aarnikunnas, J. S., A. Pihlajaniemi, A. Palva, M. Leisola, and A. Nyyssola. 2006. Cloning and expression of a xylitol 4-dehydrogenase gene from *Pantoea ananatis*. *Appl. Environ. Microbiol.* 72(1): 368-377.

Baba, T., T. Ara, M. Hasegawa, Y. Takai, Y. Okumura, M. Baba, K. A. Datsenko, M. Tomita, B. L. Wanner, and H. Mori. 2006. Construction of *Escherichia coli* K-12 in-frame, single-gene knockout mutants: the Keio collection. *Mol. Syst. Biol.* 2(1): 2006.0008.

Bao, T., X. Zhang, Z. Rao, X. Zhao, R. Zhang, T. Yang, Z. Xu, and S. Yang. 2014. Efficient whole-cell biocatalyst for acetoin production with NAD^+ regeneration system through homologous co-expression of 2,3-butanediol dehydrogenase and NADH oxidase in engineered *Bacillus subtilis*. *PloS One.* 9(7): e102951

Berenguer-Murcia, A., and R. Fernandez-Lafuente. 2010. New trends in the recycling of NAD(P)H for the design of sustainable asymmetric reductions catalyzed by dehydrogenases. *Curr. Org. Chem.* 14(10): 1000-1021.

Bernofsky, B., and M. Swan. 1973. An improved cycling assay for nicotinamide adenine dinucleotide. *Anal. Biochem.* 53(2): 452-458.

Bhuiyan, S. H., Z. Ahmed, M. Utamura, and K. Izumori. 1998. A new method for the production of L-lyxose from ribitol using microbial and enzymatic reactions. *J. Ferment. Bioeng.* 86(5): 513-516.

Di Luccio, E., B. Petschacher, J. Voegtli, H. T. Chou, H. Stahlberg, B. Nidetzky, and D. K. Wilson. 2007. Structural and kinetic studies of induced fit in xylulose kinase from *Escherichia coli*. *J. Mol. Biol.* 365(3): 783-798.

Doten, R. C. and R. P. Mortlock. 1985. Production of D- and L-xylulose by mutants of *Klebsiella pneumoniae* and *Erwinia uredovora. Appl. Environ. Microbiol.* 49(1): 158-162.

Foster, J. W. and A. G. Moat. 1980. Nicotinamide adenine dinucleotide biosynthesis and pyridine nucleotide cycle metabolism in microbial systems. *Microbiol. Rev.* 44(1): 83.

Fu, D., A. Libson, L. J. Miercke, C. Weitzman, P. Nollert, J. Krucinski, and R. M. Stroud. 2002. Structure of a glycerol-conducting channel and the basis for its selectivity. *Science.* 290: 481-486.

Goodwin, T. E., K. R. Cousins, H. M. Crane, P. O. Eason, T. E. Freyaldenhoven, C. C. Harmon, B. K. King, C. D. LaRocca, R. L. Lile, and S. G. Orlicek. 1998. Synthesis of two new maytansinoid model compounds from carbohydrate precursors. *J. Carbo. Chem*. 17(3): 323-339.

Granström, T. B., G. Takata, M. Tokuda, and K. Izumori. 2004. Izumoring: a novel and complete strategy for bioproduction of rare sugars. *J Biosci Bioeng.* 97(2): 89-94.

Heller, K. B., E. C. Lin, and T. H. Wilson. 1980. Substrate specificity and transport properties of the glycerol facilitator of *Escherichia coli*. *J. Bacteriol.* 144(1): 274-278.

Hiroshi, O., S. Seui, S. Hiroshi, and O. Toshitsugu. 1976. Increased urinary excretion of L-xylulose in patients with liver cirrhosis. *Clin. Chim. Acta.* 67(2): 131-136.

Jeong, L. S., R. F. Schinazi, J. W. Beach, H. O. Kim, S. Nampalli, K. Shanmuganathan, A. J. Alves, A. McMillan, C. K. Chu, and R. Mathis. 1993. Asymmetric synthesis and biological evaluation of. beta.-L-(2R, 5S)-and. alpha.-L-(2R, 5R)-1, 3-oxathiolane-pyrimidine and-purine nucleosides as potential anti-HIV agents. *J. Med. Chem*. 36(2): 181-195.

Jokela, J., O. Pastinen, and M. Leisola. 2002. Isomerization of pentose and hexose sugars by an enzyme reactor packed with cross-linked xylose isomerase crystals. *Enzyme Microb. Technol.* 31(1-2): 67-76.

Khan, A. R., H. Tokunaga, K. Yoshida, and K. Izumori. 1991. Conversion of xylitol to L-xylulose by *Alcaligenesp*. 701B-cells. *J. Ferment. Bioeng.* 72(6): 488-490.

Kroger, M., K. Meister, and R. Kava. 2006. Low-calorie sweeteners and other sugar substitutes: A review of the safety issues. *Compr. Rev. Food Sci. Food Saf.* 5(2): 35-47.

Lutz, R. and H. Bujard. 1997. Independent and tight regulation of transcriptional units in *Escherichia coli* via the LacR/O, the TetR/O and AraC/I1-I2 regulatory elements. *Nucleic. Acids Res.* 25(6): 1203-1210.

Ma, T., J. S. Lin, M. G. Newton, Y. C. Cheng, and C. K. Chu. 1997. Synthesis and anti-hepatitis B virus activity of 9-(2-deoxy-2-fluoro-beta-L-arabinofuranosyl) purine nucleosides. *J. Med. Chem*. 40(17): 2750-2754.

Mathé, C. and G. Gosselin. 2006. L-Nucleoside enantiomers as antivirals drugs: a mini-review. *Antivir. Res*. 71(2): 276-281.

Moran, E. J., J. E. Tellew, Z. Zhao, and R. W. Armstrong. 1993. Dehydroamino acid derivatives from D-arabinose and L-serine: Synthesis of models for the azinomycin antitumor antibiotics. *J. Org. Chem.* 58(27): 7848-7859.

Muniruzzaman, S., Y. T. Pan, Y. Zeng, B. Atkins, K. Izumori, and A. D. Elbein. 1996. Inhibition of glycoprotein processing by L-fructose and L-xylulose. *Glycobiology*. 6(8): 795-803.

Poonperm, W., G. Takata, K. Morimoto, T. B. Granström, and K. Izumori. 2007. Production of L-xylulose from xylitol by a newly isolated strain of *Bacillus pallidus* Y25 and

characterization of its relevant enzyme xylitol dehydrogenase. *Enzyme Microb. Technol.* 40(5): 1206-1212.

San, K. Y., G. N. Bennett, S. J. Berríos-Rivera, R. V. Vadali, Y. T. Yang, E. Horton, F. B. Rudolph, B. Sariyar, and K. Blackwood. 2002. Metabolic engineering through cofactor manipulation and its effects on metabolic flux redistribution in *Escherichia coli*. *Metab. Eng.* 4(2): 182-192.

Shen, C. R. and J. C. Liao. 2008. Metabolic engineering of *Escherichia coli* for 1-butanol and 1-propanol production via the keto-acid pathways. *Metab. Eng.* 10(6): 312-320.

Sweet, G., C. Gandor, R. Voegele, N. Wittekindt, J. Beuerle, V. Truniger, E. C. Lin, and W. Boos. 1990. Glycerol facilitator of *Escherichia coli*: cloning of *glpF* and identification of the *glpF* product. *J. Bacteriol.* 172(1): 424-430.

Takata, G., W. Poonperm, K. Morimoto, and K. Izumori. 2010. Cloning and overexpression of the xylitol dehydrogenase gene from *Bacillus pallidus* and its application to L-xylulose production. *Biosci. Biotechnol. Biochem.* 74(9): 1807-1813.

Vemuri, G. N., E. Altman, D. P. Sangurdekar, A. B. Khodursky, and M. A. Eiteman. 2006a. Overflow metabolism in *Escherichia coli* during steady-state growth: transcriptional regulation and effect of the redox ratio. *Appl. Environ. Microbiol.* 72(5): 3653-3661.

Vemuri, G. N., M. A. Eiteman, and E. Altman. 2006b. Increased recombinant protein production in *Escherichia coli* strains with overexpressed water-forming NADH oxidase and a deleted ArcA regulatory protein. *Biotechnol. Bioeng.* 94(3): 538-542.

Table 1-1. Strains and plasmids used in this study.

Strain or Plasmid	Relevant Characteristics	Reference
Strains		
MG1655	*E. coli* F$^-$ □$^-$ *ilvG rfb*50 *rph*-1	wild-type
MEC342	MG1655 *lyxK763*::Kan	This study
Plasmids		
pZE12-*luc*	$P_L$lacO$_1$::*luc* ColE1 Amp^r	Lutz et al., 1997
pCS27	$P_L$lacO1::MCS1 p15A Kan^r;	Shen et al., 2008
pZE12-*xdh*	Codon optimized *xdh* gene from *Pantoea ananatis* (ATCC 43072)	This study
pZE12-*xdh-glpF*	*glpF* gene from *E. coli* MG1655	This study
pCS27-*glpF*	*glpF* gene from *E. coli* MG1655	This study
pCS27-*nox*	*nox* gene from *Streptococcus pneumoniae*	This study

Table 1-2. Specific enzyme activities (Units/mg protein) for xylitol 4-dehydrogenase (XDH) and NADH oxidase (NOX) in *E. coli* MG1655 expressing these two enzymes on plasmids. Values represent the average (standard deviation) of activity after 48 h of growth in independent 50 mL shake flask cultures.

Strains & plasmids	Growth on glucose		Growth on glycerol	
	XDH	NOX	XDH	NOX
MG1655 pZE12-*xdh*	5.3 (0.1)	0.11 (0.02)	1.1 (0.1)	0.21 (0.02)
MG1655 pCS27-*nox*	N/A	6.9 (0.6)	N/A	7.8 (0.4)
MG1655 pZE12-*xdh*/pCS27-*nox*	0.7 (0.1)	4.6 (0.5)	1.9 (0.1)	4.1 (0.4)

CHAPTER 4

ENHANCEMENT OF NAD(H) POOL FOR FORMATION OF OXIDIZED BIOCHEMICALS IN *ESCHERICHIA COLI*[2]

[2] Han, Q. and M.A. Eiteman. 2018. *Journal of Industrial Microbiology and Biotechnology*. 1-12.

Reprinted here with permission of publisher.

Abstract

Total NAD(H) (i.e., NAD^+ plus NADH) plays an important role in maintaining a sufficient driving force for the oxidative processes. However, NAD(H) degradation after exhaustion of the carbon sources might contribute to a decline in the rate of desired conversion. In this study, methods of preventing or reducing the native rate of NAD(H) degradation were examined. We demonstrated that a high phosphate concentration (50 mM) slowed NAD(H) degradation after carbon source depleted. In shake flask experiments, comparison of knockout strains with the deletion of genes coding enzymes involved in NAD^+ degradation demonstrated that the total NAD(H) were positively correlated with L-xylulose formation from xylitol, and the greatest conversion (80%) was observed in MG1655 *nadR-nudC-mazG*/ pZE12-*xdh*/pCS27-*nox*. Batch processes further confirmed that L-xylulose conversion was greater in the *E. coli* triple knockout *nadR nudC mazG* than in the wild-type background as control (0.66 g/g vs 0.53 g/g). As a potential platform for enhancing formation of the oxidized biochemical product, MG1655 *nadR-nudC-mazG* was also successfully applied in the conversion of galactitol to L-tagatose: 9.4 g/L of L-tagatose was generated with 90% conversion and a yield of 0.95 g L-tagatose/g galactitol consumed. The results proved the importance of reducing NAD(H) degradation in the NAD^+-dependent biotransformation and provide a method for enhancing the production of oxidized biochemical.

Introduction

The whole-cell biotransformations represents attractive methods for the production of chiral chemicals with high yields, cost-effectiveness, and simple operations. The reactions utilizing NAD^+ or NADH as the cofactor are typically suitable for the whole-cell catalysts due to the native own of NAD(H) and cellular metabolism for cofactor recycling. In order to maintain a desired redox level of intracellular pyridine nucleotide pool, the whole-cell catalysts depend on an efficient cycle for electron donation or reception. A corresponding compound for electron acceptor or donator should readily be taken up by the cells and ideally should yield no by-products upon the reaction. In whole-cell biotransformations with recombinant *Escherichia coli*, the applications of water-form NADH oxidase and formate dehydrogenase have been demonstrated for chiral acetoin synthesis (Xiao et al., 2010) and for the formation of L-amino acid (Galkin et al., 1997).

The use of oxidoreductases on oxidize sugar alcohols selectively is one method for the production of rare sugars. Unfortunately, the need for expensive cofactors (e.g., NAD^+ or $NADP^+$) as cosubstrates and for additional purified enzymes to recycle these cofactors reduces the prospect for large-scale enzymatic production. Whole-cell catalysts using either growing or non-growing cells provide the advantages of *in vivo* cofactor synthesis and regeneration, typically from oxidation of the reduced cofactors in the presence of oxygen as the terminal electron acceptor. A continued metabolic driving force is required for the desired oxidative processes. Moreover, the total amount of NAD(H) (i.e., NAD^+ plus NADH) available plays an important role in maintaining a sufficient driving force for the desired oxidation, especially when living cells naturally degrade NAD(H) after the carbon energy source is depleted. Methods

which prevent or reduce the native rate of NAD(H) degradation may enhance or prolong a NAD^+-mediated sugar alcohol to sugar conversion.

NAD(H) is generated by two pathways in *E. coli* (Fig. 1-1): 1) a *de novo* pathway from aspartate and dihydroxyacetone phosphate via quinolinate synthetase (coded by *nadB* and *nadA* genes) and quinolinate phosphoribosyltransferase (*nadC* gene), and 2) a salvage pathway from nicotinate via nicotinate phosphoribosyltransferase (*pncB* gene). Both pathways converge at nicotinate mononucleotide (NaMN), an important precursor in NAD(H) synthesis. NaMN adenylyltransferase (*nadD*) catalyzes the conversion of NaMN to nicotinate adenine dinucleotide, which is finally aminated with NH_3 via NAD^+ synthetase (*nadE*) to form nicotinamide adenine dinucleotide (NAD^+).

To recycle the structural components of the cofactor, *E. coli* degrades intracellular NAD^+ via the pyridine nucleotide cycle (Fig. 1-1). One route converts NAD^+ to nicotinamide mononucleotide (NMN) via NADH pyrophosphatase coded by *nudC* and *nudE* (Frick and Bessman, 1995; O'Handley et al., 1998). Other enzymes with similar function have also been described in NAD(H) degradation. For example, nucleoside triphosphate pyrophosphohydrolase (*mazG*) and UDP-sugar hydrolase (*ushA*) show high NAD(H) hydrolytic activity (Zhang and Inouye, 2002; Wang et al., 2014). In addition to the enzymes directly involved in NAD(H) metabolism, the trifunctional protein NadR (*nadR*) regulates the biosynthesis of NAD(H): when NAD(H) level increases, NadR represses the transcription of *pncB, nadA* and *nadB* by increasing the binding affinity for the operator regions of target genes (Foster et al., 1990). The deletion of *nudC* and *nudE* has been previously demonstrated to decrease the pyrophosphatase activity (Heuser et al., 2007).

In this study, we examined environmental and genetic strategies to reduce NAD(H) degradation and maintain relatively high concentrations of these cofactors. We applied these strategies specifically to the oxidative formation of two rare sugars, L-xylulose and L-tagatose, from their respective sugar alcohols, xylitol and galactitol.

Materials and Methods

Strains

Escherichia coli MG1655 was used as the host strain in this study. The *ushA* coding UDP-sugar hydrolase, *nudE* coding NADH hydrolase, *nudC* coding NADH pyrophosphatase, *mazG* coding nucleoside triphosphate pyrophosphohydrolase, *nadR* coding transcriptional regulator and *gatB* coding galactitol-specific PTS system EIIB component were knocked out by transducing MG1655 with the corresponding Keio (FRT)Kan deletion (Baba et al., 2006) (Table 2-1). The Kan antibiotic marker was removed using pCP20 (Datsenko and Wanner, 2000). In knockout strains, forward primers external to the target gene and reverse primers within the kanamycin resistance cassette were used in the PCR verification to confirm proper chromosomal integration.

Plasmids construction

Plasmids pZE12-*xdh* expressing NAD^+-dependent xylitol 4-dehydrogenase (XDH) and pCS27-*nox* expressing NADH oxidase were constructed previously. The *gdh* gene from *Rhodobacter sphaeroides* expressing NAD^+-dependent galactitol 2-dehydrogenase (GDH) was synthesized by GenScript (Piscataway, USA) as a codon optimized gene for *E. coli*. Using synthesized sequence as template, the *gdh* gene was PCR-amplified with forward primer containing KpnI site (underlined) 5'-GGAAGGTACCATGGATTATCGTACCG-3' and reverse

primer containing sphI site (underlined) 5'-GGAAGCATGCTCACCAAACGGTATAACCAC-3'. The PCR products were gel-isolated, restriction enzyme digested, and ligated into the pZE12-*luc* to construct pZE12-*gdh*. In this study, pZE12-*xdh*, pZE12-*gdh* and pCS27-*nox* were transformed into the selected strains by electroporation.

Growth Medium

The defined medium contained (per L): 2.5 g K_2SO_4, 4.38 g NH_4Cl, 25.0 mg $Na_2(EDTA)\cdot 2H_2O$, 0.15 g $MgSO_4\cdot 7H_2O$, 20 mg citric acid, 0.25 mg $ZnSO_4\cdot 7H_2O$, 0.125 mg $CuCl_2\cdot 2H_2O$, 1.25 mg $MnSO_4\cdot H_2O$, 0.875 mg $CoCl_2\cdot 6H_2O$, 0.06 mg H_3BO_3, 0.25 mg $Na_2MoO_4\cdot 2H_2O$, 5.5 mg $FeSO_4\cdot 7H_2O$ and 20 mg thiamine·HCl. A first experiment examined the effect of initial phosphate concentration, and five phosphate concentrations (2, 25, 50, 75 and 100 mM) using KH_2PO_4 and K_2HPO_4 were added to this medium, and subsequent media used contained the single phosphate concentration as described. The pH of all media was adjusted to 7.0 with 30% (w/v) NaOH. For strains containing plasmids, 50 mg ampillicin/L and 100 mg kanamycin/L were added as appropriate.

Fermentation

Shake flask experiments were accomplished by first inoculating from plate culture a strain into 3 mL Lysogeny Broth (LB) and grown overnight at 37°C. Then, 1 mL of this culture was transferred to 50 mL defined medium containing 10 g/L sugar alcohol substrate and 5 g/L glycerol in a 250 mL baffled shake flask. For xylitol, triplicate shake flask cultures were maintained at 37°C with an agitation of 250 rpm, and cultures were induced at the time of inoculation with 0.5 mM IPTG. For D-galactitol, triplicate shake flask cultures were maintained at 32°C with an agitation of 250 rpm, and cultures were induced with 0.75 mM IPTG when the

OD reached 0.5. In all cases, samples were withdrawn to measure sugar alcohol, rare sugar product, and intracellular NAD^+ and NADH.

Duplicate batch bioreactor experiments used an inoculum from shake flask cultures grown as described above to an OD of 3. This 50 mL volume was used to inoculate a 2.5 L bioreactor (Bioflo 2000, New Brunswick Scientific Co., Edison, NJ) containing 1 L of defined medium with 10 g/L xylitol and 10 g/L glycerol for L-xylulose conversion, or with 10 g/L galactitol and 15 g/L glycerol for L-tagatose conversion. During cultures with xylitol leading to L.-xylulose, induction occurred at 2 h with 0.5 mM IPTG, and the temperature was 37°C. During cultures of galactitol leading to L-tagatose, induction occurred when the OD reached 0.6 with 0.75 mM IPTG, and the temperature was 32°C. For both sugar conversions, agitation was maintained at 400 rpm, and air flow rate was controlled at 1.0 L/min to ensure a dissolved oxygen concentration above 40% of saturation. The pH was maintained at 7.0 with automatic addition of 30% (w/v) NH_4OH.

Analytical methods

The optical density at 600 nm (OD) was used to monitor cell growth (UV-650 spectrophotometer, Beckman Instruments, San Jose, CA). Liquid chromatography with a refractive index detector and a Coregel 64-H ion-exclusion column (Transgenomic Ltd., Glasgow, United Kingdom) using a mobile phase of 4 mN H_2SO_4 was used for analysis of organic chemicals (Eiteman and Chastain, 1997). For dry cell weight (DCW) measurement, three 25.0 mL samples were centrifuged (8,400 × g for 10 min), and the cell pellets were washed with 30 mL deionized (DI) water three times then dried at 60°C for 24 h.

Enzyme kinetics

The kinetic parameters of XDH and GDH in whole cells were determined using 50 mM Tris/glycine buffer (pH 7.0 adjusted with 20% NaOH), containing 1 mM $MgCl_2$, 1 mM NAD^+, and 1-100 mM of substrate (xylitol or galactitol). The kinetic constants were calculated from measurements of triplicate samples, the parameters K_M and V_{MAX} were determined by nonlinear regression of the data to the Michaelis-Menten equation.

Quantification of NAD^+ and NADH

For the measurement of NAD^+ and NADH, two separate 1 mL samples from a batch culture were centrifuged (20,000×g for 1 min). The two cell pellets were separately resuspended in 250 μL 0.2 M HCl (for NAD^+ extraction) or 250 μL 0.2 M NaOH (for NADH) in a 50°C water bath for 10 minutes. After cooling in an ice bath, the samples were neutralized with 0.1 M NaOH or 0.1 M HCl, the extracts centrifuged (20,000×g for 5 min), and the supernatants used to determine the concentration of NAD^+ or NADH, using the enzymatic cycling assay (Bernofsky and Swan, 1973). The reaction mixture contained 1.0 M Bicine buffer (pH 8.0 adjusted with 20% NaOH), 40 mM EDTA (pH 8.0 adjusted with 20% NaOH), 16.6 mM phenanzinium ethylsulfate (PES), 4.2 mM thiazolyl-blue (MTT), absolute ethanol, and 500 U/mL alcohol dehydrogenase (EC 1.1.1.1, Sigma-Aldrich C., St. Louis, MO, Cat.A7011). The alcohol dehydrogenase uses NAD^+ to oxidize ethanol into acetaldehyde, and NAD^+ or NADH transfers the reducing equivalents from ethanol ultimately to MTT. The rate of formation of reduced MTT measured at 570 nm is proportional to the amount of NAD^+or NADH.

Results

Effect of phosphate on L-xylulose formation and NAD(H) maintenance

Since the phosphate concentration has been proposed to be critical for maintaining NAD(H) during stationary phase (Schurig-Briccio et al., 2008), we first examined the effect of medium composition on the NAD(H) concentration and its relationship to the conversion of xylitol to L-xylulose as a model biotransformation. Five different initial phosphate compositions (2 mM, 25 mM, 50 mM, 75 mM, or 100 mM) were tested in shake flask culture of MG1655/pZE12-*xdh*/pCS27-*nox* grown on 5 g/L glycerol supplemented with 10 g/L xylitol. In triplicate experiments, no difference in L-xylulose formation occurred among the phosphate concentrations after 24 h, which approximately corresponded to the time that glycerol was depleted (Fig. 3-1). However, after 48 h those cultures with 50 mM – 100 mM phosphate generated significantly more L-xylulose than flasks with 2 mM or 25 mM phosphate. At 96 h, the flask with 50 mM phosphate provided a xylitol-to-L-xylulose conversion of 0.63 g/g, while the 25 mM phosphate medium resulted in a conversion of only 0.13 g/g.

The intracellular concentrations of NAD^+ and NADH were measured during the xylitol-to-L-xylulose conversion in the media with 25 mM and 50 mM phosphate. After 24 h no difference was observed in NAD^+ and NADH between the 25 mM and 50 mM phosphate media (Fig. 3-2). For both phosphate concentrations, the total NAD(H) (i.e., NAD^+ plus NADH) as well as NAD^+ and NADH decreased with time. However, the rate of NAD(H) loss was much greater in cells growing in 25 mM phosphate compared to cells growing in 50 mM phosphate. After 96 h, 51% of the intracellular NAD(H) remained in cells grown in 50 mM phosphate, while only 11% of the original NAD(H) remained in cells grown in 25 mM phosphate (Fig. 3-2). The medium composed of 50 mM phosphate appears to delay the degradation of NAD(H) after cell

growth, a result which correlated with the increased L-xylulose formation at that phosphate concentration. The defined medium with 50 mM phosphate was used in all subsequent studies.

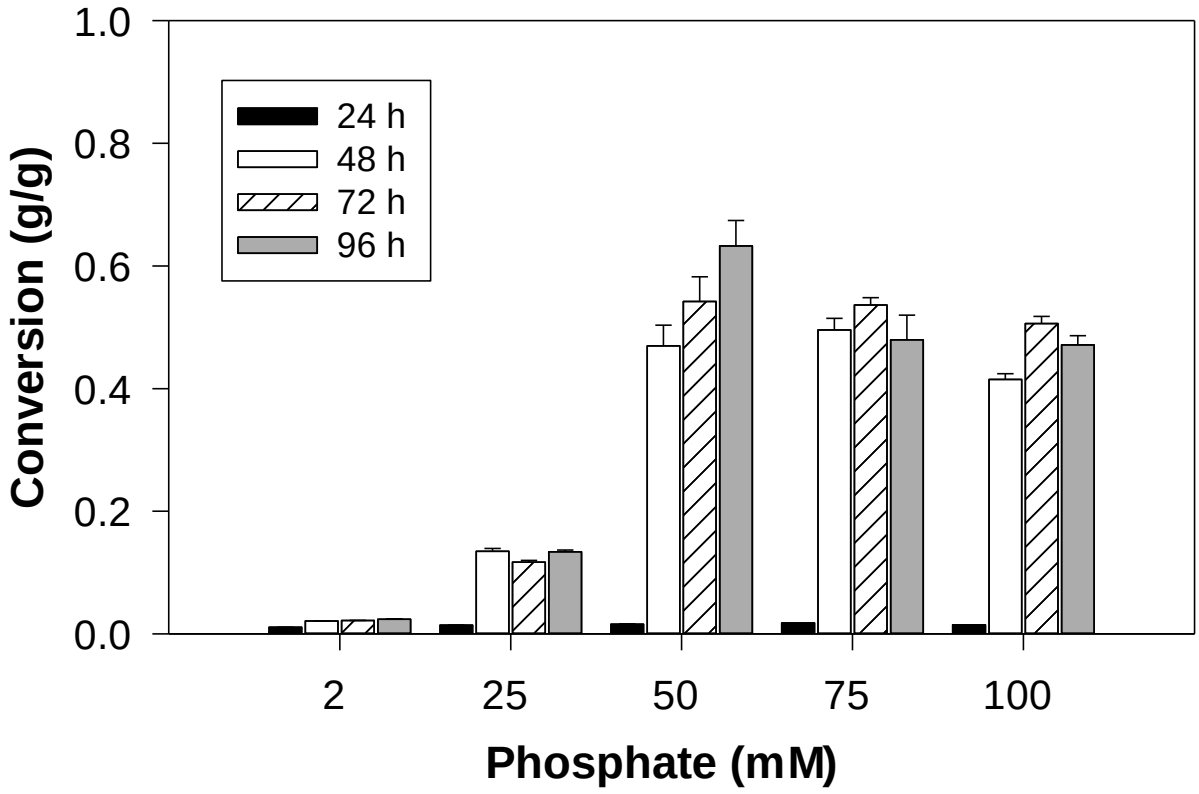

Figure 3-1. Conversion of xylitol to L-xylulose in a defined medium with different phosphate concentrations. MG1655/pZE12-*xdh*/pCS27-*nox* was cultured in 5 g/L glycerol supplemented with 10 g/L xylitol. Conversion is the quantity of L-xylulose generated divided by the initial quantity of xylitol provided. Error bars indicate standard deviation.

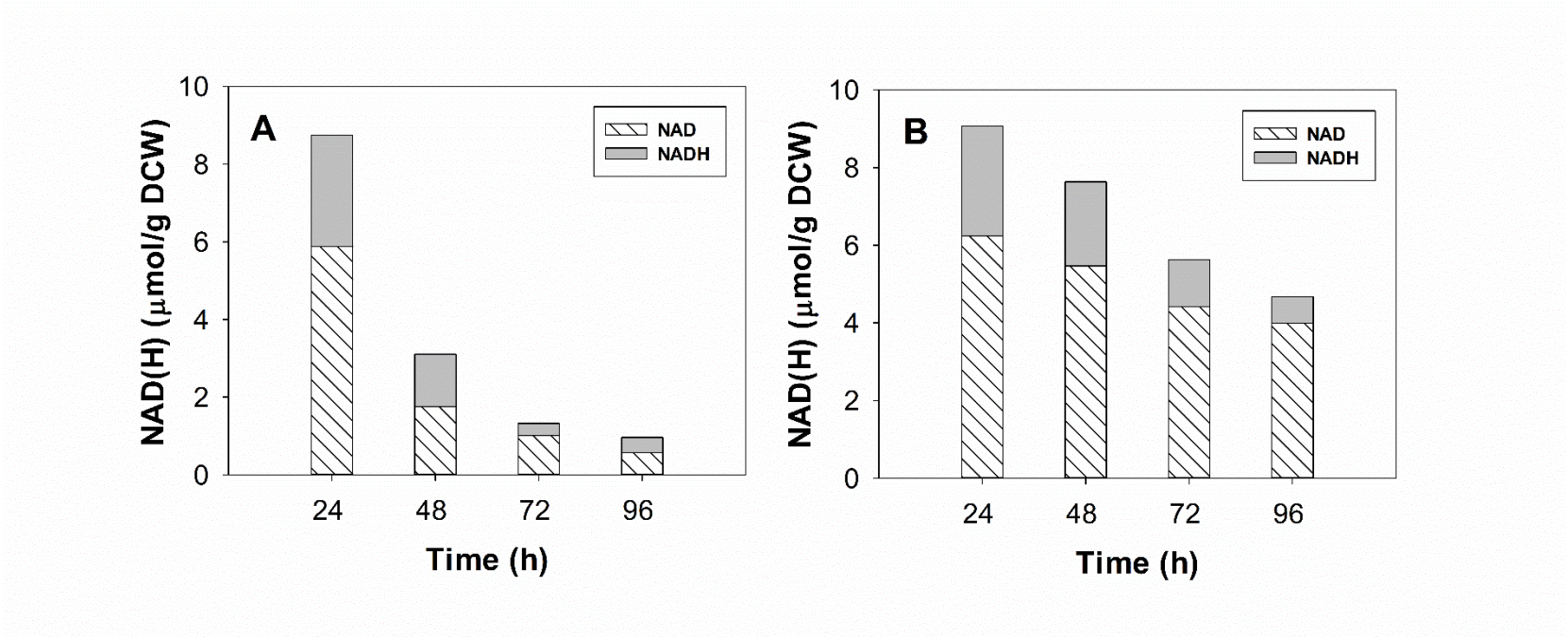

Figure 3-2. Intracellular NAD(H) in cells grown in medium containing A) 25 mM or B) 50 mM phosphate. MG1655/pZE12-*xdh*/pCS27-*nox* was cultured in 5 g/L glycerol supplemented with 10 g/L xylitol.

Effect of modifications in the NAD(H) pathway on L-xylulose formation and NAD(H) maintenance

The cofactor NAD^+ is generated and degraded by a network of pathways (Fig. 1-1). We hypothesized that deletion of genes encoding enzymes involved in NAD^+ degradation would prolong the NAD(H) pool and facilitate the biotransformation of xylitol into L-xylulose. The *ushA* gene encodes UDP-sugar hydrolase, *nudC* gene encodes NADH pyrophosphatase, *nudE* gene encodes NADH hydrolase, and *mazG* gene encodes nucleoside triphosphate pyrophosphohydrolase (Frick and Bessman, 1995; O'Handley et al., 1998; Zhang and Inouye, 2002; Wang et al., 2014). Moreover, the *nadR* gene encodes a repressor acting on the transcription of several genes in the NAD^+ biosynthetic pathway including *nadA*, *nadB*, and *pncB* (Foster et al., 1990). To examine whether these proteins affect L-xylulose formation and intracellular NAD(H) availability, we compared several single-gene knockout strains expressing pZE12-*xdh* and pCS27-*nox* for the conversion of xylitol to L-xylulose in shake flasks (Fig. 3-3). For each strain, to account for slight differences in growth rate, we measured the conversion at the time that the glycerol was depleted (Td), and then at 24 h and 48 h after Td. Single-gene knockouts MG1655 *nadR* (MEC517), MG1655 *nudC* (MEC516) or MG1655 *mazG* (MEC695) showed significantly greater conversion at Td + 48 h, while MG1655 *ushA* (MEC495) and MG1655 *nudE* (MEC504) showed significantly less conversion compared to wild-type MG1655, all expressing pZE12-*xdh*/pCS27-*nox* (Fig. 3-3). Further improvement in conversion was observed with the double knockouts MG1655 *nadR nudC* (MEC518) and MG1655 *nudC mazG* (MEC696) and the triple knockout MG1655 *nadR nudC mazG* (MEC697) expressing pZE12-*xdh*/pCS27-*nox*. The triple knockout resulted in a conversion of 0.87 g L-xylulose/g xylitol at Td + 48 h, 50% greater than the wild-type expressing pZE12-*xdh*/pCS27-*nox*.

In these shake flask studies using MG1655 and knockout strains with the two plasmids (pZE12-*xdh* and pCS27-*nox*), intracellular NAD(H) concentrations were also quantified. When glycerol was exhausted (at Td), most knockout strains maintained a greater total NAD(H) concentration than the wild-type (Fig. 3-4). In the subsequent 48 h after glycerol was depleted, NAD(H) degradation proceeded at differing rates. For example, at Td + 48 h the Δ*ushA* strain showed over 80% NAD(H) degradation, whereas the Δ*mazG* strain showed about 25% NAD(H) degradation. Among the nine strains, the greatest NAD(H) remaining after 48 h was observed in the double knockout MEC696 (9.7 μmol/g DCW) and the triple knockout MEC697 (8.2 μmol/g DCW). Moreover, we observed a correlation between xylitol-to-L-xylulose conversion (shown in Fig. 3-3) and intracellular NAD(H) at Td + 48 h (shown in Fig. 3-4). The greater the NAD(H) remaining 48 h after the carbon source glycerol was depleted, the greater the observed conversion of xylitol into L-xylulose at that time (Fig. 3-5).

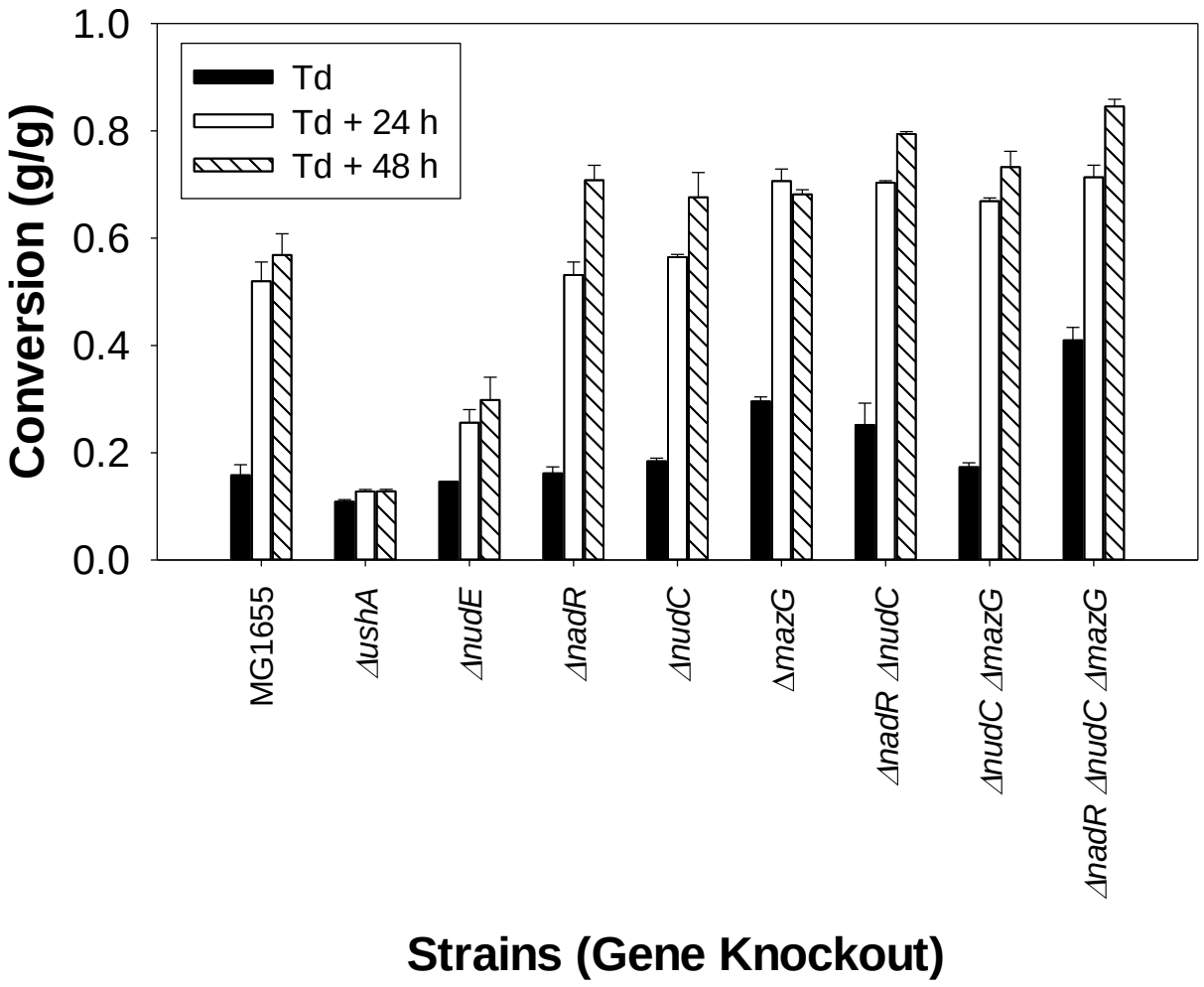

Figure 3-3. Comparison of *E. coli* strains for the conversion of 10 g/L xylitol to L-xylulose at the time that the 5 g/L glycerol carbon source was depleted (Td), or 24 h (Td + 24 h) and 48 h (Td + 48 h) after the time carbon source was depleted in shake flask cultures. Specific knockouts are indicated for each strain. Error bars indicate standard deviation. See Table 2-1 for more information about the knockout strains.

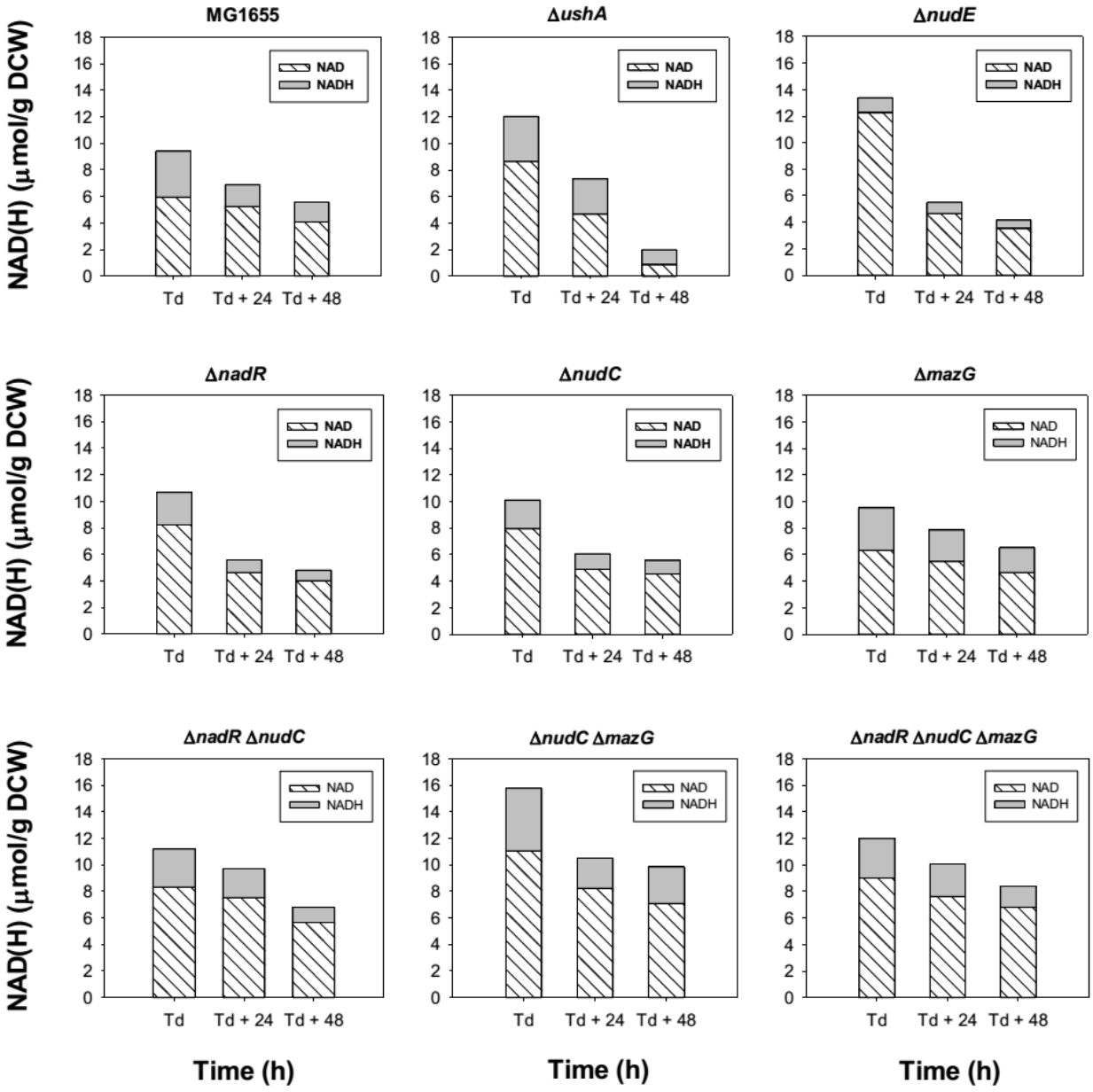

Figure 3-4. Intracellular NAD(H) concentrations in the wild-type and knockout *E. coli* strains at Td, Td + 24h, Td + 48 h during growth in shake flask cultures. Strains were cultured in 5 g/L glycerol supplemented with 10 g/L xylitol. Specific knockouts are indicated for each strain.

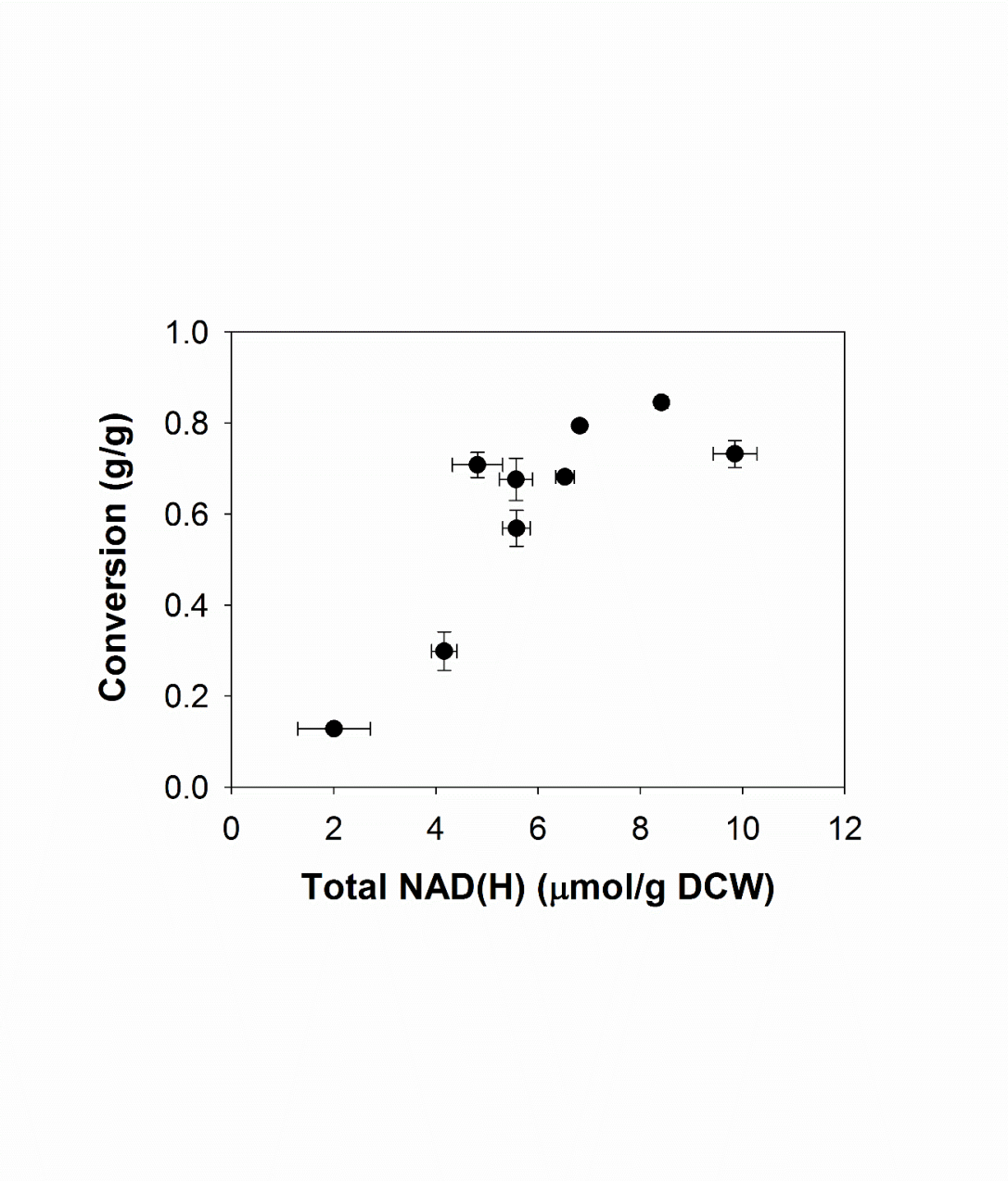

Figure 3-5. Relationship between total NAD(H) concentration and xylitol conversion to L-xylulose among all strains at Td + 48 h. Error bars indicate standard deviation.

Batch process for L-xylulose formation

In shake flask cultures the greatest conversion of xylitol to L-xylulose occurred in MEC697/pZE12-*xdh*/pCS27-*nox*. However, shake flask cultures offer limited control of several environmental conditions (e.g., pH, oxygenation), and therefore controlled batch processes were examined on the 1 liter scale. In duplicate experiments, we compared MG1655/pZE12-*xdh*/pCS27-*nox* (Fig. 3-6) with MEC697/pZE12-*xdh*/pCS27-*nox* (Fig. 3-7). MG1655/pZE12-*xdh*/pCS27-*nox* reached an OD of 12 in 30 h with a specific growth rate of 0.32 h^{-1}, and had accumulated 1.9 (±0.0) g/L of L-xylulose when glycerol was depleted (Fig. 3-6). Ultimately by 54 h, 6.8 (±0.1) g/L of xylitol was consumed, generating 5.6 g/L (±0.1) of L-xylulose with a yield of 0.81 (±0.02) g L-xylulose/g xylitol. For MEC697/pZE12-*xdh*/pCS27-*nox*, an OD of 8.8 was attained in 31 h with a specific growth rate of 0.23 h^{-1}. At the time glycerol was depleted, 2.9 (±0.0) g/L of L-xylulose was generated, and eventually 9.2 (±0.1) g/L of xylitol was converted to 7.3 (±0.1) g/L of L-xylulose with a yield of 0.79 (±0.07) g L-xylulose/g xylitol (Fig. 3-7). Although the triple knockout strain showed a lower specific growth rate, the conversion of xylitol to L-xylulose was greater by MEC697/pZE12-*xdh*/pCS27-*nox* than by MG1655/pZE12-*xdh*/pCS27-*nox* (0.66 g/g vs 0.53 g/g).

As noted previously, shake flask experiments revealed a greater level of NAD(H) in the triple knockout than in the wild-type background (Fig. 3-4). Identical measurements were made in the controlled bioreactors. For MG1655/pZE12-*xdh*/pCS27-*nox* (Fig. 3-6), the total NAD(H) concentration at the time of glycerol depletion was 6.7 μmol/g DCW. At the end of the biotransformation 43 h later, the NAD(H) concentration had decreased 42% to 4.0 μmol/g DCW. In contrast for MEC697/pZE12-*xdh*/pCS27-*nox* (Fig. 3-7), the total NAD(H) concentration at any given time was always over 50% greater than the NAD(H) concentration observed for

MG1655/pZE12-*xdh*/pCS27-*nox*. The NAD(H) concentration was 10.8 μmol/g DCW at the time of glycerol depletion and ultimately decreased 36% to 6.9 μmol/g DCW.

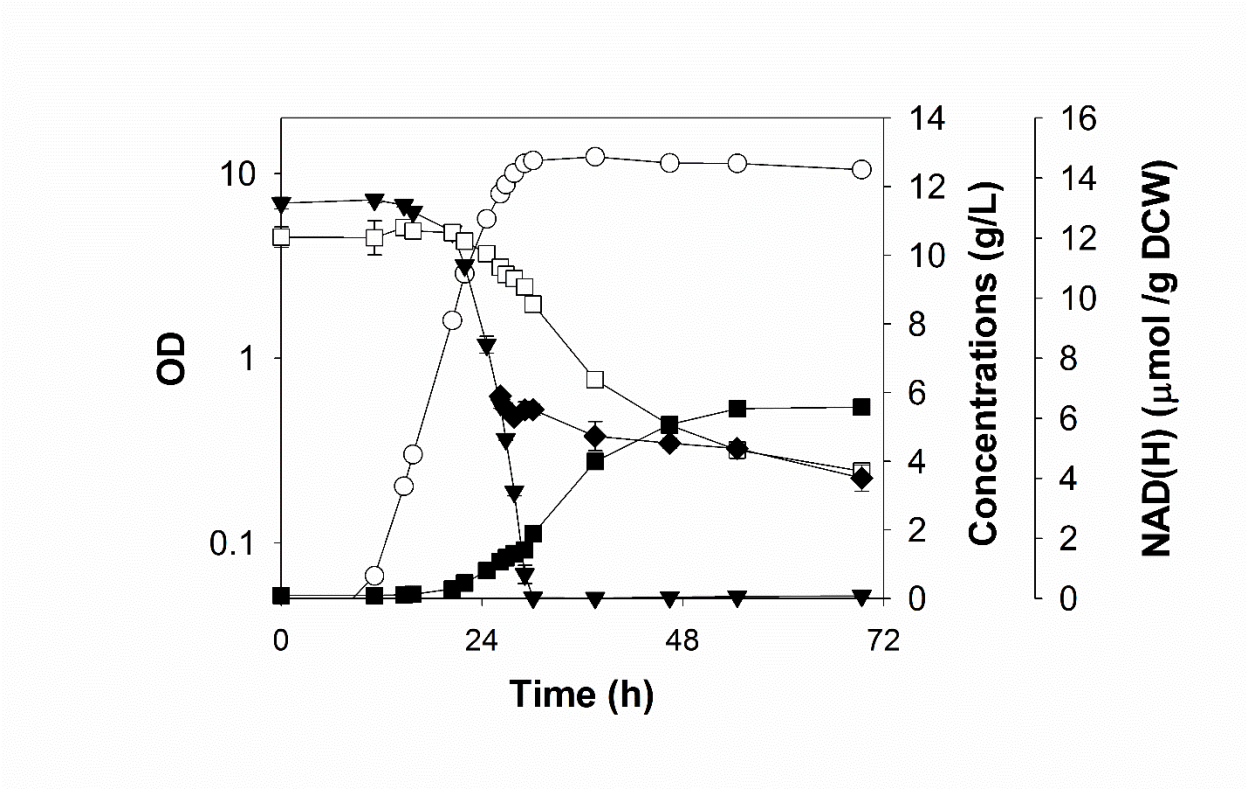

Figure 3-6. L-xylulose formation from 10 g/L xylitol during batch growth of MG1655/pZE12-*xdh*/pCS27-*nox* on 10 g/L glycerol: OD (○); glycerol (▼); xylitol (□); L-xylulose (■); Total NAD(H) (◆).

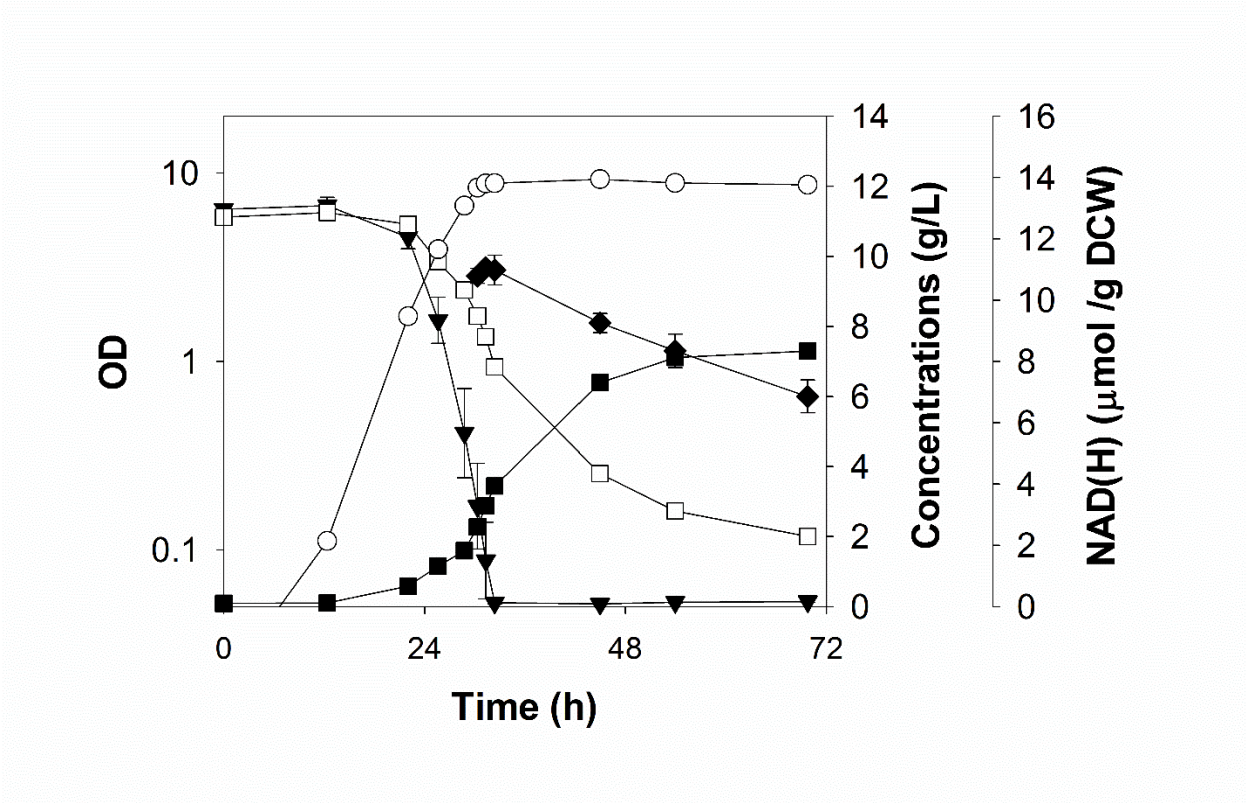

Figure 3-7. L-xylulose formation from 10 g/L xylitol during batch growth of MEC697/pZE12-*xdh*/pCS27-*nox* on 10 g/L glycerol: OD (○); glycerol (▼); xylitol (□); L-xylulose (■); Total NAD(H) (◆).

Kinetic comparison between xylitol dehydrogenase and galactitol dehydrogenase

The conversion of xylitol to L-xylulose in an *E. coli* strain expressing NAD^+-dependent xylitol 4-dehydrogenase correlated strongly with the prolonged availability of NAD(H) after the carbon source was depleted. To examine the utility of the triple knockout MEC697 as a platform strain to enhance other oxidative whole-cell biotransformations, we examined an NAD^+-dependent galactitol 2-dehydrogenase (GDH) from *Rhodobacter sphaeroides* (Huwig et al., 1997) to catalyze the conversion of galactitol into L-tagatose. Before the testing of MEC697 on L-tagatose conversion, we determined the kinetic parameters for both GDH and XDH on xylitol or galactitol. For XDH the K_M for xylitol was measured to be 7.3 mM with an observed maximum activity (V_{MAX}) of 7.0 IU/mg DCW. For GDH, the K_M for galactitol was 96 mM with an observed maximum activity of 1.9 IU/mg DCW. Although the intracellular concentrations of the sugar alcohol substrates were not determined, these results indicate that XDH is the superior biotransformation enzyme, and the enzyme results account for the comparatively slow conversion of galactitol to L-tagatose.

Biotransformation of galactitol to L-tagatose

Although *E. coli* does not naturally metabolize xylitol, this bacterium is able to metabolize galactitol for cell growth (Nobelmann and Lengeler, 1996). Therefore, before testing the performance of MEC697 for L-tagatose formation, the galactitol-specific PTS gene *gatB* in the wild-type and triple knockout strain was deleted to result in MG1655 *gatB* (MEC763) and MG1655 *nadR nudC mazG gatB* (MEC766). These strains were additionally transformed with pZE12-*gdh* expressing GDH and pCS27-*nox* expressing NADH oxidase. Shake flasks studies using 10 g/L galactitol and 5 g/L glycerol found that the total NAD(H) in MEC766/pZE12-*gdh*/pCS27-*nox* (Fig. 3-8B) was consistently greater than the total NAD(H) in the

MEC763/pZE12-*gdh*/pCS27-*nox* (Fig. 3-8A) after the glycerol was depleted. Similarly, the conversion of galactitol to L-tagatose was much greater in MEC766/pZE12-*gdh*/pCS27-*nox* (0.12 g L-tagatose/g galactitol at Td + 48 h) than the MEC763/pZE12-*gdh*/pCS27-*nox* (0.06 g L-tagatose/g galactitol) (Fig. 3-9).

L-tagatose production in the batch process

Because of the comparatively poor affinity shown by GDH for galactitol, we performed a controlled batch process using an increased concentration of glycerol (15 g/L) to carry out the conversion of galactitol to L-tagatose. In duplicate experiments, MEC763/pZE12-*gdh*/pCS27-*nox* generated 5.7 g/L L-tagatose after 198 h with a conversion of 0.62 g/g and a yield of 0.94 (±0.38) g L-tagatose/g galactitol (Fig. 3-10). In comparison, MEC766/pZE12-*gdh*/pCS27-*nox* generated 9.5 (±0.0) g/L L-tagatose in 178 h, with a conversion of 0.96 g/g and a yield of 0.96 (±0.01) g L-tagatose/g galactitol (Fig. 3-11). During the course of these processes, the total NAD(H) concentration observed in MEC766/pZE12-*xdh*/pCS27-*nox* (13.3 ±0.2 μmol/g DCW at time of glycerol depletion and ultimately 8.0±0.8 μmol/g DCW) was consistently greater than the concentration in MEC763/pZE12-*xdh*/pCS27-*nox* (6.6 ±0.4 μmol/g DCW at time of glycerol depletion and ultimately 3.4 ±0.7 μmol/g DCW).

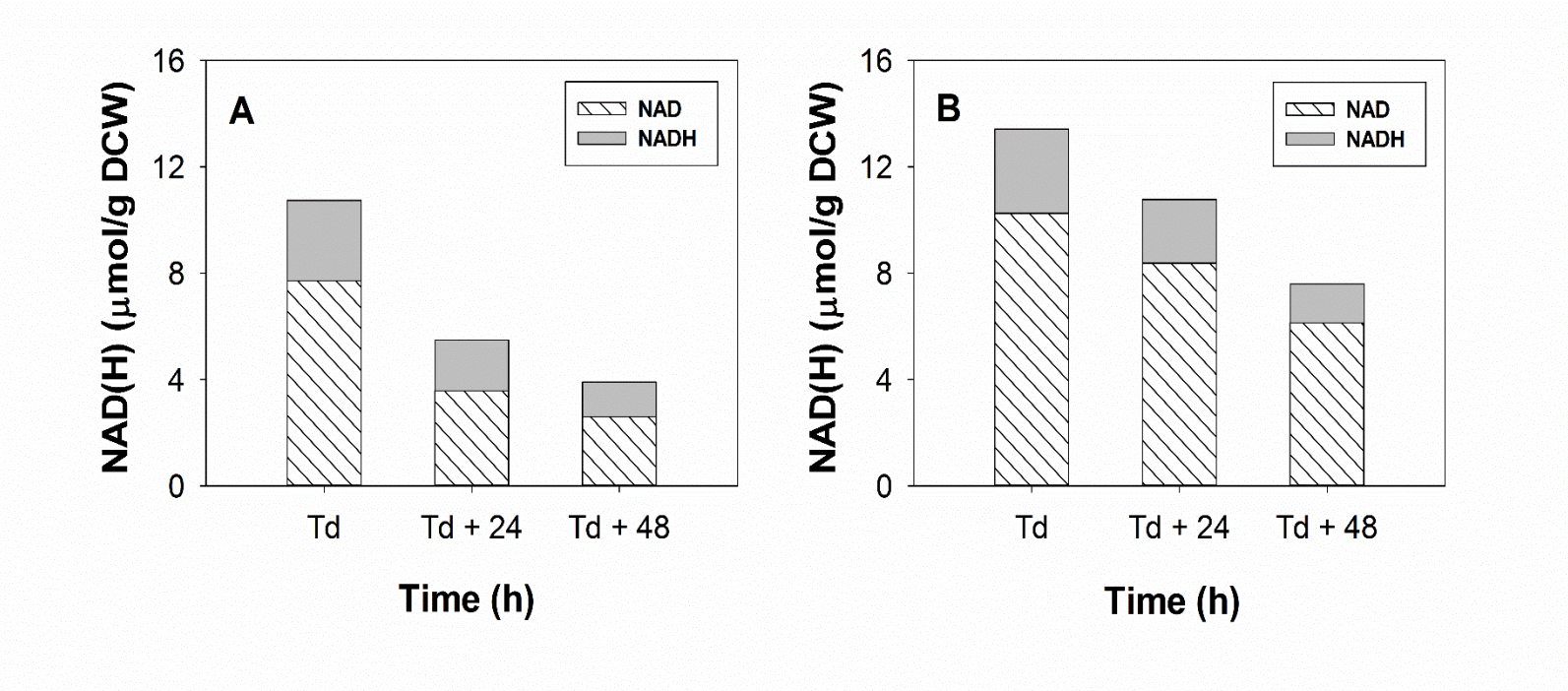

Figure 3-8. Intracellular NAD(H) concentrations in the MEC763 (Δ*gatB*) /pZE12-*gdh*/pCS27-*nox* (A) and MEC766 (Δ*nadR nudC mazG gatB*) /pZE12-*gdh*/pCS27-*nox* (B) at Td, Td + 24h, Td + 48 h in 5 g/L glycerol shake flask cultures.

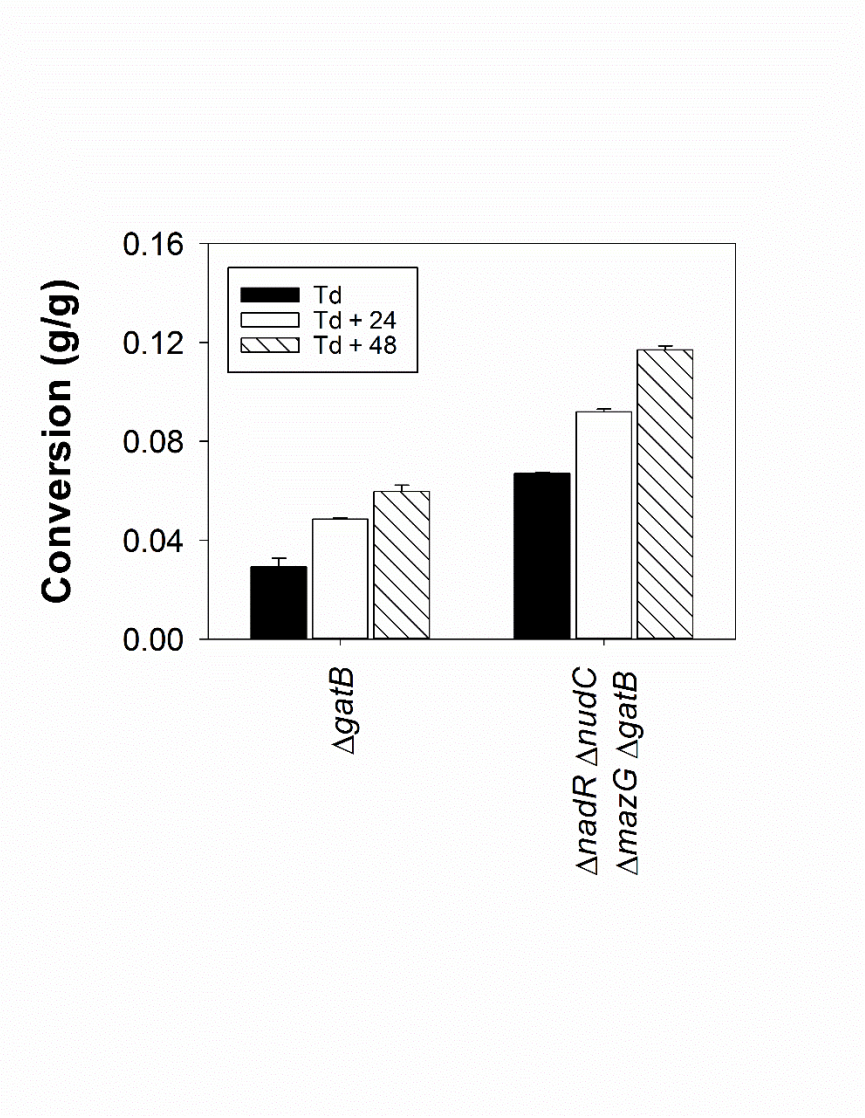

Figure 3-9. Comparison of MEC763 (Δ*gatB*) /pZE12-*gdh*/pCS27-*nox* and MEC766 (Δ*nadR nudC mazG gatB*) /pZE12-*gdh*/pCS27-*nox* for the conversion of 10 g/L galactitol to L-tagatose at Td, Td + 24h, Td + 48 h during growth in 5 g/L glycerol shake flask cultures. Error bars indicate standard deviation.

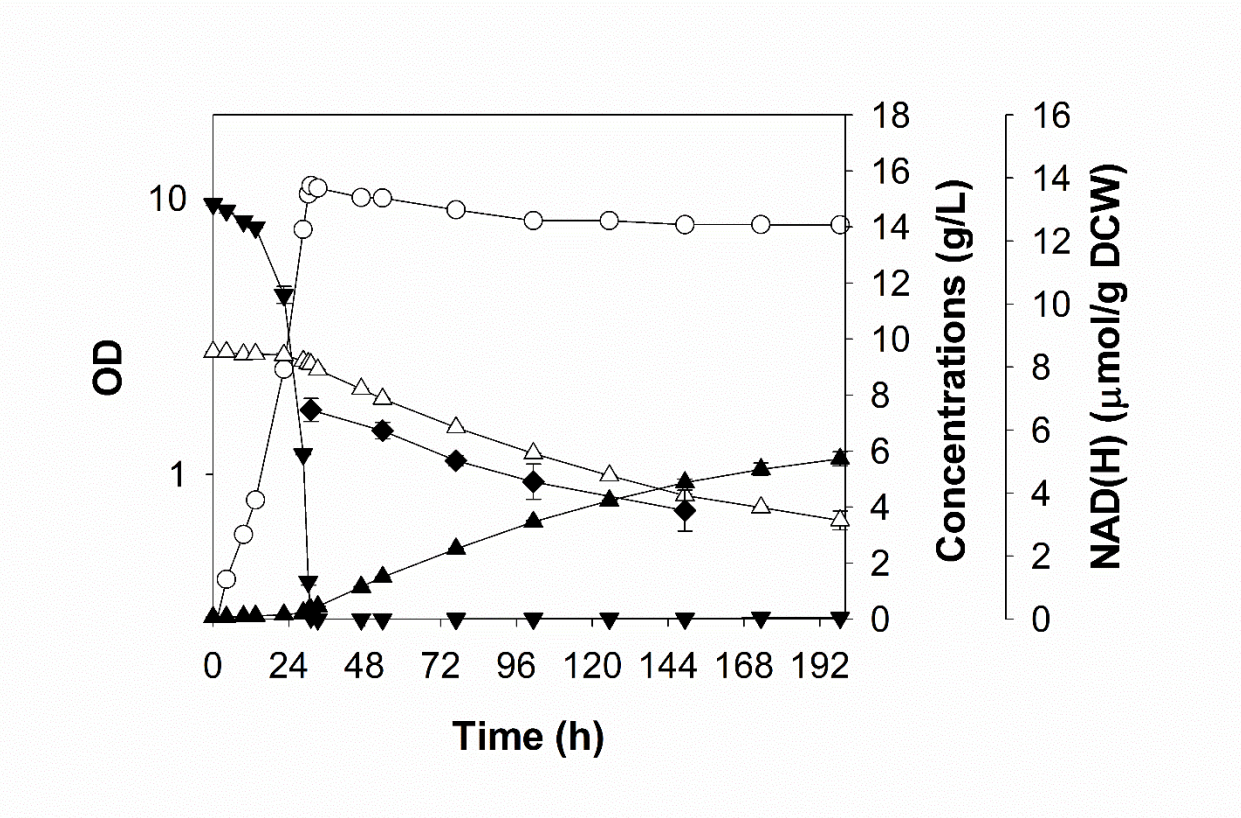

Figure 3-10. L-tagatose formation from 10 g/L galactitol during controlled batch culture of MEC763/pZE12-*gdh*/pCS27-*nox* on 15 g/L glycerol: OD (○); glycerol (▼); galactitol (△); L-tagatose (▲); Total NAD(H) (◆).

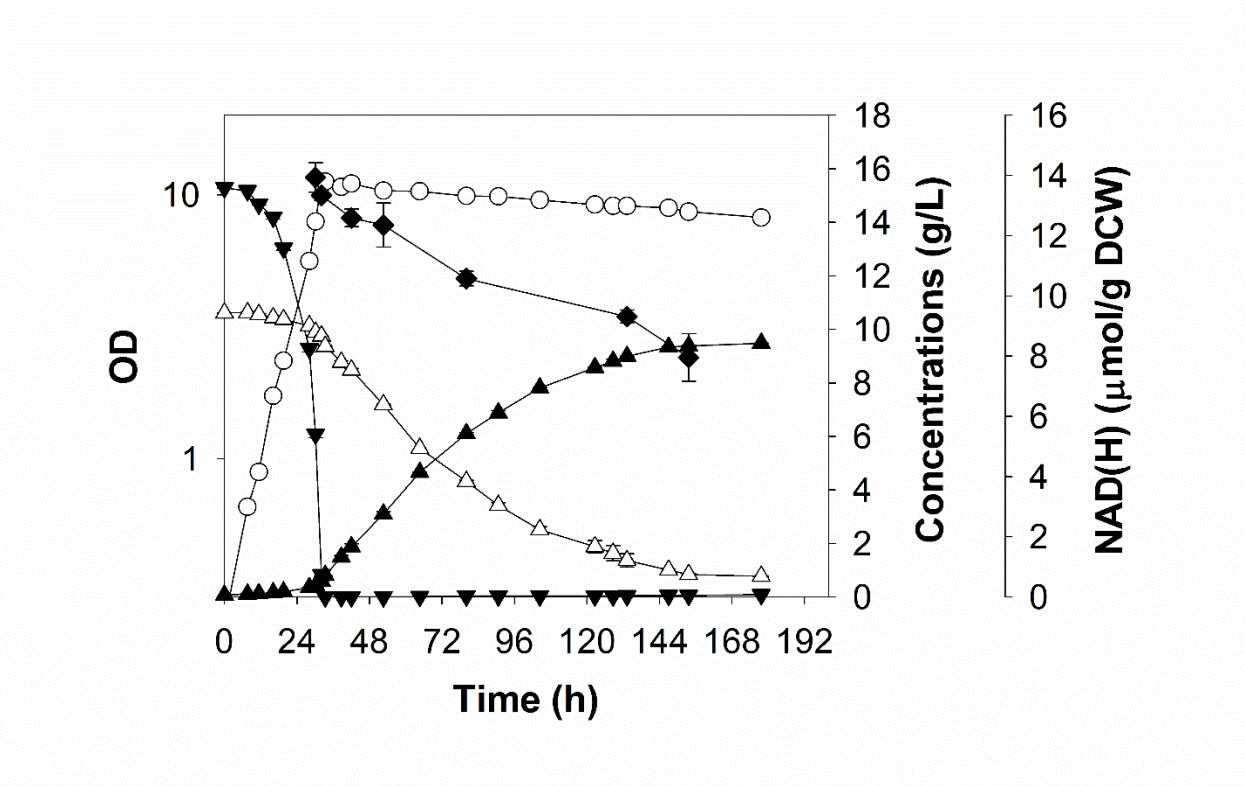

Figure 3-11. L-tagatose formation from 10 g/L galactitol during controlled batch culture of MEC766/pZE12-*gdh*/pCS27-*nox* on 15 g/L glycerol: OD (○); glycerol (▼); galactitol (△); L-tagatose (▲); Total NAD(H) (◆).

Discussion

NAD^+-mediated oxidative biotransformations are improved by increasing the relative concentration of oxidized cofactor NAD^+ compared to the reduced cofactor NADH. For example, increasing the NAD^+/NADH ratio in *Bacillus subtilis* from 0.83 to 2.5 was associated with a 2-fold increase in the conversion of 2, 3-butanediol to the oxidized product, acetoin (Bao et al., 2014). In addition to the importance of maintaining an elevated NAD^+/NADH ratio for oxidative processes, we also speculated that NAD(H) degradation after exhaustion of the growth substrate contributed to a dramatic decline in the rate of L-xylulose formation. Indeed, a major factor attributed to the slowing of reductive biotransformation of D-tagatose to D-mannitol in a recombinant *E. coli* was the degradation of NAD(H) (Heuser et al., 2009). In this present study, methods of preventing or reducing the native rate of NAD(H) degradation were examined, and the results demonstrated that the total intracellular NAD(H) was strongly correlated with the conversion of sugar alcohols to sugars.

Numerous factors including cellular and environmental conditions are likely responsible for the rate of NAD(H) degradation. In this study, we demonstrated that a high phosphate concentration (50 mM) slowed NAD(H) degradation after the carbon source was depleted, and resulted in improved biotransformation. Note that 25 mM phosphate corresponds with 0.77 g P/L, sufficient to generate over 26 g/L cells (Battley, 1991, 2003); therefore the cells in this study exposed to 25 mM phosphate concentration were not phosphate-limited. Others have shown that 35 mM marks a critical phosphate concentration in the growth medium at which the activity of a native NADH dehydrogenase is sustained (Schurig-Briccio et al., 2008). Moreover, elevated phosphate maintains cell viability by elevating intracellular polyphosphate (poly-P) (Schurig-Briccio et al., 2009a). A phosphate concentration over 35 mM was correlated to an

increased level of poly-P, which is thought to prolong the supply of amino acid and support tolerance to starvation (Kuroda et al., 2001). High phosphate appears to protect *E. coli* from oxidative stress during the stationary phase (Schurig-Briccio et al., 2009b). Although the mechanism is unclear, our results confirm that phosphate composition is a key parameter supporting prolonged NAD(H) availability during oxidative biotransformations.

In addition to consideration of medium components, cellular approaches could be applied to maintaining NAD(H). During the non-growing phase, the cofactors degradation was thought to be predominate since the cell adaptions for starvation. Therefore, it's reasonable to consider the potential approaches in the aspects of native NAD^+ synthesis or degradation for maintaining the stability of NAD(H) pool in the energy-limited phase: deletion of genes encoding prominent NAD(H) degrading enzymes. The enzymes coded by *nudC* and *nudE* of *E. coli* belong to the "Nudix" hydrolases family, and have been characterized as NADH pyrophosphatase with a high activity toward NAD(H) degradation (Frick and Bessman, 1995; O'Handley et al., 1998). Deletions of *nudC*, *nudE* or both genes resulted in over 50% reduction of pyrophosphatase activity (Heuser et al., 2007). Several other candidates, such as *ushA* coding a UDP-sugar hydrolase and *mazG* coding a nucleoside triphosphate pyrophosphohydrolase, also hydrolyze NAD^+ and NADH (Wang et al., 2014; Zhang et al., 2002).

Generally, single gene knockouts reduced the rate of NAD(H) degradation and increased the conversion of xylitol to L-xylulose. The two exceptions were *ushA* or *nudE* single knockouts in shake flask cultures, in which NAD(H) decreased quickly after the depletion of the carbon source (Fig. 3-4). We attribute these results to the vital role these genes appear to have in cell growth and viability: the growth rate for these two strains was lower than for any other single-gene knockout. Although the current study did not eliminate NAD(H) degradation, the *nadR*,

nudC, and *mazG* triple knockout diminished the rate of NAD(H) degradation. In addition to showing consistently higher levels of intracellular NAD(H), this strain showed increased oxidative biotransformations with a small decrease in maximum specific growth rate.

We also examined blocking the negative-regulator protein NadR as a way to elevate the expression of genes involved in the synthesis of NAD(H). When NAD(H) is present at a high concentration, the NadR protein represses the transcription of *pncB*, *nadA*, and *nadB* involved in NAD^+ biosynthesis (Foster et al., 1990). Overexpression of *pncB* gene with a mutation on its operator region resulted in an increase of NAD(H) due to preventing the repressor NadR from site-specific binding. (Berríos-Rivera et al., 2002). Excluded this repressor by deleting *nadR* gene were also suspected to lead the cell consistently express the key enzymes in NAD^+ synthesis pathway. In the current study, the *nadR* deletion enhanced xylitol-to-L-xylulose conversion, particular in the *nudC* and *nudC mazG* strains.

The conversion of xylitol to L-xylulose and galactitol to L-tagatose is catalyzed by the NAD^+-dependent enzymes, xylitol 4-dehydrogenase from *Pantoea anantatis* (Aarnikunnas et al., 2006) or galactitol 2-dehydrogenase from *Rhodobacter sphaeroides* (Huwig et al., 1997), respectively. NADH oxidase was also overexpressed because this enzyme has been shown to increase NADH recycling to NAD^+ (Vemuri et al., 2006; Xiao et al., 2010; Zhou et al., 2013). In the current study, production of the rare sugars from the sugar alcohol using these enzymes was elevated in the *E. coli* triple knockout *nadR nudC mazG* compared to the wild-type background as control. This study demonstrates that reducing NAD(H) degradation is important for driving NAD^+-dependent biotransformations and can be a methodology for enhancing formation of the oxidized biochemical product.

Acknowledgments

The authors thank Sarah Lee for her technical assistance. The authors declare she has no conflicts of interests.

References

Aarnikunnas, J. S., A. Pihlajaniemi, A. Palva, M. Leisola, and A. Nyyssola. 2006. Cloning and expression of a xylitol 4-dehydrogenase gene from *Pantoea ananatis*. *Appl. Environ. Microbiol.* 72(1): 368-377.

Baba, T., T. Ara, M. Hasegawa, Y. Takai, Y. Okumura, M. Baba, K. A. Datsenko, M. Tomita, B. L. Wanner, and H. Mori. 2006. Construction of *Escherichia coli* K-12 in-frame, single-gene knockout mutants: the Keio collection. *Mol. Syst. Biol. 2*(1).

Bao, T., X. Zhang, Z. Rao, X. Zhao, R. Zhang, T. Yang, Z. Xu, and S. Yang. 2014. Efficient whole-cell biocatalyst for acetoin production with NAD^+ regeneration system through homologous co-expression of 2, 3-butanediol dehydrogenase and NADH oxidase in engineered *Bacillus subtilis*. *PloS One*. 9(7): e102951.

Battley, E. H. 1991. Calculation of the heat of growth of *Escherichia coli* K-12 cells on succinic acid. *Biotechnol. Bioeng.* 37(4): 334-343.

Battley, E. H. 2003. Absorbed heat and heat of formation of dried microbial biomass. *J. Therm. Anal. Calorim.* 74(3): 709-721.

Berríos-Rivera, S. J., G. N. Bennett, and K. Y. San. 2002. The effect of increasing NADH availability on the redistribution of metabolic fluxes in *Escherichia coli* chemostat cultures. *Metab. Eng*. 4(3): 230-237.

Bernofsky, C., and M. Swan. 1973. An improved cycling assay for nicotinamide adenine dinucleotide. *Anal. Biochem*. 53(2): 452-458.

Datsenko, K. A. and B. L. Wanner. 2000. One-step inactivation of chromosomal genes in *Escherichia coli* K-12 using PCR products. *Proc. Natl. Acad. Sci*. 97(12): 6640-6645.

Eiteman, M. A. and M. J. Chastain. 1997. Optimization of the ion-exchange analysis of organic acids from fermentation. *Anal. Chim. Acta*. 338

Foster, J. W., Y. K. Park, T. Penfound, T. Fenger, and M. P. Spector. 1990. Regulation of NAD metabolism in *Salmonella typhimurium*: molecular sequence analysis of the bifunctional nadR regulator and the nadA-pnuC operon. *J. Bacteriol*. 172(8): 4187-4196.

Frick, D. N. and M. J. Bessman. 1995. Cloning, purification, and properties of a novel NADH pyrophosphatase evidence for a nucleotide pyrophosphatase catalytic domain in MutT-like enzymes. *J. Biol. Chem.* 270(4): 1529-1534.

Galkin, A., L. Kulakova, T. Yoshimura, K. Soda, and N. Esaki. 1997. Synthesis of optically active amino acids from alpha-keto acids with *Escherichia coli* cells expressing heterologous genes. *Appl. Environ. Microbiol*. 63(12): 4651-4656.

Han, Q. and M. A. Eiteman. 2017. Coupling xylitol dehydrogenase with NADH oxidase improves L-xylulose production in *Escherichia coli* culture. *Enzyme Microb. Technol*. 106: 106-113.

Heuser, F., K. Schroer, S. Lütz, S. Bringer-Meyer, and H. Sahm. 2007. Enhancement of the NAD (P)(H) pool in *Escherichia coli* for biotransformation. *Eng. Life Sci*. 7(4): 343-353.

Heuser, F., K. Marin, B. Kaup, S. Bringer, and H. Sahm. 2009. Improving d-mannitol productivity of *Escherichia coli*: impact of NAD, CO2 and expression of a putative sugar permease from *Leuconostoc pseudomesenteroides*. *Metab. Eng*. 11(3): 178-183.

Huwig, A., S. Emmel, G. Jäkel, and F. Giffhorn. 1997. Enzymatic synthesis of L-tagatose from galactitol with galactitol dehydrogenase from *Rhodobacter sphaeroides* D. *Carbohydr. Res*. *305*(3-4): 337-339.

Nobelmann, B. and J. W. Lengeler. 1996. Molecular analysis of the gat genes from *Escherichia coli* and of their roles in galactitol transport and metabolism. *J. Bacteriol.* 178(23): 6790-6795.

O'Handley, S. F., D. N. Frick, C. A. Dunn, and M. J. Bessman. 1998. Orf186 represents a new member of the Nudix hydrolases, active on adenosine (5′) triphospho (5′) adenosine, ADP-ribose, and NADH. *J. Biol. Chem*. 273(6): 3192-3197.

Schurig-Briccio, L. A., M. R. Rintoul, S. I. Volentini, R. N. Farías, L. Baldomà, J. Badía, L. Rodríguez-Montelongo, and V. A. Rapisarda. 2008. A critical phosphate concentration in the stationary phase maintains *ndh* gene expression and aerobic respiratory chain activity in *Escherichia coli*. *FEMS Microbiol. Lett*. 284(1):76-83.

Schurig-Briccio, L. A., R. N. Farías, M. R. Rintoul, and V. A. Rapisarda. 2009a. Phosphate-enhanced stationary-phase fitness of *Escherichia coli* is related to inorganic polyphosphate level. *J. Bacteriol*. 191(13): 4478-4481.

Schurig-Briccio, L.A., R. N. Farías, L. Rodríguez-Montelongo, M. R. Rintoul, and V. A. Rapisarda. 2009b. Protection against oxidative stress in Escherichia coli stationary phase byy a phosphate concentration-dependent genes expression. *Arch. Biochem. Biophys.* 483:106-110.

Vemuri, G. N., E. Altman, D. P. Sangurdekar, A. B. Khodursky, and M. A. Eiteman. 2006. Overflow metabolism in *Escherichia coli* during steady-state growth: transcriptional regulation and effect of the redocx ratio. *Appl. Environ. Microbiol.* 72(5): 3653-3661.

Wang, L., Y. J. Zhou, D. Ji, X. Lin, Y. Liu, Y. Zhang, W. Liu, and Z. K. Zhao. 2014. Identification of UshA as a major enzyme for NAD degradation in *Escherichia coli*. *Enzyme Microb. Technol.* 58: 75-79.

Xiao, Z., C. Lv, C. Gao, J. Qin, C. Ma, Z. Liu, P. Liu, L. Li, and Xu, P. 2010. A novel whole-cell biocatalyst with NAD^+ regeneration for production of chiral chemicals. *PloS One*. 5(1): e8860.

Zhang, J. and M. Inouye. 2002. MazG, a nucleoside triphosphate pyrophosphohydrolase, interacts with Era, an essential GTPase in *Escherichia coli*. *J. Bacteriol*. 184(19): 5323-5329.

Zhou, Y. J., W. Yang, L. Wang, Z. Zhu, S. Zhang, and Z. K. Zhao. 2013. Engineering NAD^+ availability for *Escherichia coli* whole-cell biocatalysis: a case study for dihydroxyacetone production. *Microb. Cell Fact.* 12(1): 103.

Table 2-1. Strains and plasmids used in this study.

Strain or Plasmid	Relevant Characteristics	Reference
Strains		
MG1655	*E. coli* F$^-$ □$^-$ *ilvG rfb*50 *rph*-1	wild-type
MEC495	MG1655 □*ushA763*::(FRT)	This study
MEC504	MG1655 □*nudE732*::(FRT)	This study
MEC516	MG1655 □*nudC767*::(FRT)	This study
MEC517	MG1655 □*nadR786*::(FRT)	This study
MEC518	MEC517 *nudC767*::(FRT)	This study
MEC695	MG1655 □*mazG780*::(FRT)	This study
MEC696	MEC516 □*mazG780*::(FRT)	This study
MEC697	MEC518 *mazG780*::(FRT)	This study
MEC763	MG1655 *gatB788*::(FRT)	This study
MEC766	MEC697 □*gatB788*::(FRT)	This study
Plasmids		
pZE12-*xdh*	Codon optimized *xdh* gene coding xylitol 4-dehydrogenase from *Pantoea ananatis* (ATCC 43072)	Aarnikunnas et al., 2006; Han and Eiteman, 2017
pZE12-*gdh*	Codon optimized *gdh* gene coding galactitol 2-dehydrogenase from *Rhodobacter sphaeroides* (ATCC 43072)	Huwig et al., 1997; This study
pCS27-*nox*	*nox* gene coding water-forming NADH oxidase from *Streptococcus pneumoniae*	Vemuri et al., 2006a; Han and Eiteman, 2017

CHAPTER 5

ACETATE FORMATION DURING RECOMBINANT PROTEIN PRODUCTION IN *ESCHERICHIA COLI* WITH AN ELEVATED NAD(H) POOL[3]

[3] Han, Q. and M. A. Eiteman. To be submitted to *Journal of Industrial Microbiology and Biotechnology*.

Abstract

Acetate formation is a disadvantage in the use of *Escherichia coli* for recombinant protein production, and many studies have focused on optimizing fermentation processes or altering metabolism to eliminate acetate accumulation. In this study, we found *E. coli* MEC697 (MG1655 *nadR nudC mazG*) maintaining a larger pool of NAD(H) compared to the wild-type control, also accumulated lower concentrations of acetate when grown in batch culture on glucose. In steady-state cultures, the elevated total NAD(H) found in MEC697 delayed the threshold dilution rate for acetate formation to a growth rate of 0.27 h^{-1}. Batch and fed-batch processes using MEC697 were examined for the production of β-galactosidase as a model recombinant protein. Fed-batch culture of MEC697/pTrc99A-*lacZ* compared to MG1655/pTrc99A-*lacZ* at a growth rate of 0.22 h^{-1} showed only a modest increase of protein formation. However, 1-liter batch growth of MEC697/pTrc99A-*lacZ* resulted in 50% lower acetate formation compared to MG1655/pTrc99A-*lacZ* and a two-fold increase in recombinant protein production.

Introduction

Escherichia coli is often used for the commercial production of chemicals and recombinant proteins. However, acetate formation in aerobically grown cultures of *E. coli* is undesirable because the chemical inhibits cell growth and protein formation (Jensen and Carlsen, 1990; El-Mansi, 2004) and induces stress responses even at a low concentration (Nakano et al., 1997). Moreover, the formation of acetate constitutes a diversion of carbon that might have contributed to biomass or protein synthesis (March et al., 2002).

Under aerobic batch growth on glucose as the sole carbon source, acetate accumulates as a result of overflow metabolism. Comparison of several common *E. coli* strains led to a range of 0.88 – 5.12 g/L acetate when grown in batch cultures with 20 g/L glucose (Luli and Strohl, 1990). In *E. coli*, the complete oxidation of 1 mol of glucose via glycolysis and the tricarboxylic acid (TCA) cycle generates 10 mol of NAD(P)H and 2 mol of $FADH_2$ (Neidhardt et al., 1990). Those reduced cofactors can theoretically be reoxidized within the electron transport chain to maintain a redox balance and generate ATP by oxidative phosphorylation. However, if the capacity to oxidize reduced cofactors is lower than the rate of glucose consumption, cells respond as though they are oxygen limited (Andersen and Meyenburg, 1980). Specifically, NADH accumulates (Vemuri et al., 2006a), and this cofactor acts as an allosteric inhibitor of citrate synthase (Weitzman and Danson, 1976), reducing the flux of acetyl CoA into the TCA cycle (Iuchi et al., 1994). The redox ratio of $NADH/NAD^+$ correlates with acetate overflow in *E. coli*, with a ratio greater than a critical redox ratio of 0.06 marking the onset of acetate formation. Acetate formation can be delayed by reducing the $NADH/NAD^+$ ratio, for example, by overexpression of a water-form NADH oxidase (Vemuri et al., 2006a). Acetate is generated mainly via the enzymes phosphotransacetylase and acetate kinase when carbon from acetyl-CoA

is directed to acetate. Since the TCA cycle generates NADH while acetate formation does not, acetate formation is a means to modulate the redox balance (Andersen and Meyenburg, 1977; Andersen and Meyenburg, 1980; Reiling et al., 1985).

Various strategies have been applied to reduce acetate formation, including metabolic engineering (Chou et al., 1994; San et al., 1994; Aristidou et al., 1999) and process control (Konstantinov et al., 1990; Kleman et al., 1991; Riesenberg and Guthke, 1999; Åkesson et al., 2001; Johnston et al., 2003). As noted above, acetate formation commences when the cell growth rate or glucose uptake rate surpasses a threshold (Vemuri et al., 2006a), and since the oxygen consumption rate also reaches a maximum at this threshold (Varma and Palsson, 1994), many metabolic engineering and process strategies address the balance between growth rate and oxygen utilization.

Because of the relationship between acetate formation and NAD(H), we hypothesized that curtailing the natural degradation of NAD(H) by the cell would directly impact acetate formation and thus would affect recombinant protein production. An *E. coli* strain (MEC697) with *nadR nudC mazG* gene knockouts associated with NAD(H) degradation pathway elevates the NAD(H) pool during the cell growth (Han and Eiteman, 2018). An increase of total NAD(H) is believed to encourage a lower NADH/NAD^+ ratio (San et al., 2002). Thus, in this study we examined growth and metabolism of MEC697 compared to the wild-type on several carbon sources. A decrease of acetate formation was indeed found during growth on glucose as the sole carbon source. We further examined MEC697 for the production of β-galactosidase as a model recombinant protein.

Materials and Methods

Strains and Plasmids

Escherichia coli MG1655, MEC697 (MG1655 *nadR nudC mazG*) were used in this study (Han and Eiteman, 2018). The plasmid pTrc99A-*lacZ* expressing β-galactosidase (March et al., 2002) was transformed into each strain.

Growth Medium

The defined medium contained (per L): 2.8 g KH_2PO_4, 5.1 g K_2HPO_4, 2.5 g K_2SO_4, 4.38 g NH_4Cl, 25.0 mg $Na_2(EDTA)\cdot 2H_2O$, 0.15 g $MgSO_4\cdot 7H_2O$, 20 mg citric acid, 0.25 mg $ZnSO_4\cdot 7H_2O$, 0.125 mg $CuCl_2\cdot 2H_2O$, 1.25 mg $MnSO_4\cdot H_2O$, 0.875 mg $CoCl_2\cdot 6H_2O$, 0.06 mg H_3BO_3, 0.25 mg $Na_2MoO_4\cdot 2H_2O$, 5.5 mg $FeSO_4\cdot 7H_2O$, and 20 mg thiamine·HCl. The pH of the medium was adjusted to 7.0 with 30% (w/v) NaOH. This medium was supplemented with 20 g/L glucose, gluconate, or sorbitol, or 10 g/L glucose for recombinant protein production. For a fed-batch study, the bioreactor initially contained this defined medium with 2.5 g/L glucose; and the feed solution contained (per L): 250 g glucose, 7.0 g $MgSO_4\cdot 7H_2O$, 2 mg $CoCl_2\cdot 6H_2O$, 7.85 mg $MnCl_2\cdot 4H_2O$, 0.8 mg $CuCl_2\cdot 2H_2O$, 1.67 mg H_3BO_3, 4.0 mg $Na_2MoO_4\cdot 2H_2O$, 21 mg $FeSO_4\cdot 7H_2O$, and 4.5 mg EDTA. Cultures using strains harboring the pTrc99A-*lacZ* plasmid contained 50 mg ampillicin/L.

Batch processes

Shake flask cultures (50 mL) grown to an OD of 3 in defined medium were used to inoculate a 2.5 L bioreactor (Bioflo 2000, New Brunswick Scientific Co., Edison, NJ) containing 1.3 L of defined medium to compare carbon sources or 1.0 L of medium for β-galactosidase production. In both cases, agitation was maintained at 400 rpm, and temperature was 37°C. Air flow rate was controlled at 1.0 L/min with oxygen mixed as necessary to ensure a dissolved

oxygen (DO) concentration above 40% of saturation. The pH was maintained at 7.0 with automatic addition of 15% KOH/5% NH_4OH. Additionally, cultures for β-galactosidase production were induced with 0.75 mM IPTG when the OD reached 0.5.

Steady-state processes

Carbon-limited chemostats were initiated in batch mode in the 2.5 L bioreactor containing 1 L of defined medium with 5 g/L glucose. When the OD reached 4, a continuous process commenced using a selected constant feed/effluent rate and 10 g/L glucose. A steady-state condition was assumed after five residence times, at which time the oxygen and CO_2 concentrations in the effluent gas remained unchanged. During the entire process, the pH was maintained at 7.0 with 15% KOH/5% NH_4OH, the temperature at 37°C, and the agitation at 400 rpm. An airflow rate of 1.0 liter/min using mass flow controllers (Unit Instruments, Orange, CA) ensured the DO concentration remained above 40% of saturation.

Fed-batch processes

Fed-batch processes were carried out in the 2.5 L bioreactor (Bioflo 310, New Brunswick Scientific Co., Edison, NJ) with 0.8 L initial volume. When the initial glucose was nearly exhausted under batch conditions, the fed-batch mode was commenced by exponentially feeding the medium so that cell growth was a constant specific rate of 0.22 h^{-1}. The pH was maintained at 7.0 with 15% NH_4OH, the temperature at 37°C, and the agitation at 400 rpm. Air and oxygen were mixed as necessary at 1.0 - 1.5 liter/min flow rate to maintain a DO concentration above 40% of saturation.

Quantification of NAD^+/NADH and pyruvate/phosphoenolpyruvate

NAD^+ and NADH concentration were measured by a cycling enzymatic method (Bernofsky and Swan, 1973), where alcohol dehydrogenase uses NAD^+ to oxidize ethanol into

acetaldehyde, and NAD^+ or NADH transfers the reducing equivalents from ethanol ultimately to MTT. The rate of formation of reduced MTT measured at 570 nm is proportional to the amount of NAD^+ or NADH.

The cell extracts for intracellular pyruvate and phosphoenolpyruvate (PEP) measurements were prepared by a modified perchloric acid method (Schaefer et al., 1999). Briefly, 10 mL culture was promptly combined with 30 mL of 60% (v/v) methanol (-50°C), and then centrifuged (10,300 × g for 5 min at -20°C). The pellet was resuspended in 2 mL of 35% (w/v) $HClO_4$ (-25°C). After 10 min in ice, the $HClO_4$ treated samples were centrifuged (42,000 × g for 30 min at 4°C), and neutralized with 5 M K_2CO_3 to pH 7.0. The resulting precipitate was centrifuged (42,000 × g for 10 min at 4°C), and the supernatant assayed enzymatically to determine the concentration of pyruvate or PEP. For pyruvate measurement, the reaction mixture contained 50 mM TEA/EDTA buffer (adjusted with 20% NaOH to pH 7.6), 12 mM $MgSO_4$, 44 mM KCl, 1 mM ADP, 0.3 mM NADH, and 50 U/mL lactate dehydrogenase (Sigma-Aldrich, St. Louis, MO). For PEP measurement, 50 U/mL pyruvate kinase was also added (Sigma-Aldrich, St. Louis, MO). The rate of decline of NADH measured at 420 nm is proportional to the quantity of pyruvate or PEP.

Enzyme Activity

In this study, a whole cell measurement was used to measure the activity of β-galactosidase (Pardee et al., 1959). Briefly, 100 μL of a cell sample was added into 900 μL pretreatment mixture, which contained 0.1 M sodium phosphate buffer (pH 7.0), 10 mM KCl, 10 mM $MgSO_4$, 0.9 μM SDS, 0.3 mM β-mercaptoethanol, and 0.6 mM chloroform. After incubation at 30°C for 5 min, the measurement was initiated by adding 200 μL of 13.2 mM ortho-nitrophenyl-β-D-galactoside, while 500 μL of 1 M Na_2CO_3 terminated the reaction. One

unit of β-galactosidase was defined as the amount of enzyme to generate 1 μmol of o-nitrophenol per min at 30°C.

Analytical methods

The optical density at 600 nm (OD) was used to monitor cell growth (UV-650 spectrophotometer, Beckman Instruments, San Jose, CA). Liquid chromatography with a refractive index detector and a Coregel 64-H ion-exclusion column (Transgenomic Ltd., Glasgow, United Kingdom) with a mobile phase of 4 mN H_2SO_4 was used for analysis of organic chemicals (Eiteman and Chastain, 1997). For dry cell weight (DCW) measurement, three independent 10.0 mL samples were centrifuged (8,400 × g for 10 min), and the cell pellets washed with 30 mL deionized (DI) water three times then dried at 60°C for 24 h. Oxygen uptake rate and CO_2 evolution rate were calculated by measuring the influent and effluent concentrations of oxygen and CO_2 (Ultramat 23 gas analyzer, Siemens, Germany).

Results

Batch growth of E. coli MG1655 and MEC697 on various carbon sources.

In a previous study, *E. coli* MEC697 having knockouts in three genes associated with NAD(H) degradation (MG1655 *nadR mudC mazG*) showed an increased intracellular pool of NAD(H) (Han and Eiteman, 2018). Since the use of carbon sources with different oxidation states affects the intracellular NAD(H) pool (San, et al., 2002), MEC697 and MG1655 were each grown on 20 g/L of gluconate, glucose, or sorbitol as the sole carbon source in a batch process using a controlled bioreactor.

With 20 g/L glucose as the carbon source, MG1655 attained 6.5 g/L biomass and 2.1 g/L acetate in 10.3 h with a specific growth rate of 0.53 h^{-1} (Fig. 4-1). During the exponential growth phase, MG1655 maintained a concentration of total NAD(H) (i.e., NAD^+ plus NADH) of 4.6

μmol/g DCW. For MEC697 on glucose, 6.7 g/L biomass and 1.1 g/L acetate was obtained in 11 h with a specific growth rate of 0.60 h^{-1} (Fig. 4-2). MEC697 maintained about 6.7 μmol/g DCW NAD(H).

Using gluconate as carbon source, the average NAD(H) for MG1655 was 11.6 μmol/g DCW, and ultimately 2.5 g/L acetate accumulated in the culture (Fig. 4-3). For MEC697, the NAD(H) was 16.8 μmol/g DCW, and about 2.9 g/L acetate accumulated when the gluconate was exhausted (Fig. 4-4). Using sorbitol as carbon source, a greater amount of NAD(H) was also observed during growth of MEC697: 12.4 μmol/g DCW for MG1655 compared to 18.2 μmol/g DCW for MEC697 (Fig. 4-5 & 4-6). For both strains the acetate accumulation was very low: 0.11-0.12 g/L.

For each of these three carbon sources, MEC697 exhibited a greater total NAD(H) concentration than MG1655 during the exponential growth phase (Table 3-1). The culture grown on gluconate led both strains to accumulate more acetate than cultures grown on glucose or sorbitol. Although acetate accumulation from glucose was twice as great in MG1655 than in MEC697, no significant difference between acetate formation was observed between these two strains when grown on gluconate or sorbitol. Interestingly, significant pyruvate accumulated (about 0.4-1.6 g/L) when either strain was grown on gluconate as the sole carbon source.

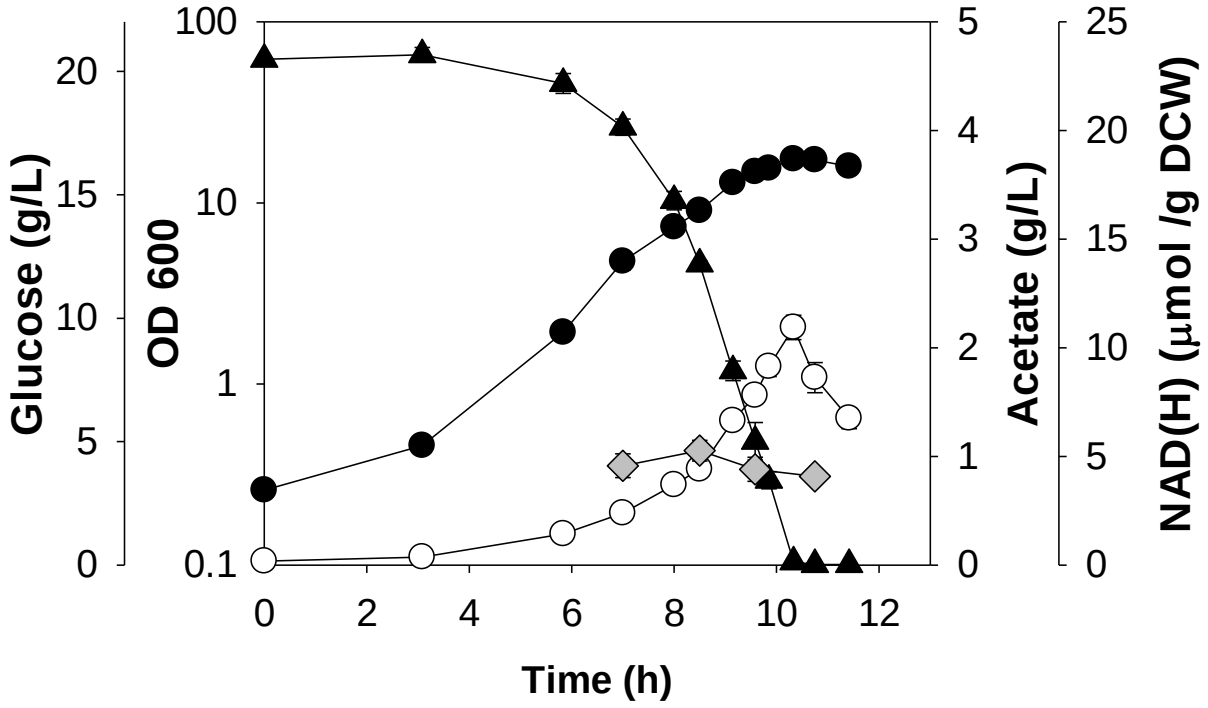

Figure 4-1. Acetate formation during batch growth of MG1655 on 20 g/L glucose: OD (●); glucose (▲); Acetate (○); Total NAD(H) (◆). Error bars indicate standard deviation.

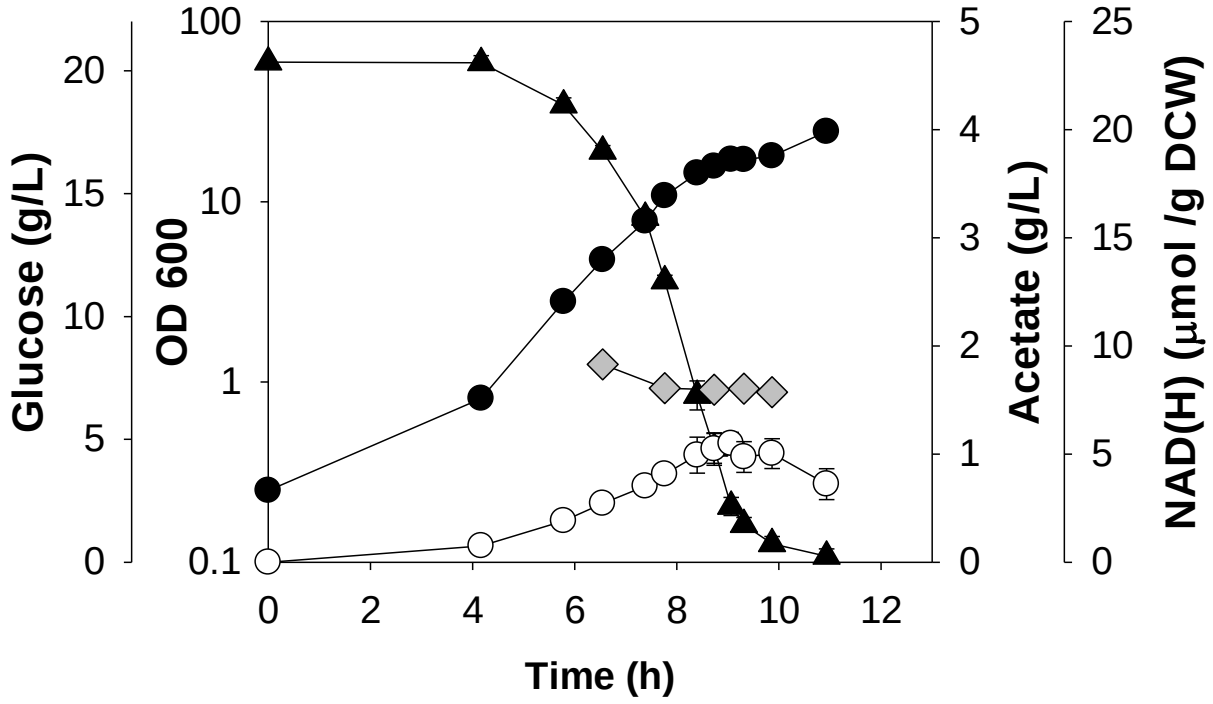

Figure 4-2. Acetate formation during batch growth of MEC697 on 20 g/L glucose: OD (●); glucose (▲); Acetate (○); Total NAD(H) (◆). Error bars indicate standard deviation.

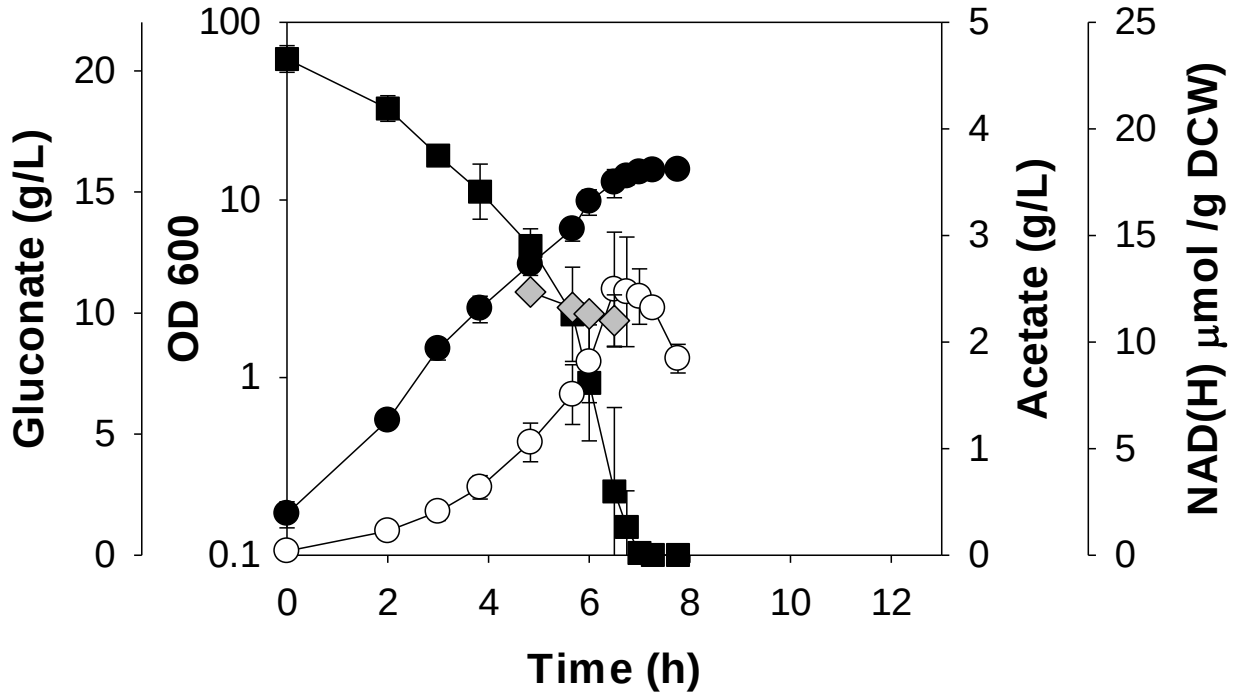

Figure 4-3. Acetate formation during batch growth of MG1655 on 20 g/L gluconate: OD (●); gluconate (■); Acetate (○); Total NAD(H) (◆). Error bars indicate standard deviation.

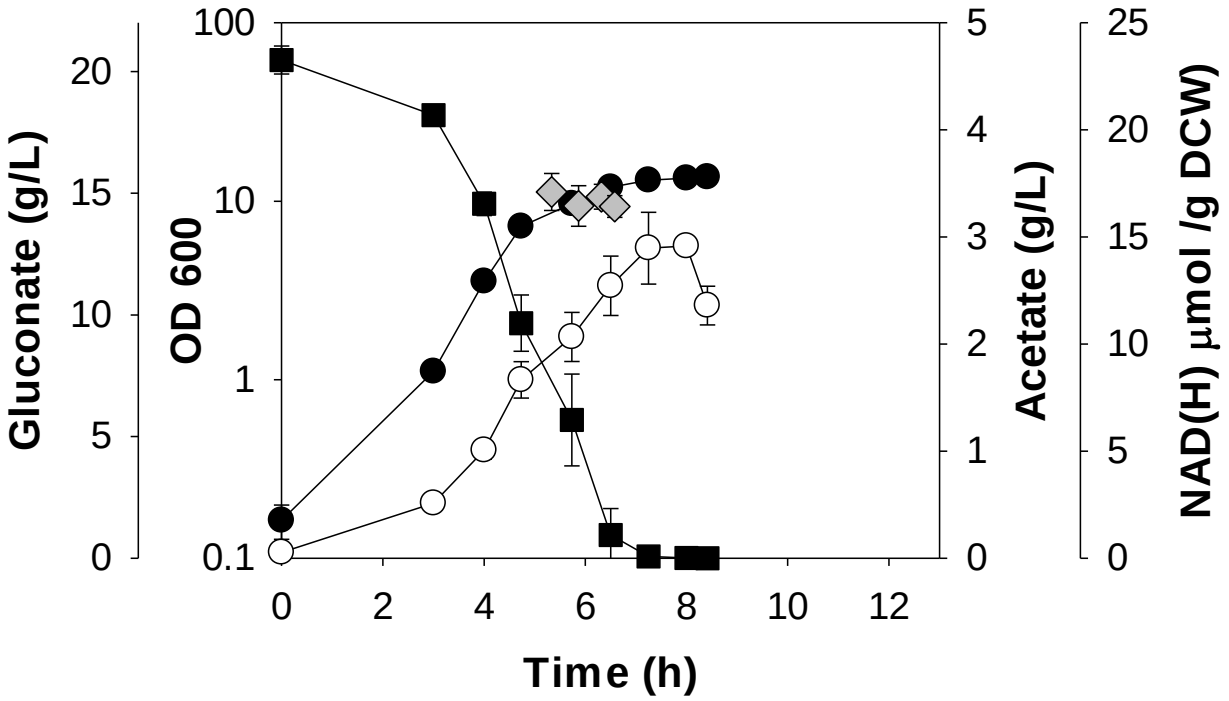

Figure 4-4. Acetate formation during batch growth of MEC697 on 20 g/L gluconate: OD (●); gluconate (■); Acetate (○); Total NAD(H) (◆). Error bars indicate standard deviation.

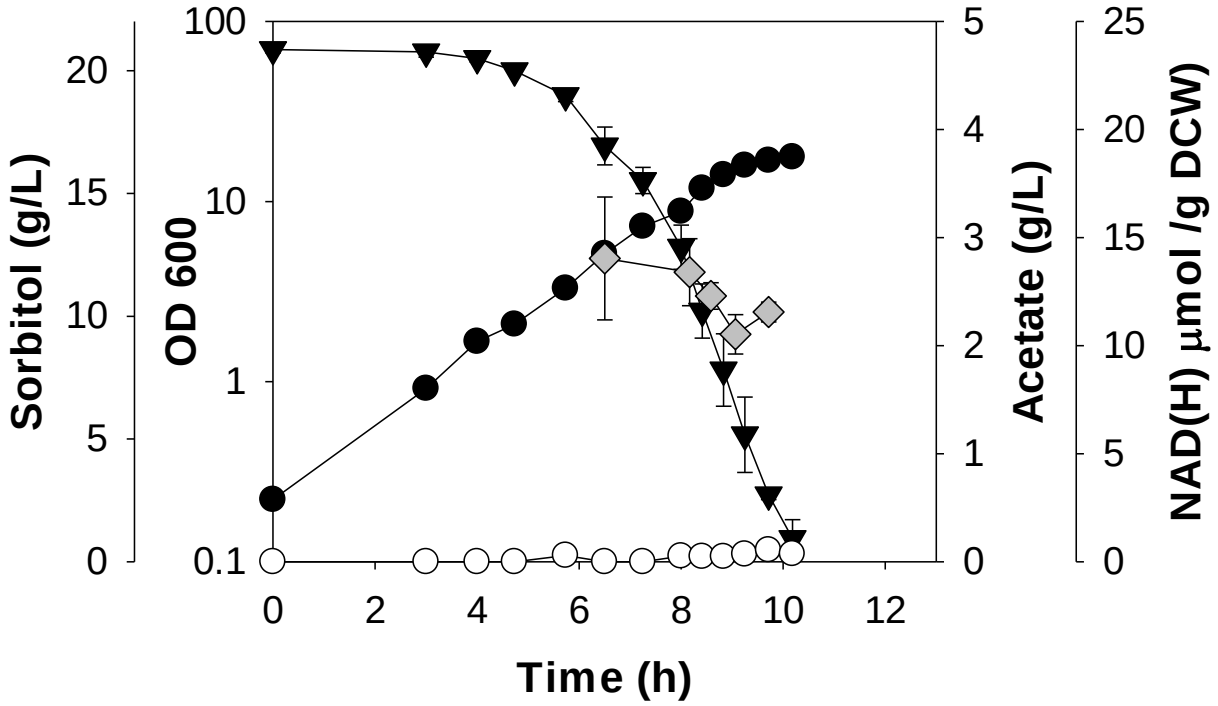

Figure 4-5. Acetate formation during batch growth of MG1655 on 20 g/L sorbitol: OD (●); sorbitol (▼); Acetate (○); Total NAD(H) (◆). Error bars indicate standard deviation.

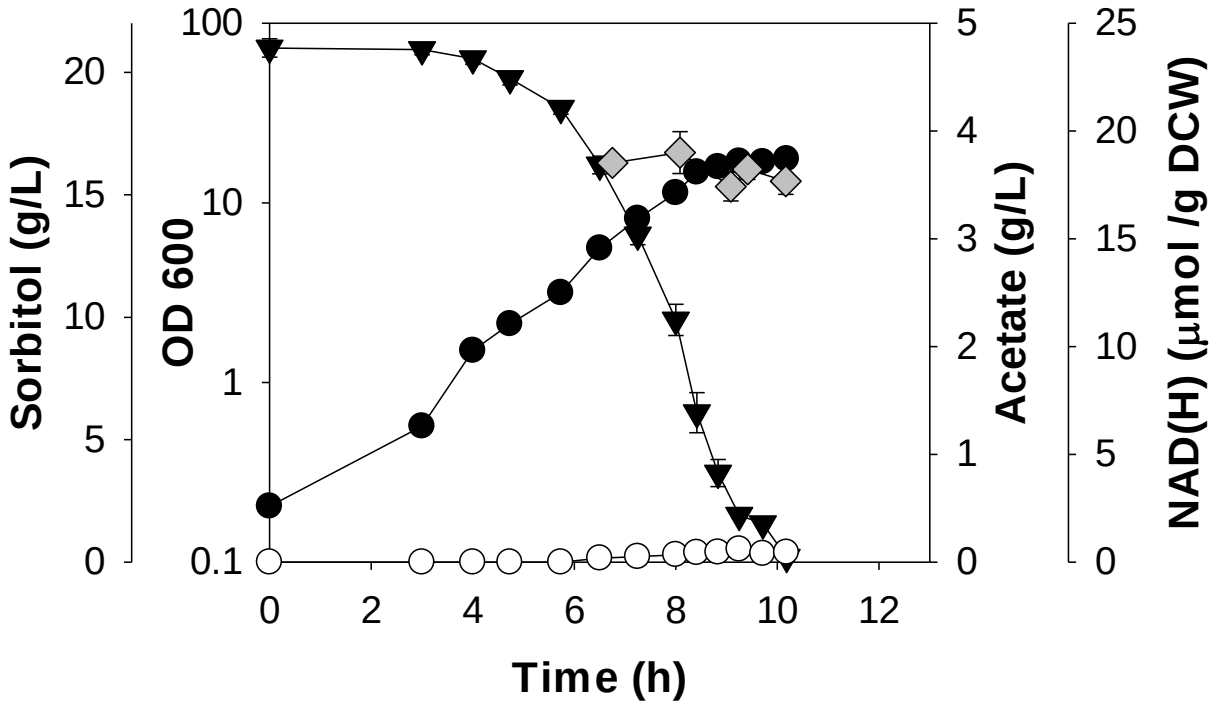

Figure 4-6. Acetate formation during batch growth of MEC697 on 20 g/L sorbitol: OD (●); sorbitol (▼); Acetate (○); Total NAD(H) (◆). Error bars indicate standard deviation.

Steady-state growth of MG1655 and MEC697 on glucose

A chemostat permits microbial growth to achieve a constant nutrient-limited growth rate, and therefore a constant specific glucose consumption rate. Such a system allows a comparatively precise analysis of metabolism. Previous research found that acetate formation correlates with the specific glucose consumption rate: acetate formation ("overflow") commenced only when the glucose consumption surpassed a threshold rate which itself correlated with NAD(H) (Vemuri et al., 2006a). To examine such overflow metabolism when NAD(H) degradation pathways were knocked out, we compared MG1655 and MEC697 under steady-state glucose-limited growth at different dilution rates. As shown in Fig. 4-7, no acetate accumulated when either strain grew at a low growth rate (low glucose consumption rate, q_S). When the glucose consumption rate exceeded a threshold value, acetate accumulation commenced, and this threshold occurred at a specific glucose consumption rate (q_S) of about 0.50 g/g DCW h for MG1655 and about 0.70 g/g DCW h for MEC697. Furthermore, as the specific glucose consumption rate further increased, MEC697 exhibited lower acetate formation. For example, at the dilution rate of 0.27 h^{-1}, MG1655 achieved a steady-state acetate concentration of 1.39 g/L (q_A = 0.13 g/g DCW h), while MEC697 achieved a steady-state acetate concentration of only 0.11 g/L (q_A = 0.01 g/g DCW h). Acetate accumulation in MG1655 led to a decrease in biomass yield ($Y_{X/S}$) from 0.42 to 0.29 (g DCW/ g glucose consumed), while biomass yield for MEC697 was maintained above 0.40 g DCW/g even after acetate accumulated (Fig. 4-7). The specific oxygen consumption rate (q_{O2}) and CO_2 evolution rate (q_{CO2}) for MG1655 and MEC697 increased with increasing q_S (or growth rate) (Fig. 4-8), with no significant difference between MG1655 and MEC697. The carbon balance for both strains was 90-100% under all conditions.

Since the batch processes revealed a greater NAD(H) concentration in MEC697 than in MG1655, the concentrations of these two cofactors were also measured in the steady-state experiments. At any given value of q_S, the total NAD(H) concentration in MG1655 was 6.5 to 9.0 μmol/g DCW (Fig. 4-9A)., while the total NAD(H) concentration in MEC697 was consistently greater than MG1655, which was 12.9 to 17.7 umol/g DCW (Fig. 4-9B). Although this same difference between total NAD(H) concentration was observed at low growth rates when acetate did not accumulate, lower acetate formation was found in the strain with greater NAD(H) availability

We also measured the steady-state intracellular concentrations of two key glycolytic intermediates in order to identify imbalances that might exist in the two strains as the glucose consumption rate increased (Fig 4-10). Pyruvate and PEP participate in a large number of biochemical reactions, and a change in the intracellular level of these two important intermediates could indicate the shift of fluxes in pathways using pyruvate or PEP (Vemuri et al, 2006a). For MG1655, acetate accumulation correlated with an elevated pyruvate and decreased PEP concentration (Fig. 4-10A). For MEC697, the steady-state concentrations for pyruvate and PEP did change as abruptly with increasing glucose consumption (Fig. 4-10B).

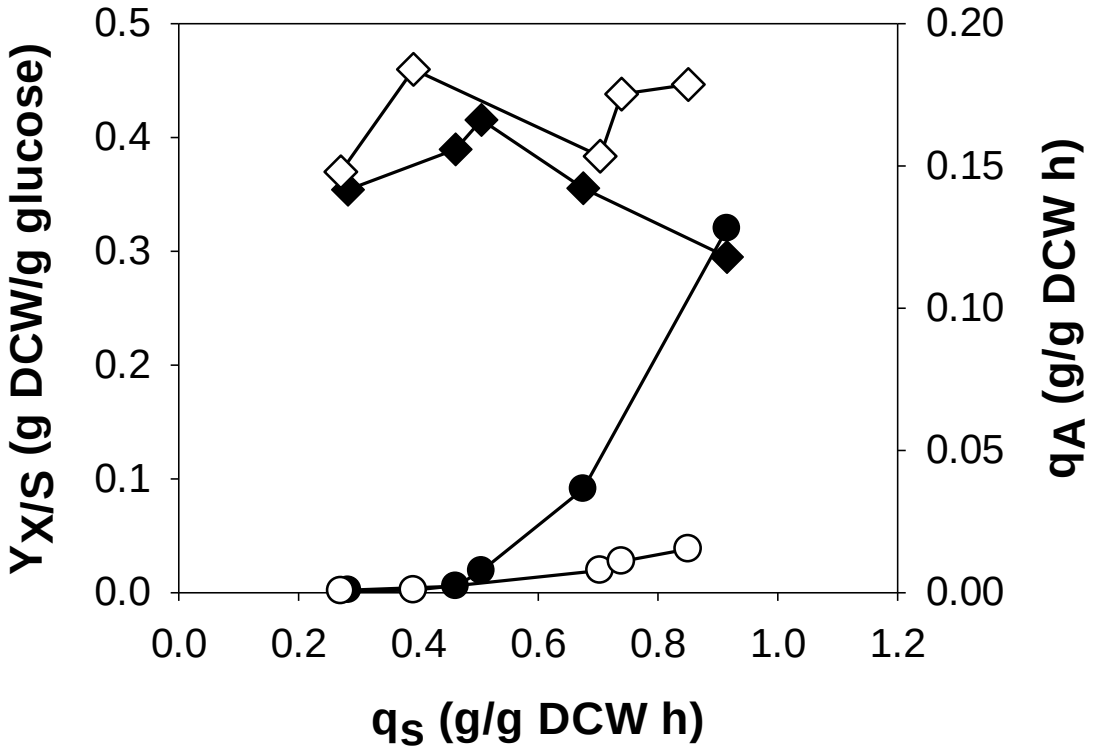

Figure 4-7. Steady-state physiological profiles of MG1655 and MEC697 on 10 g/L glucose: the biomass yield $Y_{x/s}$ (◆, ◇) and specific acetate formation rate q_A (●, ○) are shown for MG1655 (solid symbols) are and MEC697 (open symbols) as functions of the specific glucose consumption rate q_s.

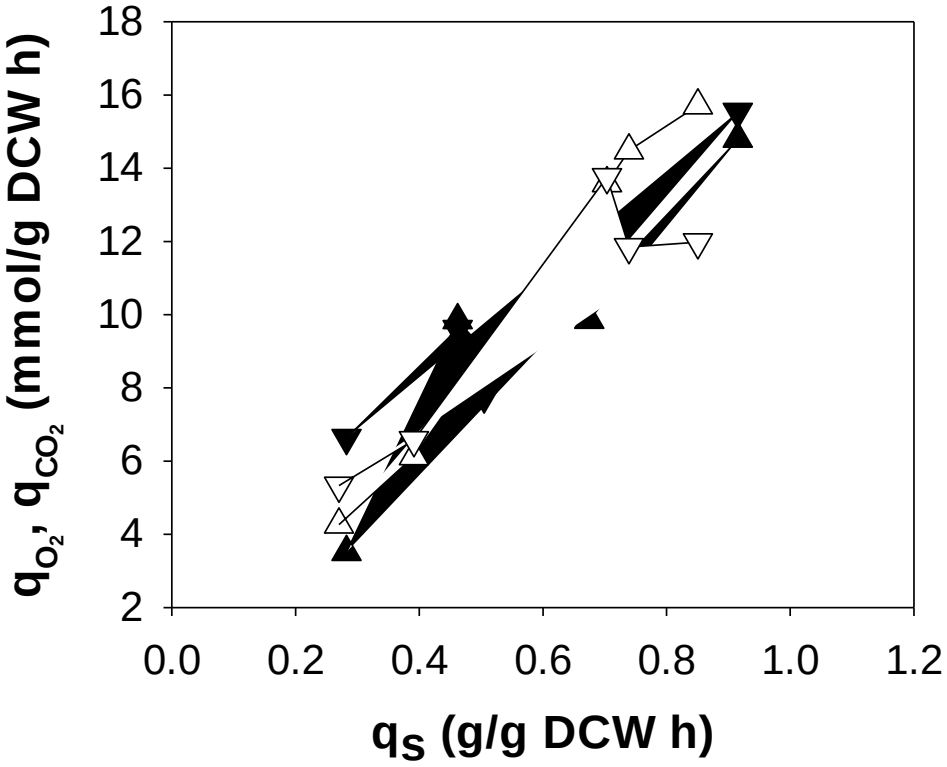

Figure 4-8. Steady-state respiration for MG1655 and MEC697: the specific oxygen consumption rate q_{O2} (▲, △) and the specific CO2 evolution rate q_{CO2} (▼, ▽) are compared for MG1655 (solid symbols) and MEC697 (open symbols) as functions of q_s.

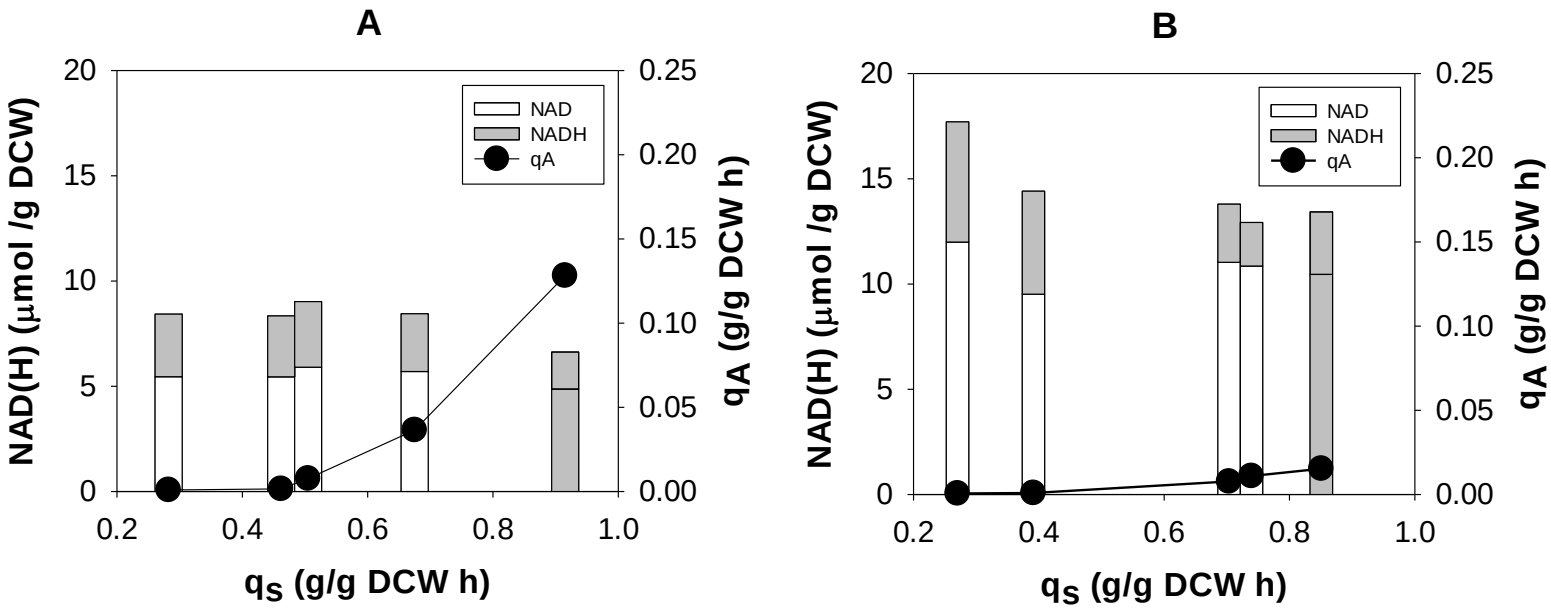

Figure 4-9. Intracellular concentrations of NAD^+ and NADH in MG1655 (A) and MEC697 (B) during growth in steady-state at different q_s. The specific acetate formation rate q_A (●) are also shown as functions of q_s.

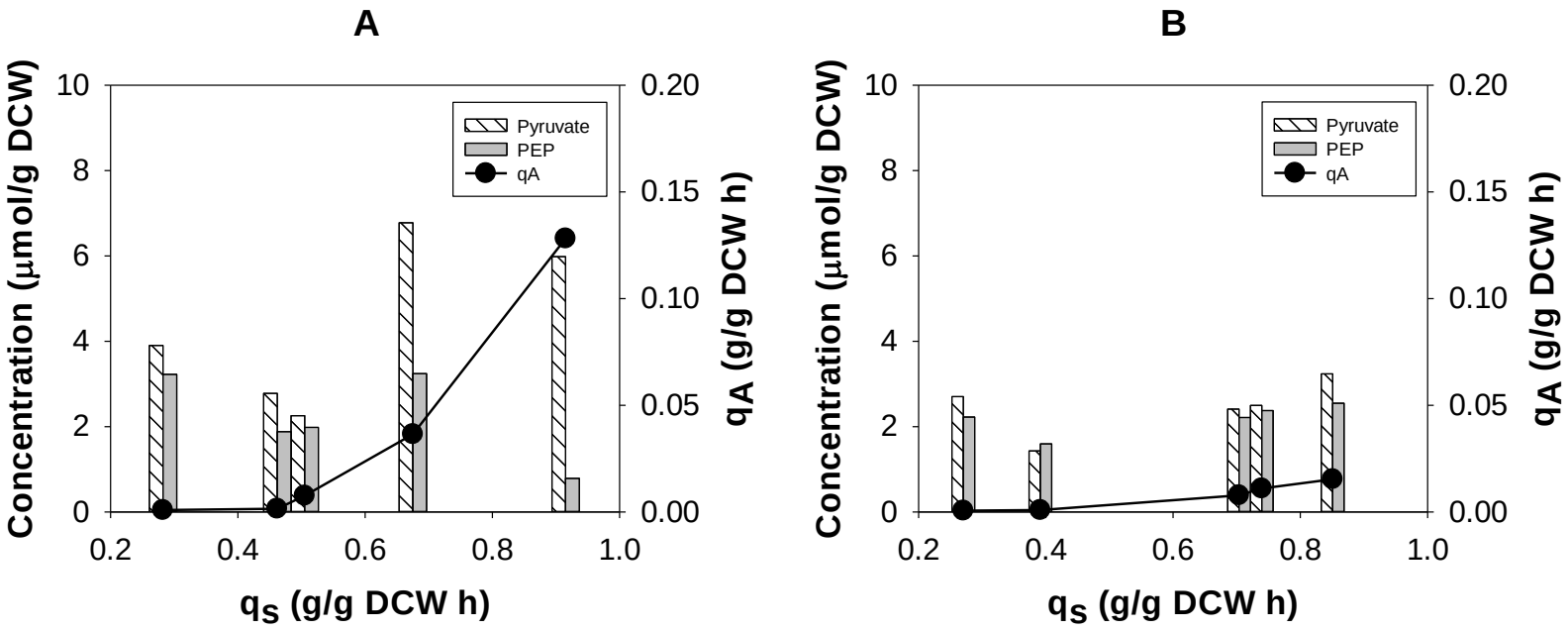

Figure 4-10. Intracellular concentrations of glycolysis metabolites pyruvate and PEP in MG1655 (A) and MEC697 (B) during growth in steady-state at different q_s. The specific acetate formation rate q_A (●) are also shown as functions of q_s.

Recombinant protein production in an exponential fed-batch process.

An exponential fed-batch process is an operational mode which provides a constant growth rate while attaining a high cell density cultivation for recombinant protein production (Korz et al., 1995; Horn et al., 1996). In order to compare MG1655 and MEC697 for recombinant protein production, we transformed the two strains with pTrc99A-*lacZ* expressing the model protein β-galactosidase and performed glucose-limited fed-batch processes using a feed to maintain a specific growth rate of about 0.22 h^{-1}. After a short initial batch process with 2.5 g/L glucose, the process was switched to fed-batch growth using a feed of 250 g/L glucose. For both MG1655 and MEC697 (Fig. 4-11 & 4-12, respectively), the biomass increased exponentially, and the glucose concentration remained at zero. MG1655 reached to 53.7 g DCW/L biomass in 14.7 h with a biomass yield of 0.21 g DCW/g glucose consumed, and ultimately generated 302 kU/L β-galactosidase with the yield of 1.21 kU/g glucose consumed (Fig. 4-11). MEC697 reached 56.1 g DCW/L biomass in 16.6 h with the yield of 0.22 g DCW/g glucose consumed, and a slightly greater β-galactosidase concentration of 344 kU/L with the yield of 1.38 kU/g glucose consumed (Fig. 4-12). Interestingly, MG1655 did not accumulate more acetate than MEC697 at that moderate growth rate. The fed-batch process with MEC697 with a constant growth rate of 0.22 h^{-1} showed at best only a modest increase in recombinant protein production compared to fed-batch growth of MG1655.

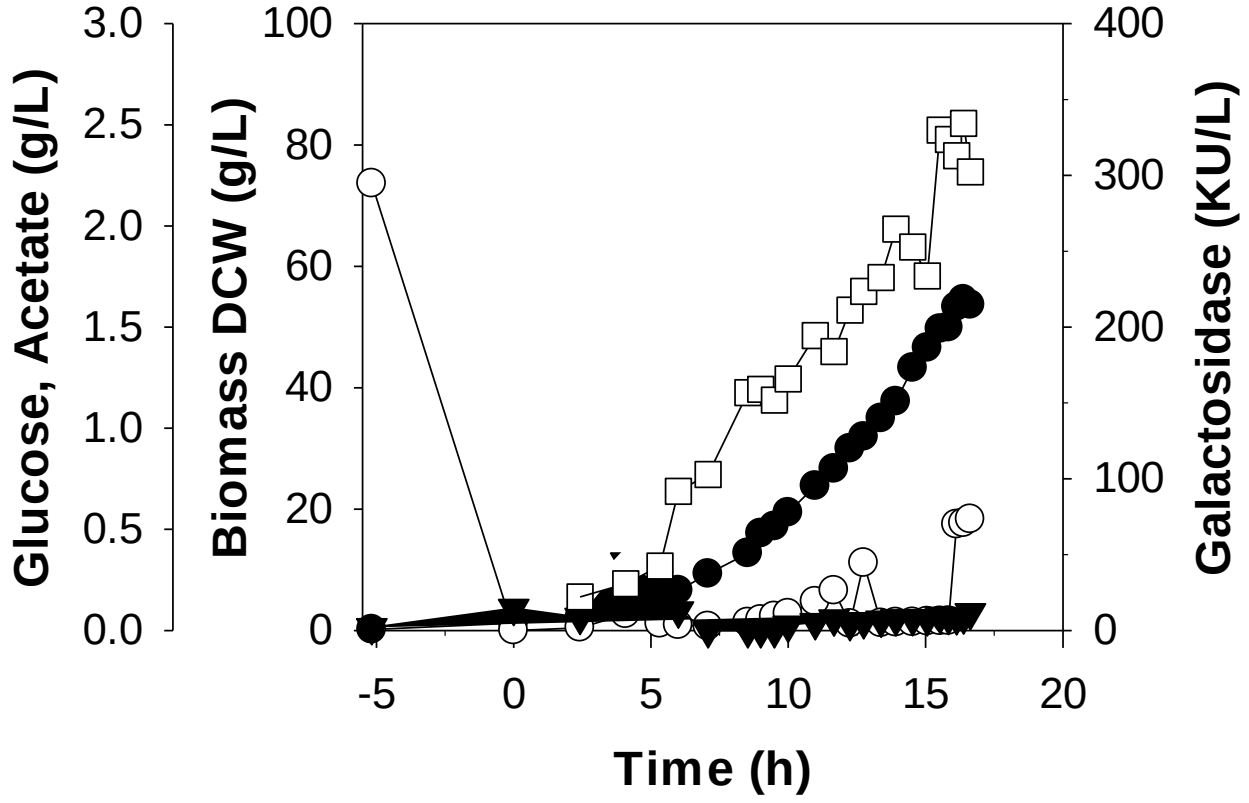

Figure 4-11. Production of b-galactosidase during exponential fed-batch growth of MG1655 pTrc99A-*lacZ* on 250 g/L glucose: biomass (▲); glucose (○); acetate (▼); β-galactosidase (□). Error bars indicate standard deviation.

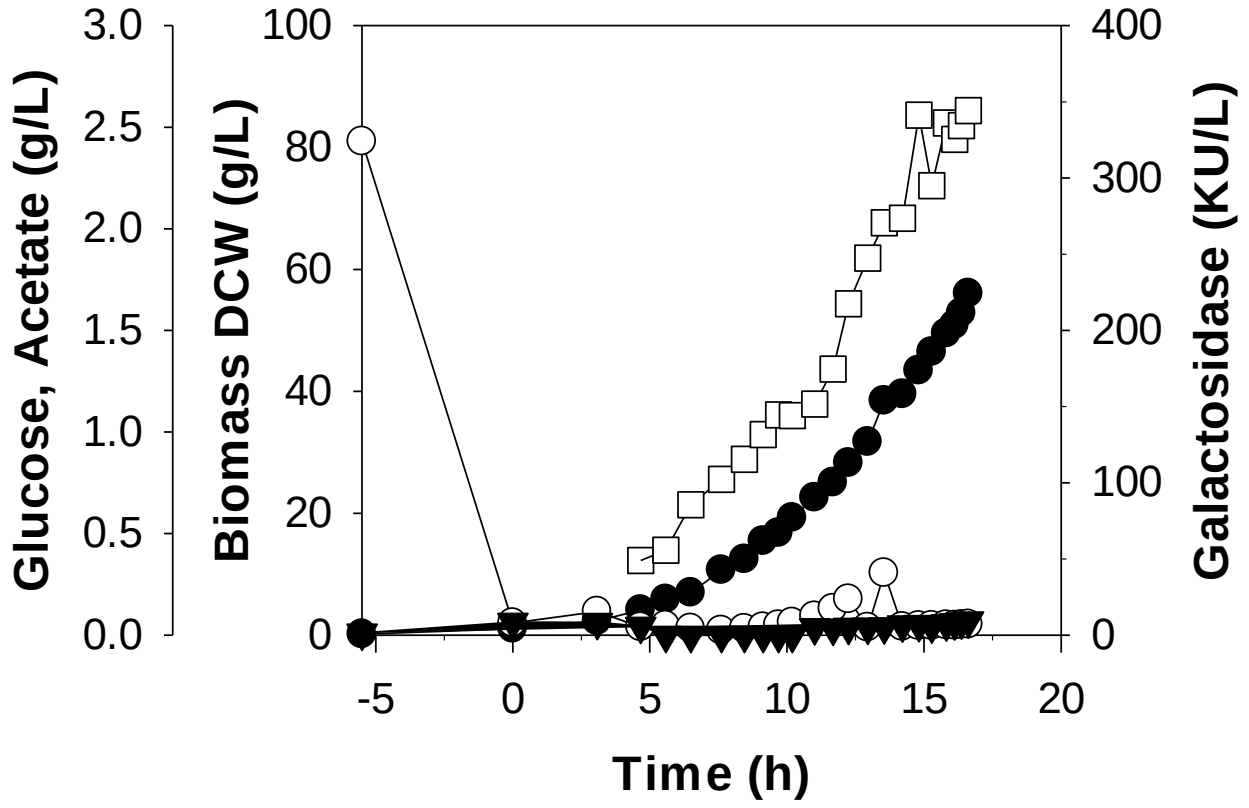

Figure 4-12. Production of b-galactosidase during exponential fed-batch growth of MEC697 pTrc99A-*lacZ* on 250 g/L glucose: biomass (▲); glucose (○); acetate (▼); β-galactosidase (□). Error bars indicate standard deviation.

Recombinant protein production in a batch process

We were also interested in whether recombinant protein formation was different in MEC697 compared to MG1655 under maximum growth rate, batch conditions. Therefore, duplicate batch processes using 10 g/L glucose compared MG1655/pTrc99A-*lacZ* with MEC697/pTrc99A-*lacZ* (Fig. 4-13 & 4-14, respectively). MG1655/pTrc99A-*lacZ* reached a biomass concentration of 3.64 g DCW/L in 10 h with a yield of 0.33 g DCW/g glucose, and had accumulated 1.09 g/L acetate (Fig. 4-13). In contrast, MEC697/pTrc99A-*lacZ* achieved 4.34 g DCW/L in about 13 h with a yield of 0.40 g DCW/g glucose, and had accumulated 0.53 g/L acetate (Fig. 4-14). At the time glucose was exhausted, MG1655/pTrc99A-*lacZ* generated 34.3 kU β-galactosidase/g DCW with a yield of 3.28 kU/g glucose consumed, while MEC697 generated 72.4 kU β-galactosidase/g DCW with a yield of 6.90 kU/g glucose (Fig. 4-15). Although MEC697/pTrc99A-*lacZ* required about 30% more time to consuming the 10 g/L glucose, less acetate and more biomass were generated using MEC697 pTrc99A-*lacZ*. Moreover, knockouts in the NAD(H) degradation pathway resulted in about twice the formation of a model recombinant protein.

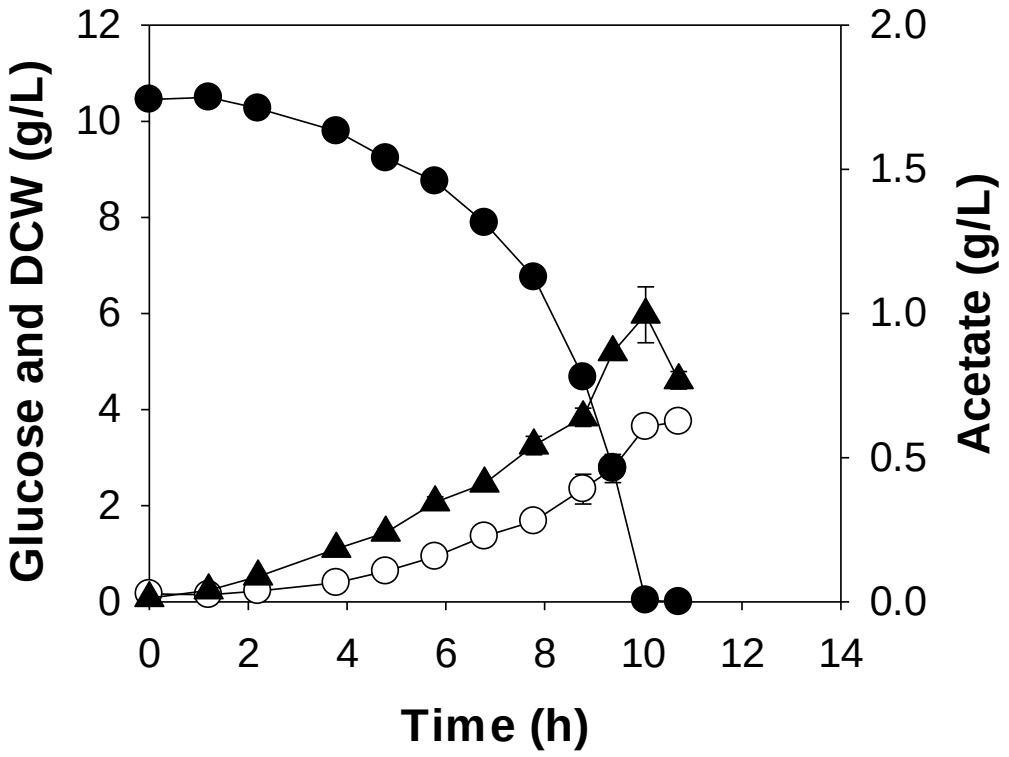

Figure 4-13. The growth profile of MG1655 pTrc99A-*lacZ* on 10 g/L glucose: biomass (▲); glucose (●); Acetate (○). Error bars indicate standard deviation.

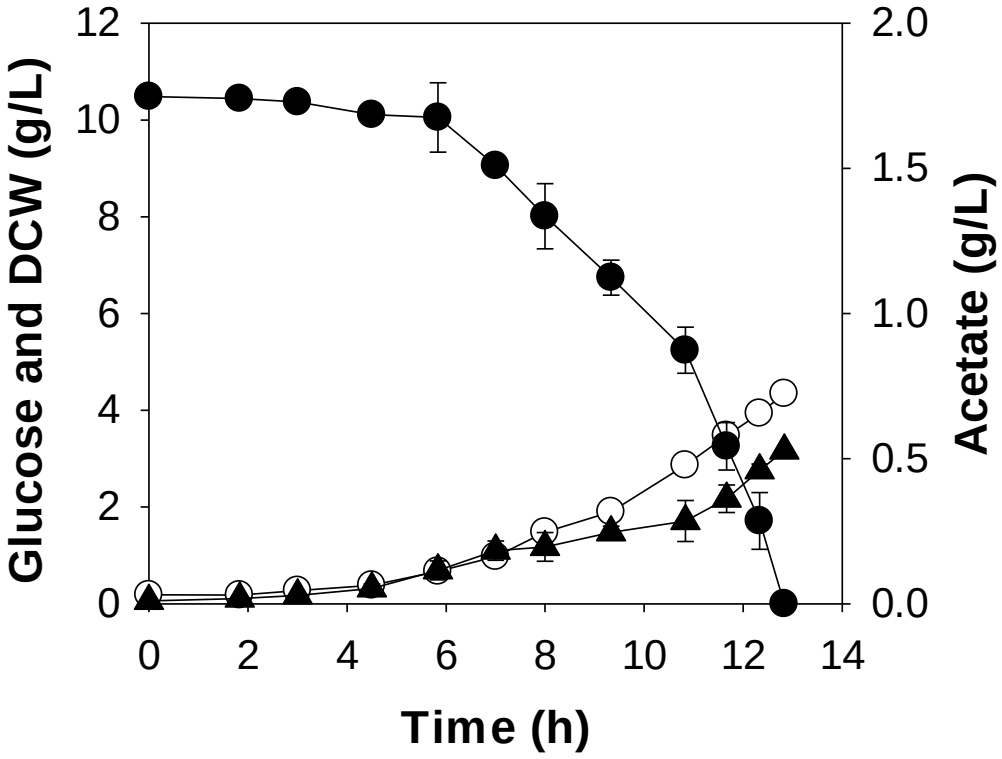

Figure 4-14. The growth profile of MEC697 pTrc99A-*lacZ* on 10 g/L glucose: biomass (▲); glucose (●); Acetate (○). Error bars indicate standard deviation.

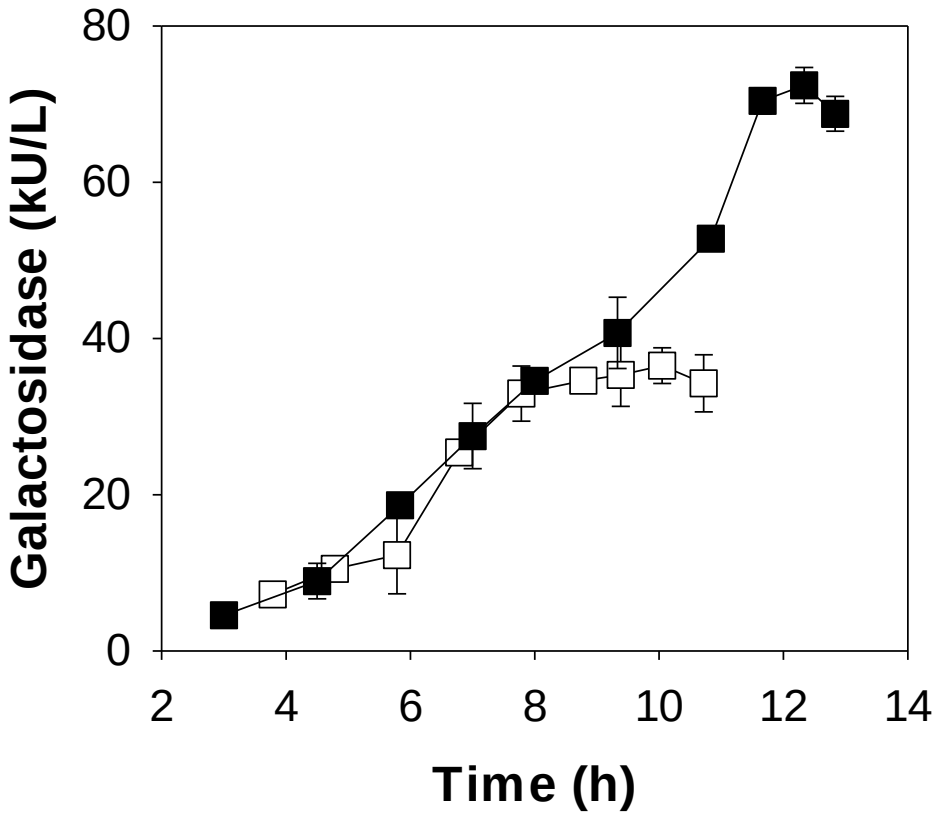

Figure 4-15. Production of β-galactosidase during batch growth of MG1655 pTrc99A-*lacZ* (□) and MEC697 pTrc99A-*lacZ* (■) on 10 g/L glucose: in. Error bars indicate standard deviation.

Discussion

During cell growth on glucose, NADH generated primarily by glycolysis and the TCA cycle is reoxidized to NAD^+ by respiration. However, the rate of oxygen consumption in *E. coli* can not match the demand for oxidizing the increasing level of NADH as glucose uptake increases (Andersen and von Meyenburg, 1980; Varma and Palsson, 1994; Eiteman and Altman, 2006). To modulate the resulting redox imbalance, *E. coli* will generate acetate as an overflow product because no NADH is generated in the conversion of acetyl-CoA to acetate (El-Mansi and Holms, 1989; Holms, 2001). In order to overcome the redox imbalance implicated in acetate overflow, a water-forming NADH oxidase expressed in *E. coli* can enhance the NADH to NAD^+ recycling and reduce acetate formation (Vemuri et al., 2006a). Overexpressing formate dehydrogenase gene from *Candida boidinii* similarly alters the NADH/NAD^+ ratio and affects acetate formation under anaerobic growth (Berríos-Rivera et al., 2002a). Altering the redox ratio by introducing enzymes which directly utilize NADH seems to be a promising way to control acetate overflow. Similarly, an increased pool of those cofactors was correlated with a reduction of NADH/NAD^+ ratio and reduced acetate formation during anaerobic *E. coli* growth with overexpression of the *pncB* gene (Berríos-Rivera et al., 2002b). In this study, curtailing NAD(H) degradation pathway did not materially alter the NADH/NAD^+ ratio, but slowing NAD(H) degradation by knockouts in the *nadR nudC mazG* genes did significantly elevate the total NAD(H) concentration and reduce acetate formation during fully aerobic growth on glucose.

The concentration of PEP and pyruvate are important indicators for carbon fluxes in glycolysis. Steady-state pools of PEP and pyruvate increased with increasing glucose uptake rate (Berríos-Rivera et al., 2002b). An elevated intracellular pyruvate concentration was previously correlated with acetate overflow (Vemuri et al., 2006a), and was also observed in the current

study (Fig 4-10). Pyruvate participates in a wide range of biochemical reactions and may contribute to acetate formation directly (De Mey et al., 2007). The triple knockout strain with an elevated NAD(H) pool did not promote pyruvate accumulation as growth rate increased. Lowering pyruvate pool has previously been described as one approach for preventing acetate formation. For example, introducing pyruvate carboxylase which converts pyruvate to oxaloacetate resulted in more carbon flux directly enter in TCA cycle and a 60% reduction in acetate (Gokarn et al., 2001; March et al., 2002). Similarly, diverting pyruvate into another benign product, such as acetolactate and acetoin using acetolactate synthase, led to lower acetate formation (Aristidou et al., 1995). Instead of redirecting pyruvate into the TCA cycle or toward other by-products, the triple knockout *E. coli* allows a high glucose uptake rate while prevents pyruvate accumulation.

PEP is also a crucial intermediate of glucose catabolism (Postma et al., 1993). The carbon flux from PEP can be directed toward two routes: PEP into pyruvate by pyruvate kinase (Muñoz and Ponce, 2003) or PEP into oxaloacetate by PEP carboxylase (Noronha et al., 2000). As the specific glucose uptake rate increased, the global flux through the route of PEP into pyruvate was increased significantly, thus results in MG1655 a greater ratio of pyruvate/PEP and more acetate. An alternative approach to lower pyruvate pool is directing more carbon from PEP into oxaloacetate and consequently reduce acetate production. For example, overexpressing PEP carboxylase led to a reduction of 60% of acetate excretion in *E. coli* VJS632 aerobic cultures (Farmer and Liao, 1997). In our study, the triple knockout strain was not influenced by the sudden changes of carbon flux due to the increased glucose uptake rate but maintained a comparatively constant PEP concentration over a wide range of growth rate.

Metabolite distribution can be influenced by carbon sources according to their oxidation states. More reduced carbon sources result in more reduced products such as ethanol, whereas the more oxidative carbon sources yield more acetate (Alam and Clark, 1989). In a comparison of aerobic growth of *E. coli* on gluconate, glucose, or sorbitol, gluconate yielded the most acetate but the least ethanol, while sorbitol yielded the least acetate but the most ethanol (Berríos-Rivera, 2002). Similar observations also were found in either MG1655 or MEC697 when compared these three carbon sources in aerobic batch growth. All those results strongly demonstrate the use of carbon sources with different oxidation states will result in the change of intracellular environment and eventually impact the metabolite distribution.

In this study a fed-batch process was designed to differentiate the high cell density growth of MG1655 and MEC697 for the goal of recombinant protein generation. An exponential fed-batch is typically an approach to prevent acetate formation and accumulate more biomass in carbon-limited cultures (Jensen and Carlsen 1990; Korz et al., 1995). These two strains growing at 0.22 h^{-1} did not materially change their acetate and biomass formation: MEC697 and MG1655 were largely indistinguishable at this growth rate and overflow metabolism was low. A higher fed-batch growth rate might have resulted in a greater difference between the strains. Indeed, batch growth (which is at each strain's maximum growth rate) resulted in 50% less acetate and 2-fold greater recombinant protein generation in MEC697 compared to MG1655. However, batch growth of *E. coli* is not an ideal process to achieve high cell density not only because the well-known acetate formation (Hollywood and Doelle, 1976; Kleman and Strohl, 1994), but also because *E. coli* growth will be inhibited when initial nutrients are present above certain concentrations (Riesenberg, 1991). Fed-batch culture through controlling a glucose concentration of 1 g/L had previously achieved a high cell density as well as maintained a high growth rate, but

in which also found acetate formation (Luli and Strohl, 1990). In order to further compare the high cell density growth of MG1655 and MEC697, a fed-batch process with controlled substrate concentration could be used in the future study.

In summary, an elevated pool of intracellular NAD(H) correlated with lower acetate formation in *E. coli* during growth on glucose as the carbon source. Considering the essential role of NAD(H) in aerobic metabolism, our study provides a new insight for *E. coli* metabolism and for the production of recombinant proteins.

Acknowledgments

The authors thank Sarah Lee and D. Brisbane Tovilla Coutiño for technical assistance. The authors declare they have no conflicts of interest.

References

Åkesson, M., P. Hagander, and J. P. Axelsson. 2001. Avoiding acetate accumulation in *Escherichia coli* cultures using feedback control of glucose feeding. *Biotechnol. Bioeng*. 73(3): 223-230.

Alam, K. Y. and D. P. Clark. 1989. Anaerobic fermentation balance of *Escherichia coli* as observed by in vivo nuclear magnetic resonance spectroscopy. *J. Bacteriol*. 171(11): 6213-6217.

Andersen, K. B. and K. von Meyenburg. 1977. Charges of nicotinamide adenine nucleotides and adenylate energy charge as regulatory parameters of the metabolism in *Escherichia coli. J. Biol. Chem*. 252(12): 4151-4156.

Andersen, K. B. and K. von Meyenburg. 1980. Are growth rates of *Escherichia coli* in batch cultures limited by respiration? *J. Bacteriol*. 144(1): 114-123.

Aristidou, A. A., K. Y. San, and G. N. Bennett. 1995. Metabolic engineering of *Escherichia coli* to enhance recombinant protein production through acetate reduction. *Biotechnol. Progr*. 11(4): 475-478.

Aristidou, A. A., K. Y. San, and G. N. Bennett. 1999. Improvement of biomass yield and recombinant gene expression in *Escherichia coli* by using fructose as the primary carbon source. *Biotechnol. Progr*. 15(1): 140-145.

Bernofsky, C. and M. Swan. 1973. An improved cycling assay for nicotinamide adenine dinucleotide. *Anal. Biochem*. 53(2): 452-458.

Berríos-Rivera, S. J. 2002. Metabolic engineering of cofactors (NADH/NAD+) in *Escherichia coli. PhD thesis*, Rice University, Houston, Tex.

Berríos-Rivera, S.J., G. N. Bennett, and K. Y. San. 2002a. Metabolic engineering of Escherichia coli: increase of NADH availability by overexpressing an NAD^+-dependent formate dehydrogenase. *Metab. Eng*. *4*(3):217-229.

Berríos-Rivera, S. J., G. N. Bennett, and K. Y. San. 2002b. The effect of increasing NADH availability on the redistribution of metabolic fluxes in *Escherichia coli* chemostat cultures. *Metab. Eng*. 4(3): 230-237.

Chou, C. H., G. N. Bennett, and K. Y. San. 1994. Effect of modified glucose uptake using genetic engineering techniques on high-level recombinant protein production in *Escherichia coli* dense cultures. *Biotechnol. Bioeng*. 44(8): 952-960.

De Mey, M., S. De Maeseneire, W. Soetaert, and E. Vandamme. 2007. Minimizing acetate formation in *E. coli* fermentations. *J. Ind. Microbiol. Biot.* 34(11): 689-700.

Eiteman, M. A. and M. J. Chastain. 1997. Optimization of the ion-exchange analysis of organic acids from fermentation. *Anal. Chim. Acta*. 338(1-2): 69-75.

Eiteman, M.A. and E. Altman. 2006. Overcoming acetate in *Escherichia coli* recombinant protein fermentations. *Trends. Biotechnol*. 24(11): 530-536.

El-Mansi, E. M. T. and W. H. Holms. 1989. Control of carbon flux to acetate excretion during growth of *Escherichia coli* in batch and continuous cultures. *Microbiology*. 135(11): 2875-2883.

El-Mansi, M., 2004. Flux to acetate and lactate excretions in industrial fermentations: physiological and biochemical implications. *J. Ind. Microbiol. Biot*. 31(7): 295-300.

Farmer, W. R. and J. C. Liao. 1997. Reduction of aerobic acetate production by *Escherichia coli*. *Appl. Environ. Microbiol.* 63(8): 3205-3210.

Gokarn, R., J. Evans, J. Walker, S. Martin, M. Eiteman, and E. Altman. 2001. The physiological effects and metabolic alterations caused by the expression of *Rhizobium etli* pyruvate carboxylase in *Escherichia coli*. *Appl. Microbiol. Biotechnol.* 56(1-2): 188-195.

Han, Q. and M. A. Eiteman. 2018. Enhancement of NAD (H) pool for formation of oxidized biochemicals in *Escherichia coli*. *J. Ind. Microbiol. Biotechnol.* 1-12.

Hollywood, N. and H. W. Doelle. 1976. Effect of specific growth rate and glucose concentration on growth and glucose metabolism of *Escherichia coli* K-12. *Microbios*, 17(67): 23-33.

Holms, H., 2001. Flux analysis: a basic tool of microbial physiology. *Adv. Microb. Physiol*. *45*: 273-340.

Horn, U., W. Strittmatter, A. Krebber, U. Knüpfer, M. Kujau, R. Wenderoth, K. Müller, S. Matzku, A. Plückthun, and D. Riesenberg. 1996. High volumetric yields of functional dimeric miniantibodies in *Escherichia coli*, using an optimized expression vector and high-cell-density fermentation under non-limited growth conditions. *Appl. Microbiol. Biotechnol*. 46(5-6): 524-532.

Iuchi, S., A. Aristarkhov, J. M. Dong, J. S. Taylor, and E. C. Lin. 1994. Effects of nitrate respiration on expression of the Arc-controlled operons encoding succinate dehydrogenase and flavin-linked L-lactate dehydrogenase. *J. Bacteriol*. 176(6): 1695-1701.

Jensen, E.B. and S. Carlsen. 1990. Production of recombinant human growth hormone in *Escherichia coli*: expression of different precursors and physiological effects of glucose, acetate, and salts. *Biotechnol. Bioeng*. 36(1): 1-11.

Johnston, W. A., M. Stewart, P. Lee, and M. J. Cooney. 2003. Tracking the acetate threshold using DO-transient control during medium and high cell density cultivation of recombinant *Escherichia coli* in complex media. *Biotechnol. Bioeng*. 84(3): 314-323.

Kleman, G. L., J. J. Chalmers, G. W. Luli, and W. R. Strohl. 1991. Glucose-stat, a glucose-controlled continuous culture. *Appl. Environ. Microbiol*. 57(4): 918-923.

Kleman, G. L. and W. R. Strohl. 1994. Acetate metabolism by *Escherichia coli* in high-cell-density fermentation. *Appl. Environ. Microbiol.* 60(11): 3952-3958.

Konstantinov, K., M. Kishimoto, T. Seki, and T. Yoshida. 1990. A balanced DO-stat and its application to the control of acetic acid excretion by recombinant *Escherichia coli*. *Biotechnol. Bioeng*. 36(7): 750-758.

Korz, D. J., U. Rinas, K. Hellmuth, E. A. Sanders, and W. D. Deckwer. 1995. Simple fed-batch technique for high cell density cultivation of *Escherichia coli*. *J. Biotechnol*. 39(1): 59-65.

Luli, G. W. and W. R. Strohl. 1990. Comparison of growth, acetate production, and acetate inhibition of *Escherichia coli* strains in batch and fed-batch fermentations. *Appl. Environ. Microbiol*. 56(4): 1004-1011.

March, J. C., M. A. Eiteman, and E. Altman. 2002. Expression of an anaplerotic enzyme, pyruvate carboxylase, improves recombinant protein production in *Escherichia coli*. *Appl. Environ. Microbiol*. 68(11): 5620-5624.

Muñoz, M. E. and E. Ponce. 2003. Pyruvate kinase: current status of regulatory and functional properties. *Comp. Biochem. Physiolo. B Biochem. Mol. Biol*. 135(2): 197-218.

Nakano, K., M. Rischke, S. Sato, and H. Märkl. 1997. Influence of acetic acid on the growth of *Escherichia coli* K12 during high-cell-density cultivation in a dialysis reactor. *Appl. Microbiol. Biotechnol*. 48(5): 597-601.

Neidhardt, F. C., J. L. Ingraham, and M. Schaechter. 1990. Physiology of the bacterial cell: a molecular approach (Vol. 20). Sunderland, MA: Sinauer Associates.

Noronha, S. B., H. J. C. Yeh, T. F. Spande, and J. Shiloach. 2000. Investigation of the TCA cycle and the glyoxylate shunt in *Escherichia coli* BL21 and JM109 using 13C-NMR/MS. *Biotechnol. Bioeng*. 68(3): 316-327.

Pardee, A. B., F. Jacob, and J. Monod. 1959. The genetic control and cytoplasmic expression of "inducibility" in the synthesis of β-galactosidase by *Escherichia coli*. *J. Mol. Biol*. 1(2): 165-178.

Postma, P.W., J. W. Lengeler, and G. R. Jacobson. 1993. Phosphoenolpyruvate: carbohydrate phosphotransferase systems of bacteria. *Microbiol. Rev*. 57(3): 543-594.

Reiling, H. E., H. Laurila, and A. Fiechter. 1985. Mass culture of *Escherichia coli*: Medium development for low and high density cultivation of *Escherichia coli* B/r in minimal and complex media. *J. Biotechnol*. 2(3-4): 191-206.

Riesenberg, D. 1991. High-cell-density cultivation of *Escherichia coli*. *Curr. Opin. Biotechnol*. 2(3): 380-384.

Riesenberg, D. and R. Guthke. 1999. High-cell-density cultivation of microorganisms. *Appl. Microbiol. Biotechnol*. 51(4): 422-430.

San, K. Y., G. N. Bennett, A. A. Aristidou, and C. H. Chou. 1994. Strategies in high-level expression of recombinant protein in *Escherichia coli*. *Ann. N.Y. Acad. Sci*. 721(1): 257-267.

Schaefer, U., W. Boos, R. Takors, and D. Weuster-Botz. 1999. Automated sampling device for monitoring intracellular metabolite dynamics. *Anal. Biochem*. 270(1): 88-96.

Varma, A. and B. O. Palsson. 1994. Stoichiometric flux balance models quantitatively predict growth and metabolic by-product secretion in wild-type *Escherichia coli* W3110. *Appl. Environ. Microbiol*. 60(10): 3724-3731.

Vemuri, G. N., E. Altman, D. P. Sangurdekar, A. B. Khodursky, and M. A. Eiteman. 2006a. Overflow metabolism in *Escherichia coli* during steady-state growth: transcriptional regulation and effect of the redocx ratio. *Appl. Environ. Microbiol.* 72(5): 3653-3661.

Vemuri, G. N., M. A. Eiteman, and E. Altman. 2006b. Increased recombinant protein production in *Escherichia coli* strains with overexpressed water-forming NADH oxidase and a deleted ArcA regulatory protein. *Biotechnol. Bioeng*. 94(3): 538-542.

Weitzman, P. D. J. and M. J. Danson. 1976. Citrate Synthase. *Current Topics in Cell Regulation*. Academic Press. 10:161-204.

Table 3-1. Summary of metabolites and growth profiles during growth of MG1655 or MEC697 on 20 g/L gluconate, glucose, or sorbitol in controlled batch bioreactor

	Gluconate		Glucose		Sorbitol	
	MG1655	MEC697	MG1655	MEC697	MG1655	MEC697
Acetate (g/L)	2.49 ± 0.54	2.92 ± 0.01	2.19 ± 0.11	1.10 ± 0.10	0.11 ± 0.07	0.12 ± 0.01
Pyruvate (g/L)	0.44 ± 0.15	1.64 ± 0.27	0.04 ± 0.01	0.06 ± 0.01	0.07 ± 0.01	0.07 ± 0.01
Lactate (g/L)	0.09 ± 0.02	0.10 ± 0.01	0.18 ± 0.11	0.23 ± 0.02	0.01 ± 0.01	0.02 ± 0.01
Succinate (g/L)	0.14 ± 0.05	0.09 ± 0.01	0.04 ± 0.03	0.01 ± 0.01	0.18 ± 0.02	0.26 ± 0.01
Ethanol (g/L)	0.04 ± 0.05	0.03 ± 0.01	0.12 ± 0.06	0.12 ± 0.09	0.21 ± 0.02	0.20 ± 0.01
Biomass (g/L)	5.30	4.81	6.54	6.73	6.63	6.58
Total NAD(H) (μmol/g DCW)	11.58 ± 0.50	16.77 ± 0.34	4.58 ± 0.43	8.21 ± 0.47	12.37 ± 1.26	18.17 ± 0.57
NAD^+/NADH	1.89	1.92	3.51	3.85	1.10	1.12
Specific Growth rate (h^{-1})	0.74	0.66	0.53	0.60	0.45	0.52
Biomass yield (g/g)	0.27	0.25	0.31	0.33	0.31	0.31

CHAPTER 6

CONCLUSIONS

The central goal of this research was to develop *E. coli* as the whole-cell biocatalysts to improve NAD^+-dependent conversions of oxidized chemicals. Maintaining sufficient concentration of NAD^+ is critical to drive such a process. Intact microbes can not only synthesize cofactors during growth but regenerate NAD^+ from NADH by transferring the reducing equivalents to the final electron acceptor, such as oxygen. In this work, we improved NAD^+ levels by expression of a water-forming NADH oxidase and the selection of glycerol as the sole carbon source. As demonstrated in Chapter 3, the biosynthesis of L-xylulose was accomplished with this strategy.

However, we were curious about the natural degradation of the cofactors. Therefore, we hypothesized that the availability of the cofactors also could impact NAD^+-dependent bioconversions by maintaining a sufficient driving force for the example oxidative process. Knocking out *nadR*, *nudC*, and *mazG* in order to minimize NAD(H) degradation resulted in a significant improvement in model conversions: xylitol to L-xylulose and galactitol to L-tagatose as described in Chapter 4. One unanticipated effect of increased total NAD(H) pool was that acetate formation was greatly diminished.

The observed reduction in acetate formation led to the hypothesis that strains having knockouts in NAD(H) degradation pathways would generate more recombinant proteins. As elucidated in Chapter 5, the engineered *E. coli* strains did indeed generate substantially more of a

model recombinant protein production, but only under batch conditions. In summary, our results revealed that maintenance of cofactors can affect several oxidative bioconversions and recombinant protein production in *E. coli*.

For the whole-cells, oxidative bioconversion under aerobic growth, coupling strategies which increase the turnover of NADH to NAD^+, for example, by expressing a water-forming NADH oxidase or, in this study, prolonging the availability of NAD(H) can be appropriate methodologies for enhancing formation of the oxidized biochemical products. On the other hand, the cofactor-dependent production systems not only include oxidative conversions but also work on reductive conversions. Thus, we believe our developed strain with an elevated total NAD(H) pool can also be combined with the approaches of NADH regeneration to increase the production of reduced chemicals under anaerobic conditions.

In this study, a new engineered *E. coli* strain resulted in an elevated pool size of intracellular NAD(H) without introducing plasmid or gene overexpression. Since there is a strong balance between NAD^+ and $NADP^+$, we believe our strain would be a good model for further investigating the relationship between NAD(H) and NADP(H) pool size as well as their influence on carbon flux distribution, which might disclose a better knowledge of the cellular metabolism responding to the increased cofactors levels.